Development and Testing of a Pre-Prototype Mach 2 Ramgen Engine
Final Report

September 29th, 2000 to August 31st, 2001

Principle Author: Ramgen Power Systems

Report Issued September 2001
DOE Award Number DE-FC26-00NT40915

Submitted By:

Ramgen Power Systems
11808 Northup Way, Suite W190
Bellevue, WA 98005

(Document Number 0800-00018)

Disclaimer

Abstract

The research and development effort of a new kind of combustion engine is presented. The engine is designed to convert the thrust from ramjet modules into shaft torque, which in turn can be used for electrical power generation or mechanical drive applications.

An aggressive test program was undertaken that included evaluation of the existing engine, as well as incorporation of novel improvements to the thrust modules and supporting systems. Fuel mixing studies with Vortex Generators and bluff body flame holders illuminated the importance of increasing the shear-layer area and spreading angle to augment flame volume. Evaluation of flame-holding configurations (with variable fuel injection methods) concluded that the heat release zone, and therefore combustion efficiency, could be manipulated by judicious selection of bluff body geometry, and is less influenced by fuel injection distribution. Air film cooling studies demonstrated that acceptable combustor life could be achieved with optimized air film distribution patterns and thermal barrier coatings.

Table of Contents

1.0 Executive Summary

This report summarizes the results of development and testing efforts of the Ramgen Engine.

The Ramgen engine represents the unique application of ramjet principles to power generation. The engine is designed to convert the thrust from a ramjet thrust module into shaft torque, which in turn can drive a generator to provide electricity or shaft power for a mechanical drive application. This effort was partially funded by Department of Energy cooperative agreement number DE-FC26-00NT40915, awarded between the period of September 29th, 2000 to July 31st, 2001.

The primary objective of advancing the research and development effort on the Ramgen engine was accomplished by reaching significant technological milestones. Major tasks completed include:

- Extended operation with satisfactory combustion and air film cooling performance at supersonic inlet conditions.
- Completion of an intensive test program, with over 500 cold flow, ignition, ramp, and high-speed engine tests. This included 216 hours of engine spin tests, 42.5 hours of hot combustor testing, and 6.3 hours above Mach 1.
- Testing three fuel mixing configurations using Vortex Generators.
- Design and testing a bluff body flame holder with integral fuel injection.
- Testing five pilot-fuel injection methods which incorporated rapid configuration-change features.
- Ignition, ramping and steady state operation using methane (natural gas) and hydrogen fuels.
- Design and testing of air film coolant improvements, including redistribution of coolant coverage, expanded protection of the Inconel and Titanium components, thermal barrier coating integration, and upgrades to the supply system.
- Direct measurement of rotor drag above Mach 1, independent of combustor geometry.
- Design and testing of a tip seal leakage mitigation scheme.
- Testing of an inlet boundary layer bleed scheme.
- Monitoring of engine emissions to evaluate combustor/engine performance.
- Direct measurement of engine acoustic noise, and evaluation of mitigation methods.

Accomplishment of these tasks has led to a greater understanding of what is required to adapt ramjet technology to a rotating reference frame. Fuel mixing studies with Vortex Generators and a bluff body flame holder illuminated the importance of increasing the shear-layer spreading angle and maximizing the shear area, thereby augmenting flame surface area. Evaluation of flame-holding configurations (with variable fuel injection methods) concluded that the heat release zone, and therefore combustion efficiency, could be manipulated by judicious selection of bluff body geometry, and is less influenced by fuel injection distribution. Air film cooling studies demonstrated that acceptable combustor life could be achieved with optimized air film distribution patterns and thermal barrier coatings.

Based on the efforts to date, it is clear that optimizing combustor residence time and velocities while dealing with unique boundary conditions is of fundamental importance. Constraints on practical flame-holder design, emissions, thrust segment weight and geometry, and materials make optimization a worthy challenge. Significant milestones toward answering these challenges have been made in the contract period. Future efforts will build on the foundation of this research and development effort, with the ultimate goal of a viable, production-ready engine.

2.0 Introduction

2.1 Project Background

This document presents the results of efforts to advance the design and development of a fundamentally new kind of power generation device known as the Ramgen Engine. These efforts have been aided by the Department of Energy, as part of an initiative to bring viable energy technologies to maturity.

The design of the Pre-Prototype Ramgen Engine represents the application of well-established ramjet principles to shaft power generation. Instead of using a ramjet to provide thrust for a supersonic aircraft or missile, the Ramgen engine is designed to convert the thrust from a ramjet into shaft torque, which in turn can drive a generator to provide electricity or shaft power for a mechanical drive application. At maturity, the production engine will have a thermal efficiency rivaling or surpassing a conventional gas turbine, with low CO and NOx emissions. The fundamental operating principal of the engine also allows the use of waste fuels, including landfill gas and coal bed methane, for energy production.

The Pre-Prototype Ramgen Engine was fully assembled in Tacoma Washington in July of 1998. Tests occurring in early 1999 validated the ignition system and flame holding at idle, the mechanical integrity of the rotor at supersonic tip speeds, and the fundamental engine design. Development work conducted from late 1999 to September 2000 focused on improving combustion stability, fuel delivery methods, and the air film cooling system. These efforts resulted in substantial progress toward operation at full rotor speeds with air film cooling and flame holding.

The continuing research, design, and development efforts were assisted by the Department of Energy from September 29th, 2000 to September 31st, 2001. Significant performance milestones were achieved during the contract period. The results of this effort have brought the Ramgen Engine significantly closer to a commercially viable power generation device.

2.2 Fundamental Principles of Ramjet Technology and the Ramgen Engine

2.2.1 Ramjet Technology

The Ramgen engine is based on ramjet technology. A ramjet engine produces propulsive force by increasing the momentum of the working fluid through some release of heat. This heat release causes the momentum of the exiting jet to exceed the momentum of the entering air stream. In contrast to other air-breathing jet engines, the working cycle of the ramjet engine is accomplished without mechanical compression of the working fluid, or intermittent semi-closed combustion cycles. This makes the ramjet engine the least complicated mechanical air-breathing engine. Figure 2.1 illustrates the working cycle of the ramjet engine. Ingestion, compression, heat release, and expansion are all achieved by the shaping of the ramjet duct, and the resulting compressible gasdynamic processes.

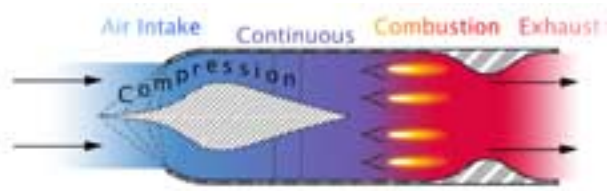

Ramjet Engine Working Cycle
Figure 2.1

The basic elements of the ramjet engine are illustrated in Figure 2.1. The air stream entering the ramjet is ingested by the inlet. The inlet is also referred to as a diffuser because the entering air stream is decelerated, or diffused, from the forward speed of the engine to a lower velocity prior to entering the combustion chamber. In engines employing liquid or gaseous fuels for heating the working fluid, the fuel is injected through orifices or nozzles at some point in the diffuser. The location of fuel injection depends upon the desired degree of atomization and vaporization of the fuel and the desired mixture pattern of the fuel and working fluid at the entrance to the combustion chamber.

A flame holder is typically located at the end of the inlet passage. A flame holder is a turbulence-generating device that serves to stabilize the combustion process. The air-fuel mixture entering the combustion chamber is ignited in the recirculating regions formed downstream of the flame holder by an independent ignition source. In most engines, this igniter is only required to function at the onset of combustion. The combustion process is self-propagating during continuous operation.

The combustion of the air-fuel mixture is completed in the combustion chamber, normally a constant-area passage. The combustion products leaving the combustion chamber are at a higher pressure than the free stream air surrounding the engine. The exhaust nozzle is used to expand the flow and convert the high pressure, high temperature gasses leaving the combustor into the high velocity exhaust jet required to generate thrust. The flow velocity after combustion is subsonic; hence, an initial contraction of the flow area (throat) is necessary to both reduce the internal pressure and to accelerate the internal flow to sonic velocity. For maximum thrust realization at these speeds, a diverging passage or nozzle is added downstream of the throat. The addition of the nozzle allows the flow to continue to expand to supersonic velocity, until ambient pressure is once again attained.

TALOS missile
Figure 2.2

Ramjets, though less commonplace than gas turbines, are used widely for many high-speed flight propulsion applications. Figure 2.2 is a picture of a TALOS missile being launched. The TALOS uses a solid propellant rocket booster to reach supersonic speeds and then

YF-12 Reconnaissance Plane
(The SR-71 Blackbird)
Figure 2.3

Ramjet Inlet for SR-71
Figure 2.4

transitions to a ramjet engine for the remainder of the mission. Note that the inlet of the ramjet flow path is clearly visible in the nose of the missile in Figure 2.2. Figures 2.3 and 2.4 are pictures of the Air Force's SR-71 "Blackbird" reconnaissance aircraft which employs ramjet propulsion to attain maximum flight speed and altitude.

A novel variation of the ramjet engine is the Ram-Accelerator. The Ram-Accelerator is a unique embodiment of the ramjet process applied to the acceleration of a projectile or payload. In the ram-accelerator, a tube or barrel is filled with a mixture of fuel and oxidant, commonly referred to as "premix". A projectile is launched into one end of the barrel. The projectile enters the barrel with a low supersonic velocity such that the local Mach number of the projectile with respect to the premix is Mach ~ 1.2. As the projectile travels through the premix in the barrel, the shaping of the projectile creates a series of oblique shock waves, which coalesce and reflect off the barrel walls as indicated in Figure 2.5.

A normal shock is stabilized in the expanding area section of the flowpath formed between the projectile and the barrel wall. This is shown in Figure 2.5. As the premix passes through the normal shock wave it is decelerated to subsonic velocities and is further decelerated in the following subsonic diffuser section of the flowpath, downstream of the normal shock. A combustion process is stabilized behind the trailing edge of the projectile. The flow is thermally choked downstream of the combustion process. The duct or flow path formed between the moving projectile and the stationary barrel wall is a complete ramjet flowpath where all the thrust is manifested on the moving projectile. The thrust developed by the ramjet process accelerates the projectile as it moves along the length of the barrel so that it emerges from the discharge end of the barrel at a significantly greater velocity than when it entered the barrel.

Two important distinctions separate the ramjet flowpath in the Ram-accelerator from a typical flight ramjet application. One of the distinctions is that the oxidant and fuel are mixed to complete homogeneity, prior to being ingested by the supersonic inlet of the ramjet. The supersonic inlet for the ramjet flowpath in the Ram-accelerator is formed by the moving nose of the projectile and the stationary barrel wall. The fact that the oxidant and fuel are mixed before entering the burner significantly simplifies the burner design and eliminates the fuel injection and mixing processes used in flight ramjet applications. Section 3 presents how the same technique of air-fuel premixing is applied in the Ramgen engine.

The second important distinction that differentiates the ramjet flowpath in the Ram-accelerator from a conventional

ramjet flowpath is that one of the defining surfaces of the ramjet flowpath is formed by a surface that is moving relative to the other surfaces. As shown in Figure 2.6, the interior wall of the barrel that forms the exterior surface of the ramjet flowpath is stationary. The exterior surface of the moving Ram-accelerator projectile forms the interior surface of the ramjet flowpath. This concept is also applied in the Ramgen engine and will be explained further in the next section.

2.2.2 The Ramgen Engine

The essential concept of the Ramgen engine is the incorporation of one or more ramjets onto the rim of a rotor such that the thrust from the ramjets acts tangentially on the rim of the rotor, causing it to rotate at high speed. In this way, the thrust from the ramjets is converted into torque on the output shaft of the high-speed rotor. This shaft torque can then

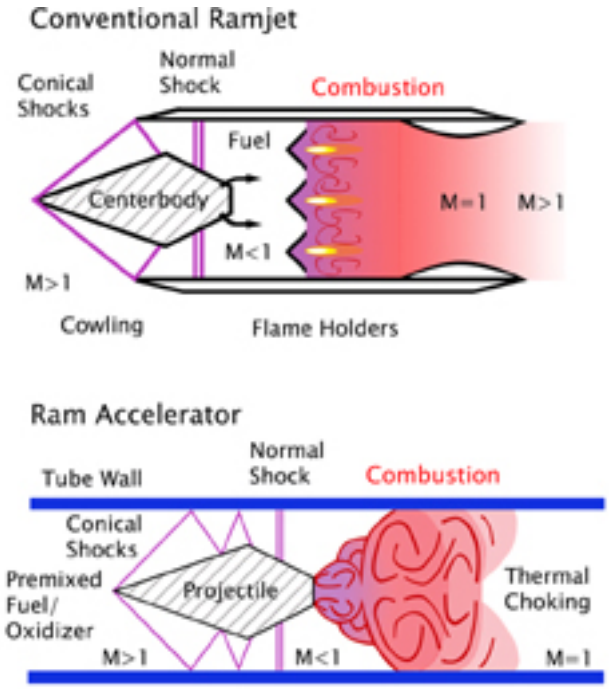

Ram-Accelerator Schematic
Figure 2.5

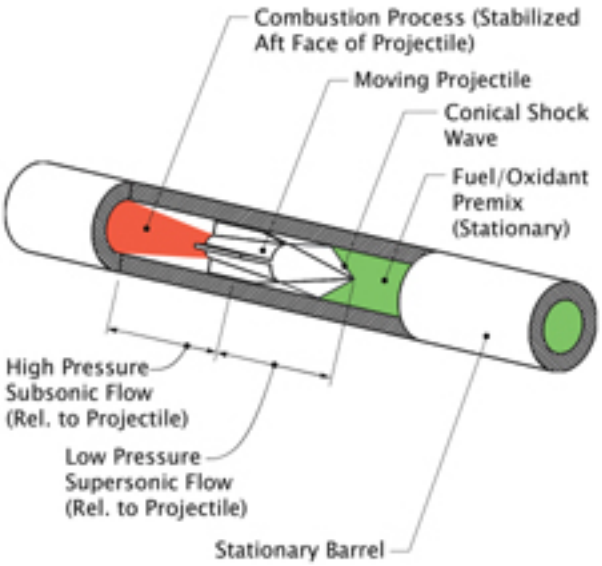

Ram-Accelerator Projectile and Barrel
Figure 2.6

be used to drive a conventional generator for stationary power production or it can be used for other mechanical drive applications. The simplicity of this concept results in a highly efficient engine compared to conventional gas turbine engines.

The two ramjet flow-paths are incorporated into the rim of the high-speed rotor. The two-dimensional ramjet flowpath is open on its exterior, or radially outer-most, surface. The closure for the ramjet flowpath is formed by the stationary interior surface of the main engine case. The combination of a ramjet flowpath where one of the ramjet surfaces is moving relative to the other is analogous to the combination of the moving projectile and stationary barrel wall in the Ram-accelerator introduced in Section 2.2.1.

The ramjet flow-paths are mounted on the rim of the rotor at a helix angle. This flow path placement allows an axial low-speed flow, in the direction of the axis of rotation of the high-speed rotor. The low speed axial flow supplies a continuous flow of premix to the ramjet inlet. The supersonic ramjet inlets in the engine continuously ingest a premix in a similar way to that of the Ram-accelerator. Because the fuel is introduced by this method, very little precompression of the fuel is

required. This enables the Ramgen engine to burn a wide variety of fuels, including sub-quality fuels such as coalmine methane, low-BTU natural gas, landfill methane, biomass gasses, and hydrogen.

Another feature of the ramjet flow path is the helical strake that separates the inflowing premix from the hot combustion products that are discharged from the ramjet nozzles.

The Ramgen engine is simple in design. It has a low part count, thus making it less costly to build and maintain in comparison to conventional gas turbine engines.

2.3 Objectives

The overall program objective, supported in part by the Department of Energy, was the continuation of the research, design, and development effort of the Ramgen Engine. This program objective was pursued by: 1) implementing and evaluating design changes to the existing Ramgen engine, and 2) assessing the issues associated with demonstrating the Ramgen engine on opportunity fuels. Item one is topic of this report. In summary, the program consisted of:

- Establishing satisfactory combustor performance and combustor cooling at design speed
- Implementing auxiliary system modifications to enhance engine control and diagnostics
- Measuring rotor drag independent of ramjet thrust modules, to assess gross thrust
- Evaluating tip leakage effects and mitigation methods
- Evaluating boundary layer bleed
- Improved monitoring of combustor integrity in real-time
- Evaluating fuel injection and mixing methods and devices
- Evaluating flame holder configurations
- Optimizing air film cooling
- Monitoring engine noise levels and evaluating noise mitigation methods
- Monitoring emissions as part of the evaluation of component-level and engine-level performance

Progress on each of these elements has resulted in a successful test and evaluation phase of the Ramgen Engine. Numerous milestones were achieved, including:

- Over five hundred tests of the spinning engine were performed, with a total hot fire time of 42.5 hours.
- Four flame holder configurations were designed and tested.
- Four vortex generator (fuel/air mixing) configurations were designed and tested.
- Multiple fuel injection distribution and injection methods were implemented and tested.
- Air film coolant distribution to the segments was redesigned for 50% more coolant coverage than previous designs.
- Thermal Barrier Coating (TBC) was added to Inconel combustor segments for improved heat protection.
- Hastelloy X seals were incorporated into the combustor assembly, for improved heat protection.
- 25% of the combustor segments were replaced, and all segments were upgraded for improved heat resistance.
- The engine casing was significantly modified for rapid and more thorough combustor inspections and configuration changes.
- The air cooling delivery system was upgraded for high flow rate and delivery pressure.
- The exhaust system was upgraded for operation above 600F.
- Proximity sensors was added to detect rim segment expansion during engine operation
- The Variable Frequency Drive, used for engine spin-up to operational speed, was replaced with a higher rated unit with regenerative capability.
- The inlet boundary layer bleed configuration was modified to promote uniform inlet conditions
- Noise monitoring was conducted and mitigation methods explored.
- Emissions monitoring of NOx, CO, O2 and unburned hydrocarbons was conducted.

Detailed discussion of these milestones and results are presented in the following sections.

3.0 Experimental

3.1 Test Facility Overview

Tests were conducted at the Ramgen test facility located in Tacoma Washington. The facility includes appropriate equipment for complete assembly and disassembly of the engine and supporting test hardware, as well as standard machining equipment for minor field modifications of engine hardware.

A schematic of the facility is shown in figure 3.1. Major features include a 12.5 MW synchronous generator (figure 3.2), 600 kW starter motor with a variable frequency drive, a 5 to 1 gearbox, 6" and 8" natural gas lines at 25 psig (see figure 3.3), a compressor with 1200 scfm air capacity at 100 psig , a 2000 psia hydrogen source, a water-cooled lube oil system with backup DC power (figure 3.4), a 120 gpm water coolant system with forced convection radiators, a fire containment hood, and a four foot diameter insulated stainless steel exhaust stack.

Monitoring and control of the engine and auxiliary equipment is conducted remotely through the control room indicated in 3.1. The engine/facility control system is described in section 3.3.

The facility is typically staffed with a facility manager, a facility assistant, a mechanical technician, an electrical technician, an engine operator, a data acquisition/mechanical engineer, and a test director. During engine assembly, disassembly and modification, this staff is augmented with additional technicians and engineering support.

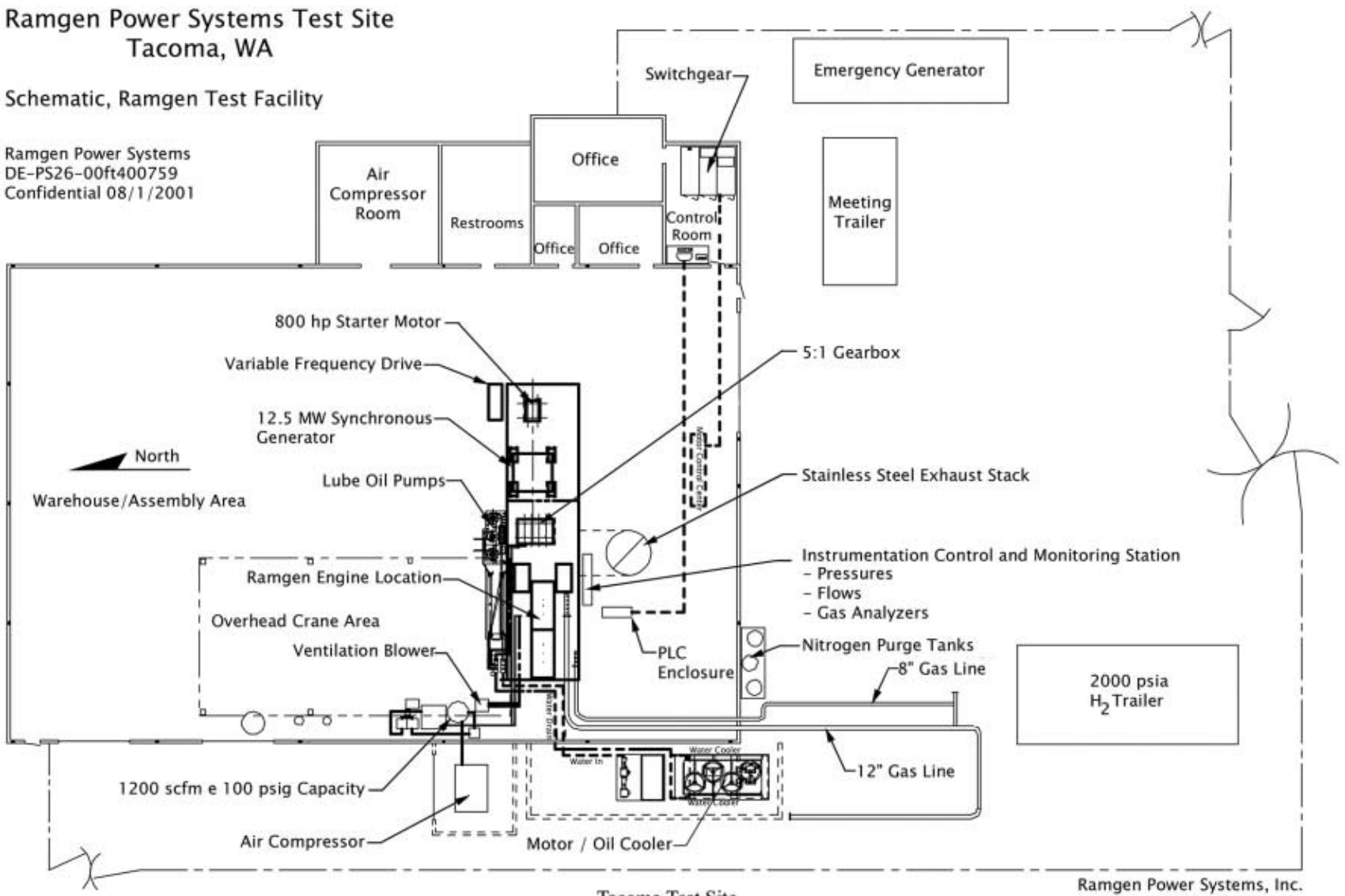
Ramgen Power Systems Test Site
Tacoma, WA
Schematic, Ramgen Test Facility
Ramgen Power Systems
DE-PS26-00ft400759
Confidential 08/1/2001
Switchgear
Emergency Generator
Air Compressor Room
Restrooms
Office
Office
Office
Control Room
Meeting Trailer
800 hp Starter Motor
Variable Frequency Drive
5:1 Gearbox
12.5 MW Synchronous Generator
North
Lube Oil Pumps
Stainless Steel Exhaust Stack
Warehouse/Assembly Area
Instrumentation Control and Monitoring Station
- Pressures
- Flows
- Gas Analyzers
Ramgen Engine Location
Overhead Crane Area
Ventilation Blower
PLC Enclosure
Nitrogen Purge Tanks
8" Gas Line
2000 psia H_2 Trailer
12" Gas Line
1200 scfm e 100 psig Capacity
Air Compressor
Motor / Oil Cooler
Tacoma Test Site
Figure 3.1
Ramgen Power Systems, Inc.
Cad Doc. 1000-00036
Graphic Doc. 0900-00102

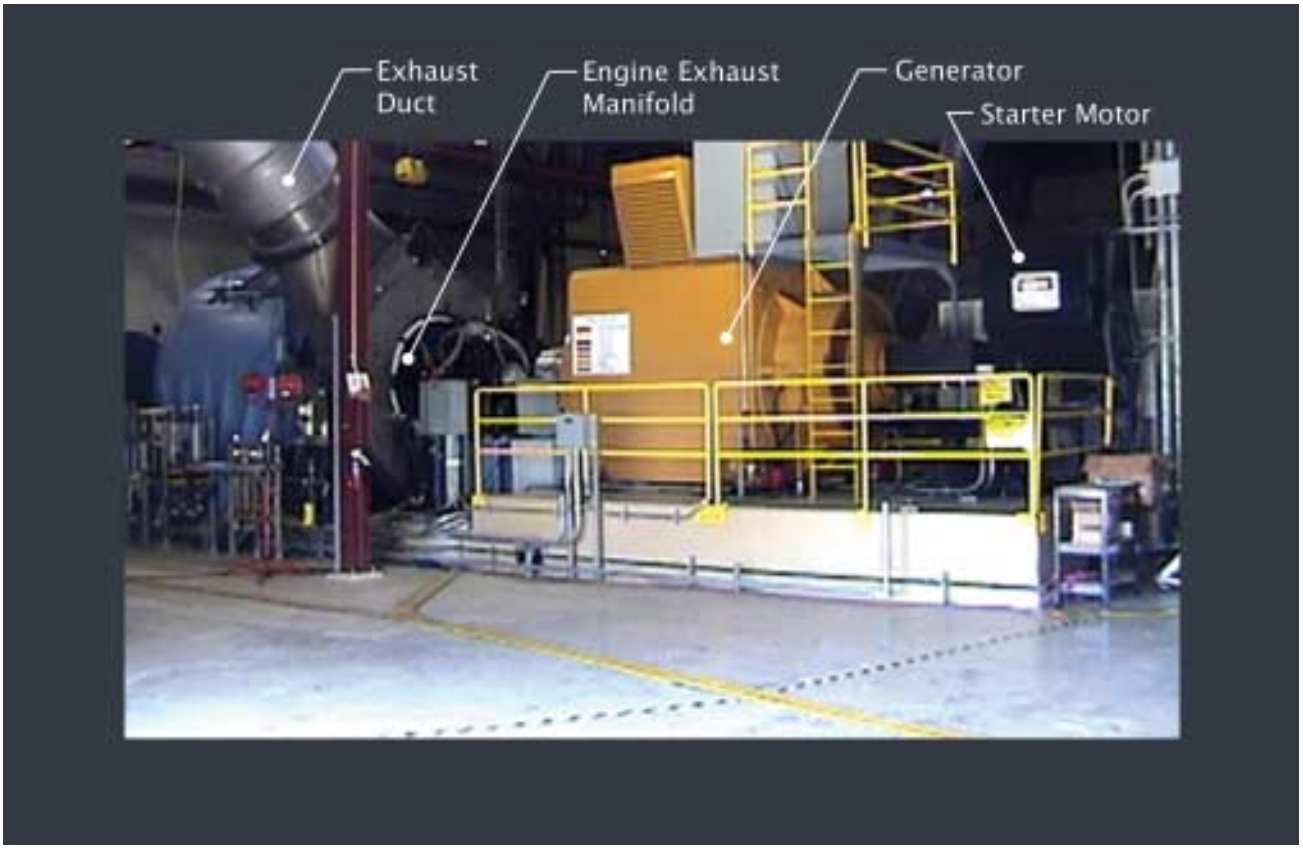

Engine and Balance of Package
Figure 3.2

Engine Prepared for Assembly
Figure 3.3

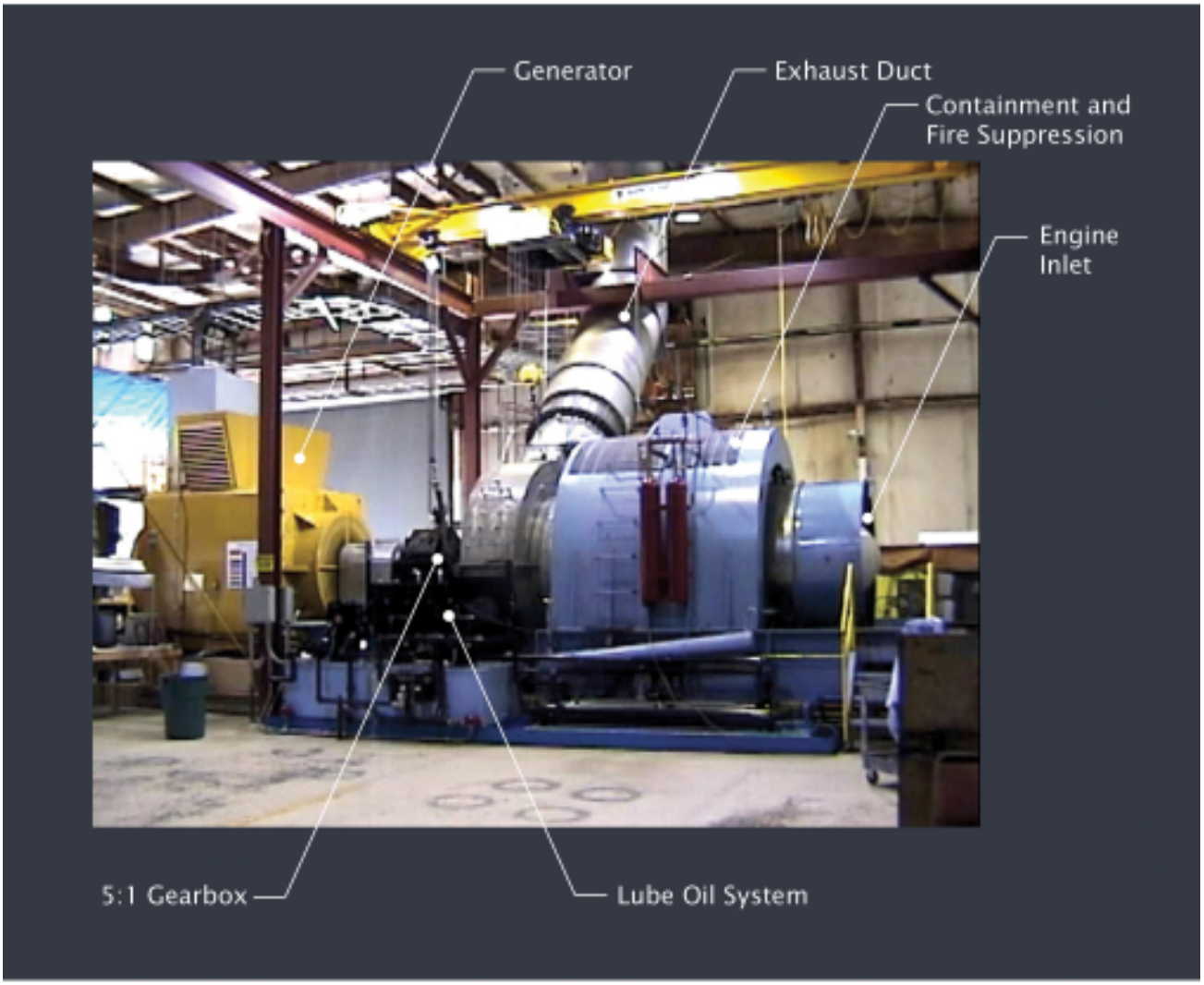

Engine and Lube Oil System
Figure 3.4

3.2 Engine Configuration

A representation of the test article is shown in figure 3.5. The major components of the Ramgen engine are the two thrust modules (ramjets) mounted tangentially on the rotor, an engine housing, an inlet duct, a primary fuel delivery system, a pilot fuel delivery system, an air film coolant delivery system, and an exhaust duct.

The engine air and fuel flow paths are shown in figure 3.6. Following these flow paths is useful for understanding the baseline engine configuration.

Ambient air is entrained at the engine inlet, shown on the far right of figure 3.6 and in 3.7. This air is not filtered or dehumidified. Inlet air passes over the bullet-nose centerbody and is accelerated by the inlet fan. The fan can be used to induce an apparent zero angle-of-attack at the thrust module inlet. A high inlet velocity also prevents flashback to the primary fuel injector struts (when the fuel injector struts are used). For consistent test conditions, the inlet fan was operated during most engine tests.

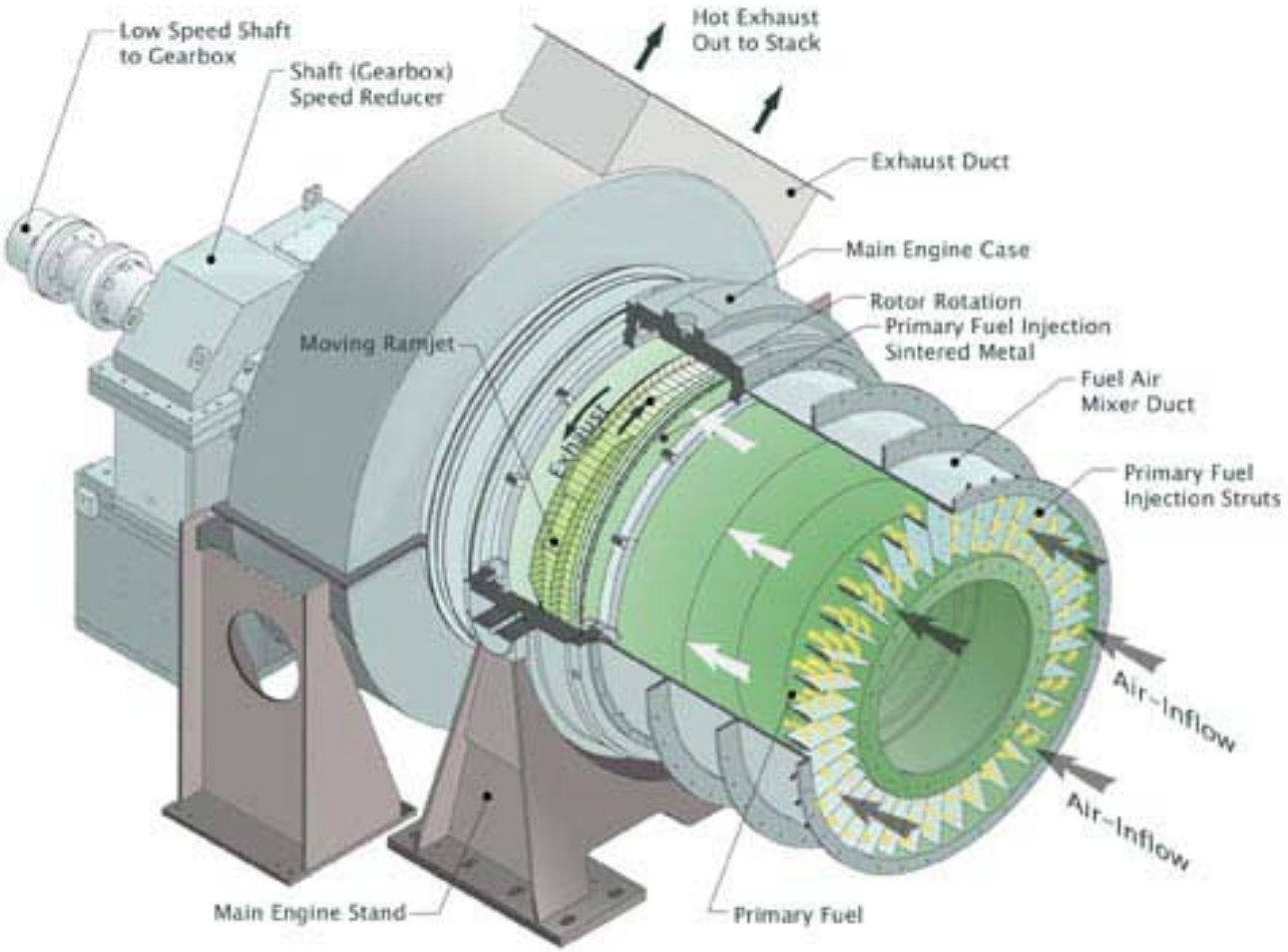

Prototype Ramgen Engine
Figure 3.5

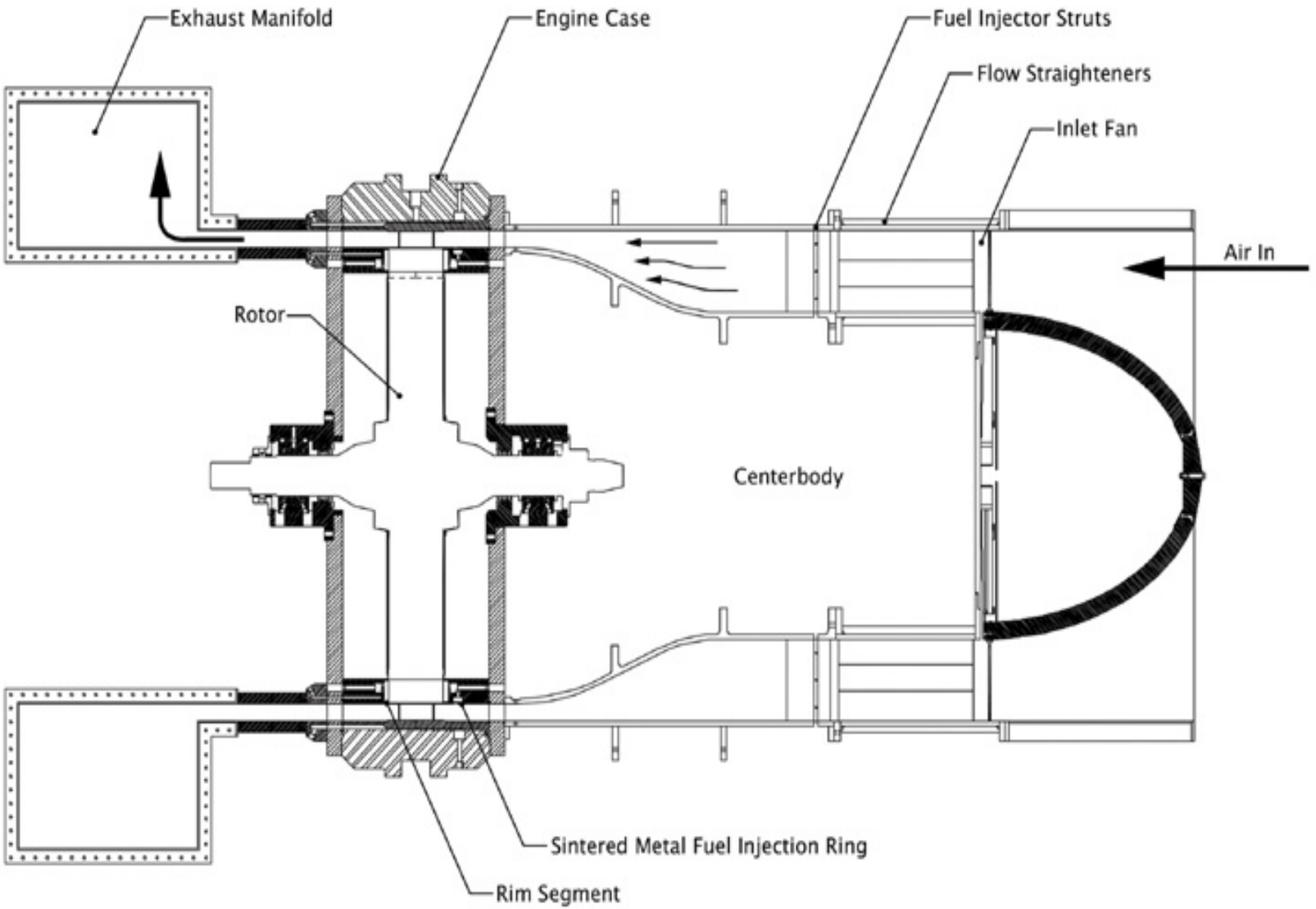

Ramgen Engine Cross Section
Figure 3.6

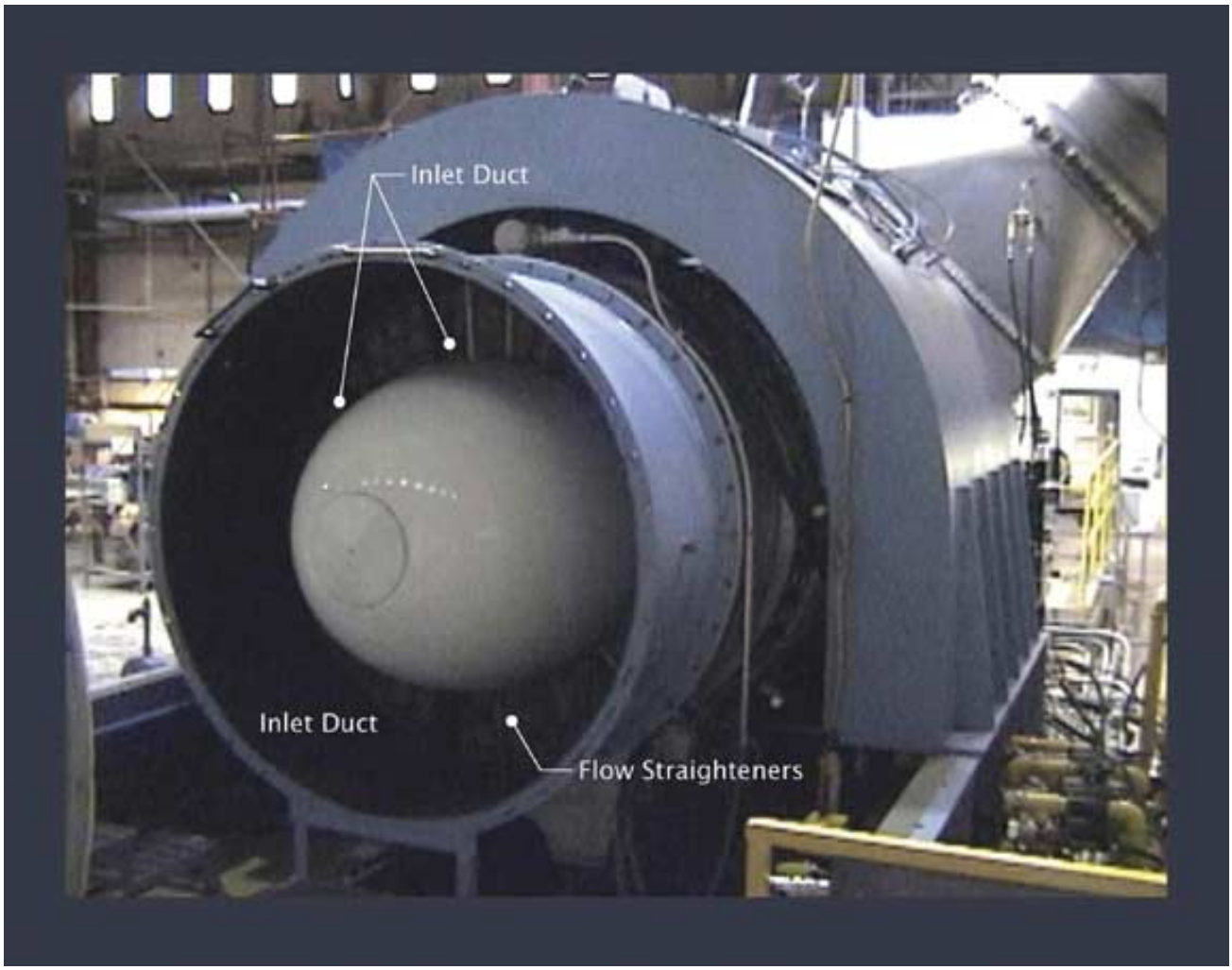

Engine Intake
Figure 3.7

Flow straighteners are installed immediately downstream of the inlet fan in order to minimize fan-induced swirl. The flow straightener array is constructed of PVC tubes 24" long by 4" diameter packed in tight groups. Tubes of 2.5" diameter and 2.75" diameter tubes are used as spacers. The array can be seen in figure 3.7.

The flow straightener array is partially restrained by the fuel injector struts, as shown schematically in figure 3.6. These hollow, symmetric NACA-airfoil struts are orificed to distribute gaseous fuel radially along the strut, and uniformly mix air and fuel prior to the thrust modules. The struts are manifolded outside the inlet housing. Fuel was not supplied to the fuel injector struts during DOE-sponsored testing.

Downstream of the fuel injector struts, the annular cross-section of the mixer duct is gradually reduced to be consistent with the flow path height of the thrust modules (2.5" nominal). The inlet centerbody is appropriately contoured to minimize flow separation, as shown in figure 3.6.

Downstream of the mixer duct but prior to the rotating thrust modules, the center body circumference is fit with a sintered metal plate mounted flush to the centerbody contour, as indicated in figure 3.6. This sintered metal fuel delivery system is discussed in detail in section 3.2.6.

The bulk flow path transforms from an axial dominated flow field to a circumferentially dominated flow field at the rotating disk. Two ramjet thrust modules are mounted on the rotor disk. Inlet gas compression, pilot fuel addition, flame holding, heat release, and thrust generation all occur along the thrust module flow path. The thrust modules and rotor disk are described in detail in section 3.2.1.

Downstream of the rotor, the hot gas is collected in the exhaust duct and vented to the roof stack. Characteristics of the exhaust and exhaust duct are discussed in section 3.2.13.

3.2.1 Thrust Modules and Rotor Disk

Tapered high strength steel discs are stacked together such that the combination of discs is 9 inches thick at the rim. There are 120 rim segments attached to the perimeter of the rotor discs, which form two complete flow paths. Note that the strake(s) of each segment are set such that the flow path is 3.05 degrees off of perpendicular to the plane of rotation, as shown in exaggerated scale in figure 3.9. This slight angle of attack results in self-pumping the engine inlet and a slight radial component to the thrust vector.

The rotor assembly turns within the stationary main engine casing such that the flow path of the ramjets is defined by the contour of the rim segments on three surfaces and the outer casing on the fourth.

A thrust module consists of three major elements: An inlet, a combustor, and a nozzle. For reference, segments making up the thrust module are numbered sequentially from 101 to 124. The first inlet segment is 101, the rear-facing step segment is 109, and the throat of the nozzle is at the end of segment 117. The details of the inlet, combustor and nozzle are described in sections 3.2.1.1 through 3.2.1.3.

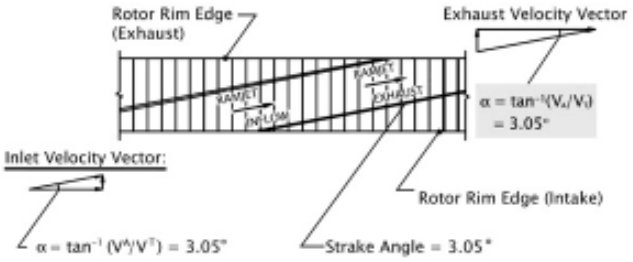

Thrust Module Helix
Figure 3.9

3.2.1.1 Thrust Module Inlet

The flow cross section is 2.5" high (measured radially relative to the rotor) and 5.2" wide (measured in the axial direction relative to the rotor). The inlet configuration used during the contract period was optimized for an inlet free stream of Mach 1.5. In order to establish a well-defined normal shock just inside the inlet, a uniform flow field upstream of the inlet is required. A dump door, or boundary layer bleed, was therefore incorporated to remove the established boundary layer formed on the upstream strake. This was accomplished by removing strakes upstream of the inlet such that a fraction of the inlet air would bypass the thrust modules and dump directly to the exhaust side. The boundary layer bleed door length was optimized prior to testing by applying CFD modeling to determine the capture stream tube.

Replaceable tip seals, starting at segment 103, minimize leakage over the stake tip. Tip seals are composed of 304 stainless steel that rub against the hardened steel (4340) engine casing at design speed, resulting in minimal sealing gap.

The cavities between inlet rim segments (i.e. below the segment floor) were modified to form a single fuel cavity by milling a passage through the web of each segment. This cavity directly feeds the fuel slot (as discussed in section 3.2.3), and is the fuel reservoir for the pylon (as discussed in section 3.2.5). Sealing of the cavity was accomplished using Hastelloy X metal strips fit into precision wire-sliced seal slots between each segment. For prototype testing, the metal-to-metal seals were augmented with high temperature silicon.

Segment pairs 106 and 107, and 108 and 109, have been modified to provide mounting locations for flame holding and mixing features. The 6061-T6 aluminum-block mounts have slots for insertion of the flame holder or mixing feature, and a passageway for retaining the feature with titanium shear pins. This method of retaining inlet features allows rapid configuration changes, as the rotor can remain in the engine case during the process. The mouning bloack is held in position by hollow steel hex-bolts when at rest, but mechanically constrained by the floor of the rim segments themselves when the rotor is spinning.

3.2.1.2 Combustor

The combustor is formed by nine rim segments. Each segment is composed of a Ni based alloy (Inconel 718) to accommodate high temperature and high g-loads. For reference, the combustor segments are numbered sequentially from segment 109, which is the location of the rear-facing step, to segment 117, which terminates at the throat of the nozzle. The combustor is 13.5" long from rear-facing step to the throat, 5.2" wide along the combustor mid-plane (measured axially relative to the rotor shaft), and 4.4" deep (measured radially, relative to the rotor shaft).

The primary flame-holding mechanism is the rear-facing step (1" tall by 5" wide) located in segment 109. The rear-facing step is augmented with an additional bluff body that increases the flame-holding volume. The bluff body (Pylon) is a changeable feature that is described in more detail in section 3.2.5.

The vertical surface of the step rear-facing step is the first location with air film cooling holes. Air film cooling orifices are distributed down the floor and walls of the combustor. A Thermal Barrier Coating (TBC) was added to reduce heat transfer to the segments and limit surface metal oxidation. Air film cooling and TBC coating is described more completely in section 3.2.2.

Limiting tip seal leakage over the thrust modules is paramount to efficient operation. Replaceable tip seals are installed from segment 103 to segment 118. Tip seals are composed of 304 series stainless steel. During full speed operation, these tip seals rub against the hardened ASTM 4340 steel engine casing, resulting in minimal sealing gap. Seals can be replaced if off-design engine operation results in excessive (momentary) seal rub.

3.2.1.3 Nozzle

The nozzle is consists of segments 118 through segment 124. Segment 118 is composed of Inconel 718 and the remaining segments are titanium. The contour of the nozzle floor was selected to expand the flow supersonically downstream of the throat without separation of the boundary layer. Note that the strakes on the exhaust side taper and open to the exhaust duct prior to an apparent recompression starting at segment 121. In January of 2001, segments 119, 120 and 121 were modified to remove the partial strakes on the engine-exhaust side of the combustor.

The rim segments have been augmented with a Thermal Barrier Coating (TBC) along the hot gas flow path. Like the combustor, the floor of the nozzle is effusion cooled. The walls of the nozzle are not air film cooled. Details of air film cooling and TBC are discussed in section 3.2.2.

3.2.2 Air Film Cooling and Thermal Barrier Coating

Effusion (air film) cooling protects the combustor and nozzle, from rim segment 109 to segment 124, starting at the vertical wall of the rear-facing step.

Air film coolant holes at the step (segment 109) are nominally 0.037" diameter and are angled at 30 degrees relative to the projected normal of the segment vertical surface, resulting in a coolant flow path complementary to the recirculation flow field direction.

Air film coolant holes continue down the floor of the combustor and through the nozzle. Nominal coolant hole size is 0.037 in. diameter, with an orientation of 30 degrees relative to the normal of the segment floor. Segment 109 to 112 floors have air film coolant holes angled forward (toward the module inlet) to be consistent with the direction of flow in the recirculation zone immediately downstream of the rear-facing step. Segments 113 through 124 AFC holes are angled back (towards the thrust module exit) to be consistent with the bulk flow field.

Additional air film coolant orifices line the walls of the combustors and are angled (30 degrees relative to normal) toward the dominant flow direction.

Both floor and wall air film cooling orifices are fed from the cavities formed between adjacent rim segments. Cooling air is supplied to the cavity between each pair of segments via two ¼" diameter holes through the lug of the dovetail. Each dovetail is supplied from a common reservoir fed from the exhaust side of the engine. The air flow distribution in the combustor can be field-modified by changing the blockage between the air cooling reservoir and an individual cavity.

Sealing of the cavity was accomplished using Hastelloy X metal strips fit into precision wire-sliced seal slots between each segment. The metal-to-metal seals were augmented with high temperature silicone

Thermal barrier coating (TBC) was applied to the combustor and nozzle rim segment surfaces that were exposed to hot combustion gasses. The coating was a composite application consisting of a bond coat layer of Metco 461 (nickel chromium-alumina-cobalt-yttria composite) and a ceramic coat layer of Metco 204NS (yttria stabilized zirconia).

3.2.3 Pilot Fuel/Fuel Slot

A reliable pilot combustion mode is required for ramping to full speed and idle. This requires precise fuel delivery to the flame-holding region of the combustor. To accomplish this, pilot fuel is supplied to the combustor from the fuel slot located at the interface of segments 107 and 108 in the thrust module inlet.

An insert plate attached to the 108 segment controls the fuel slot width. This insert plate can be removed from the fuel cavity and replaced without disassembly of the rim segments. Hence, field modification of the fuel slot geometry can be performed routinely.

The thrust modules were modified in February 2001 to accommodate the pylon flame holder. The pylon flame holder (discussed in section 3.2.5) is fed pilot fuel from the common fuel cavity via a ½" diameter hole drilled in segment 108 immediately downstream of the fuel slot. Note that the fuel insert plate is still used control the slot geometry, and is modified to provide a fuel flow path to the pylon, when installed.

3.2.4 Fuel mixing Vortex Generators

The inlet diffuser was designed such that features could be installed between the fuel slot and rear facing step, and upstream of the fuel slot. In most tests, only the downstream mounting location was used to hold mixing features.

Vortex generators were tested extensively. These devices were designed to enhance mixing between fuel injected via the fuel slot and free stream air, prior to entering the recirculation zone maintained by the rear-facing step.

Three titanium vortex generator configurations were tested in the contract period. All were fabricated with the same layout relative to a view looking in radially, but the height of the vortex generators were varied. The basic configuration consists of three pairs of zero-camber airfoils, fabricated such that the angle of attack relative to the free stream is the mirror image of the opposing air foil. Due to the high angle of attack, these airfoils were likely stalled at high rotor speeds.

The 3/8" tall vortex generators were designed for minimal mixing of the fuel layer and air free stream prior to the rear-facing step. Using ¾" tall vortex generators, the airfoil was made slightly thicker (.10") to ease manufacturing, and has a chamfered leading edge. A 1.5" tall vortex generator, was installed between the fuel slot and the rear-facing step. Like the ¾" set, the airfoil is chamfered to minimize flow separation. The 1.5" vortex generators induced the greatest mixing of the free stream air with the pilot fuel.

3.2.5 Pylon Flame Holder/ Fuel Injector

Enhanced flame-holding was investigated by adding a bluff body feature at the rear facing step. A pylon was designed to enlarge the recirculation zone formed behind the rear-facing step, increase the shear layer surface area, and increase fuel mixing by direct injection of fuel into the flame holding region. Tests were performed using the pylon with four different fuel injection plates.

The pylon is mounted just upstream of the rear-facing step, such that the fuel injection plate is coplanar with the rear facing step. The fuel cavity feeding the pilot fuel slot also feeds the pylon, via a ½" diameter hole immediately downstream of the fuel slot. During testing of the pylon, the fuel slot gap was .07", such that a fraction of the pilot fuel was ejected from the fuel slot and a fraction was ejected from the pylon fuel injection plate.

The pylon is a hollow titanium bluff body 2.5 inches tall and 1 inch wide. The pylon is secured to the thrust module with mounting lugs (identical to the vortex generator mounting lugs, as discussed in section 3.2.4) and with four additional ¼" bolts.

Note that the fuel injector plate can be removed and replaced in order to evaluate different fuel injection patterns. These Hastelloy X plates are TBC coated, machined to the desired fuel injection pattern, and secured by hastelloy screws and retaining clips.

Four fuel injection plate configurations were tested during the contract period. Hole size, number and location were varied in order to influence mixing and flame-holding.

A configuration with a single 1/8" hole in the lower half of the fuel injection plate was tested. This was the minimum fuel injection configuration tested with the pylon. The flow area split between the fuel injector plate hole and the fuel slot was 5% versus 95%. Tests conducted with this plate evaluated the pylon as a bluff body flame holder, independent of significant fuel feed. In figure Inj1, the retaining clips and Hastelloy bolts are visible.

A fuel injection plate was tested with a ½" diameter injection port. This configuration was designed to capitalize on the radial pumping along the face of the fuel injection plate, inducing rapid fuel mixing. The fuel flow area is split approximately 40% of the fuel through the pylon fuel injection plate, and 60% through the fuel slot.

A configuration with maximum flow area at the faceplate consisted of five ¼" diameter holes distributed a the top of the plate and one 15/32 inch diameter hole at the bottom of the plate resulting in a 60% / 40% area split between the hole patterns.

Tests were performed using a fuel injection plate with a hole pattern consisting of two rows eight holes of 1/8" diameter distributed on the perimeter of the plate. This mixing pattern was designed to capitalize on discrete mixing at each hole via shearing induced by the fuel jet momentum, and shear mixing at the perimeter of the injection plate. This hole pattern has 47% less flow cross-section than the maximum flow design and the same flow area as the ½" diameter hole design.

3.2.6 Sintered Metal Fuel Flow Path

During the contract period, fuel was introduced to the thrust modules through two pathways: The pilot fuel pathway, described in section 3.2.3, and upstream of the rotating disk, through a sintered metal ring.

This fuel feed system was designed to create a stratified flow field, with fuel close to the center body, prior to crossing over to the rotor. A sintered metal fuel feed system was selected because the fuel jet velocity (perpendicular to the bulk air flow vector) is negligible compared to alternative injection methods.

Fuel is routed to a ring manifold in the engine centerbody. From the manifold, fuel is fed through the bearing plate to a circumferential groove cut into the intake-side rotor housing. The open side of this groove is separated from the flow path by a sheet of stainless steel sintered metal. The sintered metal porosity was carefully selected to promote a uniform discharge of pressurized fuel.

Some mixing due to boundary layer growth and strake pumping is expected prior to entering the combustor, in contrast to fuel introduced through the fuel slot or pylon (discussed in sections 3.2.3 and 3.2.5, respectively). Most tests in the contract period focused on the use of the fuel slot and/or the pylon.

3.2.7 Wheel Space Purge and Safety Gas Analyzers

Wheel space purges were used to prevent entrainment of combustible gas mixtures on the intake side of the rotor, and limit ingestion of combustion byproducts on the exhaust side of the rotor. The stationary rotor housing and bearing plate, and the spinning rotor, define the wheel spaces.

On the intake side, two sets of nozzles are installed on the interior of the bearing plate at 28.625 inches and at 46.125 inches diameter. Six nozzles on the smaller diameter are directed at 45 degrees relative to the engine primary axis, towards the shaft. Six pairs of nozzles on the larger diameter are aligned tangent to the installation diameter, one in the

clockwise and one in the counterclockwise direction, and directed 45 degrees from the tangent line toward the rotor.

On the exhaust side, a single set of 6 nozzles is installed on the interior of the bearing plate at 28.625 inches diameter. The nozzles are directed at 45 degrees relative to the engine primary axis, towards the shaft.

Wheel space temperature, pressure and gas composition are monitored continuously during test. Both intake and exhaust wheel space temperatures are sampled at the rotor labyrinth seal and on the bearing plate. Wheel space pressures are sampled through the bearing plates at 37.875 inches diameter. using a Noshok 100-30/15-1-1-2-6 pressure transducers. Gas samples, from the wheel spaces, are analyzed using CEA Instrument gas analyzers, CEA-428-100% LEL. Redundant gas analysis is performed with Drager Multiwarn II portable gas analyzers. Gas readings for both analyzer sets are recorded as % of the Lower Explosive Limit (LEL) of methane.

3.2.8 Water Coolant System

The water coolant system cools the engine case and the lubrication oil. A flow schematic is shown in figure 3.31. Two 175 gallon-per-minute pumps supply water from the 400 gallon reservoir to a three station manifold. At the manifold, the flow is distributed by manual needle valves and monitored by Hedland HB-111-115 flow meters. The manifold feeds the lube oil system heat exchangers, the external engine casing and the internal engine casing.

Water routed to the lube oil system flows through two shell and tube coolers plumbed in series. The system is configured to keep the lubrication oil below 120 °F.

Water for cooling the external engine casing is routed to a 12-station manifold and then distributed to an annular channel at the intake side of the main engine case. The channel feeds 120 axial passages formed in the rotor cooling jacket, the exhaust bearing plate and the external exhaust ring. Flow in these passages convectively dissipates heat from the external side of the combustion and exhaust passages. In the external exhaust ring, a second annular groove directs return water flow to 12 circumferential ports, which feed to a ring manifold and the return water line.

Water for cooling the internal engine casing is routed through a pair of six station manifolds on the exhaust bearing plate. Radial passages cut through the 12 webs on the bearing plate intersect 12 of 120 annular passages in the bearing plate and the internal rotor housing. An annular groove in the internal rotor housing (beneath the exhaust side rotor labyrinth seal) connects the feed passages with the return flow passages. Return water flows through the internal rotor housing and through the bearing plate, then collects in an annular groove in the internal cooling ring. Twelve ports tap this groove and route return water to a 12-station ring manifold. This ring manifold dumps the heated water to the water return line.

All return water lines feed water into a forced air, multi-pass heat exchanger. Four fans force ambient air through a radiator bank prior to returning the coolant to the reservoir. At full engine operation, the heat exchanger is designed to reduce the return water temperature to levels below 115 °F.

3.2.9 Lube Oil System

The lube oil system provides lubrication and cooling for the starter motor, generator, gearbox and engine bearings. A flow schematic is shown in figure 3.32. Mobile DTE 724 Oil is collected in a reservoir and distributed by one of a pair of 90 GPM pumps. Oil leaving the reservoir for distribution passes through a pair of shell and tube heat exchangers. A portion of the water in the water coolant system chills the oil in the coolers to a temperature below 120 °F. A Watlow ABJ000A40UJ200, J type, thermocouple and a Data Instruments XPRO 200 PSI pressure transducer, monitors oil temperature and pressure at a manifold, upstream of the coolers. The manifold is a bank of manually set needle valves controlling the bearing oil flow rates. Each flow is monitored by Hedland H641 or H741 flow meters, depending on range. The engine guide bearing is fed at the exhaust bearing housing by a one inch hose. The thrust bearing is fed by a one inch

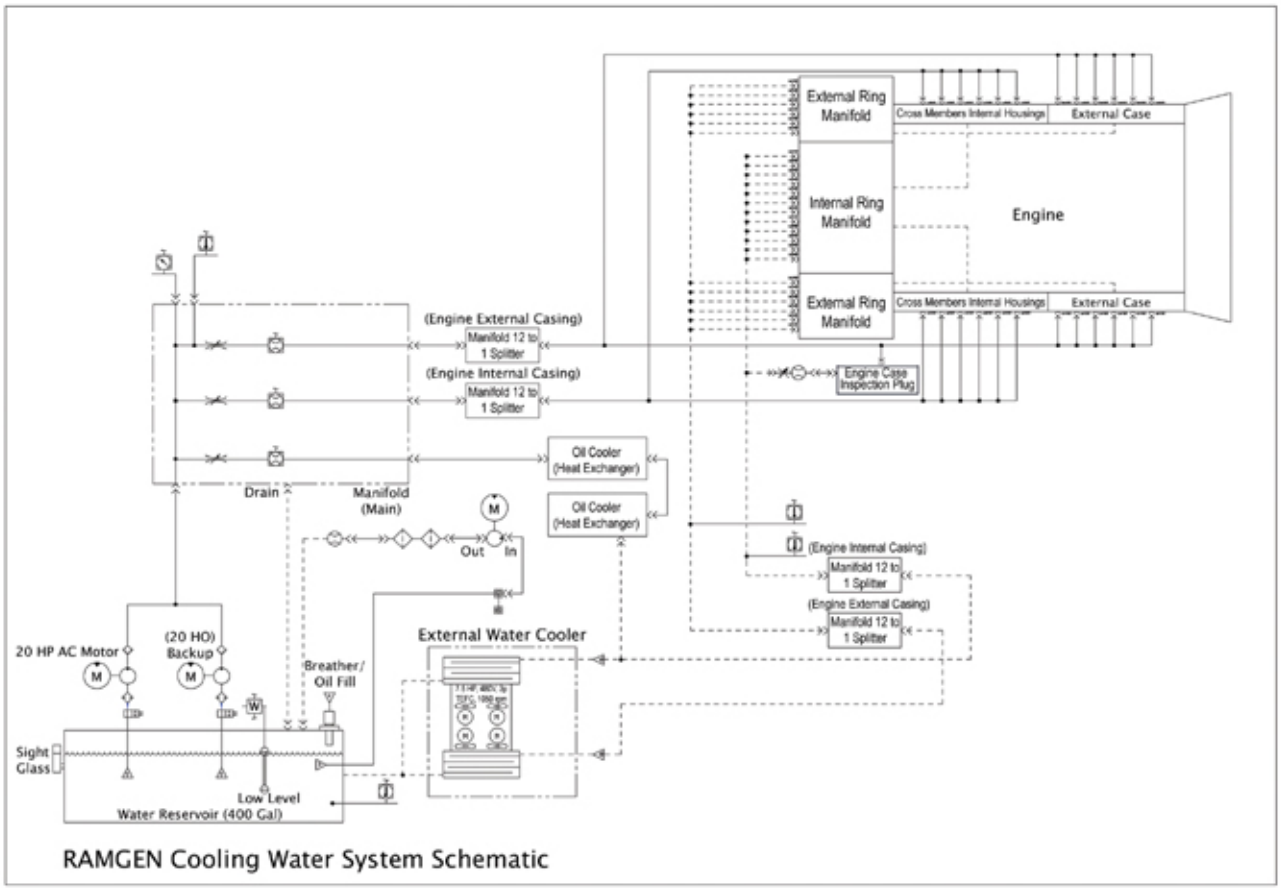

Ramgen Cooling Water System Schematic
Figure 3.31

hose at the intake bearing housing through the intake fan housing, the engine strut and the centerbody. Oil is collected in a six gallon reservoir on the underside of each bearing housing and gravity fed back to the reservoir. If the gravity feed is overwhelmed, pneumatic oil flow assist pumps, controlled by internal float switches, assist in emptying the oil reservoirs.

The control system cycles between the two primary pumps with each engine start. This dual oil pump scheme allows for life extension of both primary lubrication pumps and motors and for in operation service to one of the pumps. A third emergency shut down pump is also installed to protect the engine in the event of a power failure. This 45 GPM pump driven by a 5 HP DC motor provides the minimum oil flows required to allow the rotor to safely free spin from design speed to rest while operating on the facility's uninterruptible power supply.

3.2.10 Natural Gas Supply

The baseline fuel for engine testing was natural gas, which is supplied at 25 psig by the local gas distribution network. Natural gas in the Puget Sound region is typically >95% methane, with some higher hydrocarbons. A flow schematic is shown in figure 3.33.

The engine test facility is supplied by a six inch supply line with a fail-safe pneumatic on/off valve and a filter. The line is split to a six inch line (which feeds the pilot fuel system) and an eight inch line (which feeds the sintered metal fuel

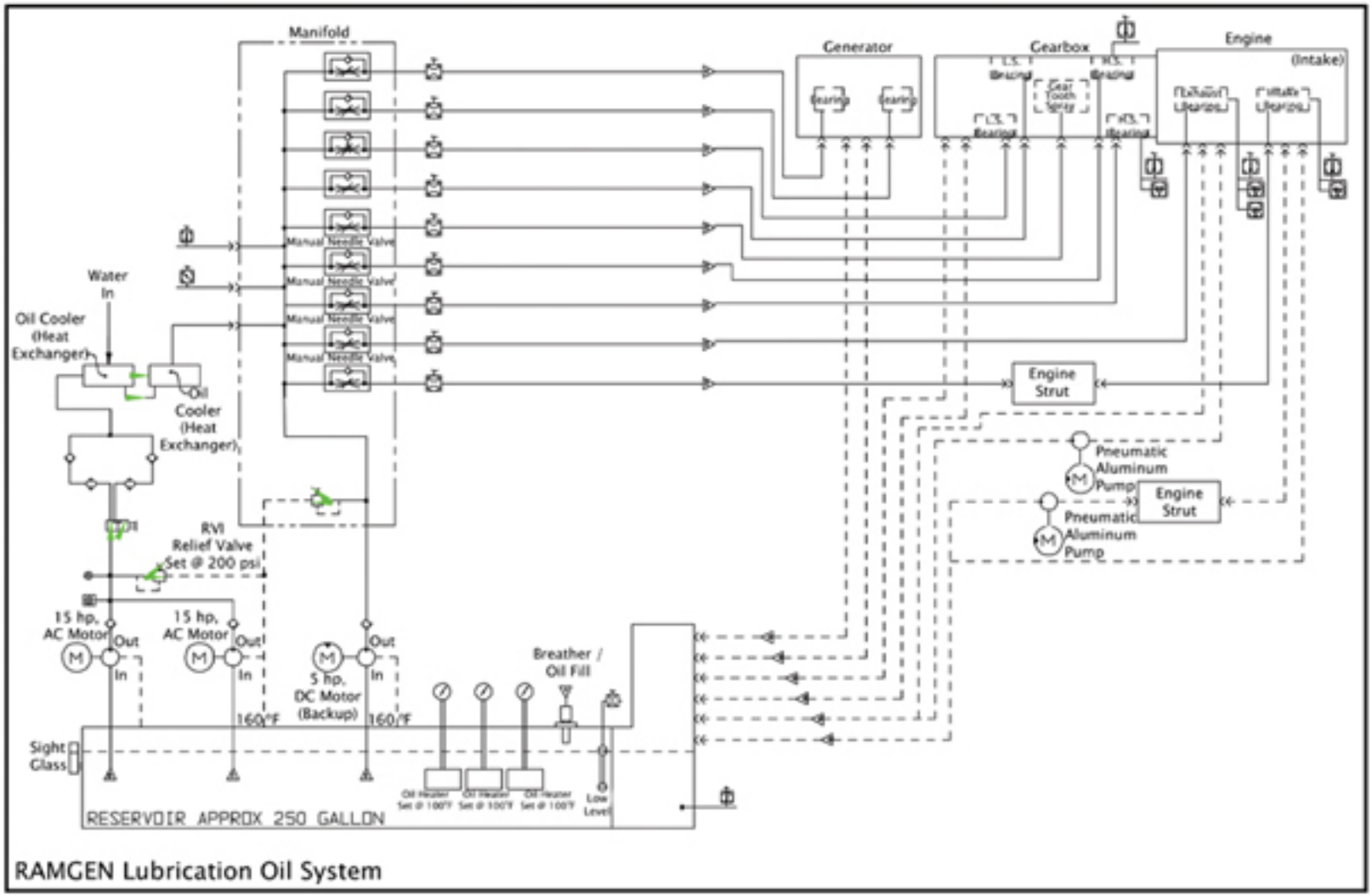

Ramgen Lubrication Oil System
Figure 3.32

system). Gas flow is monitored by a Miners & Pisani OVP-100 flow meters on each line.

Following the pilot fuel line, natural gas is routed through a fail-safe pneumatically actuated on/off valve, a turbine meter (Sponsler SP1-1/2-CB-PH12-B-4X, range of 8-130 ACFM +/-1% accuracy), and a control valve (Worchester Controls 20-755W). Feedback from the turbine meter is used for valve control. A rotometer is plumbed into the fuel line between the control valve and the engine interface for manual fuel flow verification. Downstream of the rotometer, a check-valved H2 feed system allows for the blending of hydrogen into the natural gas stream.

Like the pilot fuel leg, the sintered metal fuel leg is routed through a fail-safe pneumatically actuated on/off valve, a turbine meter (Sponsler SP2-CB-PH12-B-4X, range of 15-250 ACFM, +/- 1% accuracy), and a control valve (Worchester Controls 20-755W).

Fuel system nitrogen purges are designed into the control logic of the system. See figure 3.34. The sintered metal and the pilot fuel can be operated independently or controlled simultaneously using gas-off or full-stop commands. During a normal gas-off purge, the actuator valve closes, the control valve opens to 25% and a solenoid valve on the nitrogen line actuates. The solenoid introduces nitrogen into both fuel lines upstream of the actuator valve. Nitrogen flows through the feed line and the engine components before venting into the exhaust duct. These fifteen second nitrogen purges are initiated by closing system valves, so only active fuel lines are purged. When a full stop is commanded, a 90 second purge of the premix natural gas line occurs regardless of prior fuel flow conditions. During these purges the hydrogen system is protected from over-pressurization by a check valve and by a normally closed diverter valve.

3.2.11 Hydrogen Supply

Some testing was conducted with hydrogen blended into the natural gas. An independent hydrogen supply system was developed for accurate and safe delivery of hydrogen through re-routable pathways. The hydrogen delivery system is shown schematically in figure 3.35, and is described below.

A 25,104 cu ft hydrogen trailer is isolated from the test facility by a manual plug valve, a fail-safe actuator valve, and thirty feet of stainless steel tubing. Auxiliary ports in the supply system allow K-size bottles to be used when a hydrogen trailer is not available. Manual bleed valves can be opened to vent the trailer or the downstream lines. Inside the facility, the high pressure line is routed to a panel that supports the majority of hydrogen control and metering hardware.

Hydrogen, supplied to the facility at 2500-1000 psig by the 1 in. main line, is branched to two independent control and metering legs. A manual ball valve protects each branch system from rapid pressurization by the main line. Following a leg, hydrogen is routed through a high pressure gas regulator (Oxyweld R2327, 300-75 psig discharge), a fail-safe actuator valve, redundant turbine meters (Omega FTB-935, 2.5-28 ACFM, +/-1% of reading), and an Automax 61236 AT flow control valve. From the control valve, the hydrogen line is plumbed to the natural gas line just prior to entering the engine.

Engine testing is typically performed using fixed valve position flow control on the Hydrogen system. Experimentally predefined valve positions or ramps are utilized to meter fuel delivery. In both cases the control valve position is monitored by the valve supply current and by the valve shaft position. Downstream of the control valve, hydrogen is routed to the engine's pilot and/or sintered metal natural gas supply line through a diverter valve, which is open only while the hydrogen system is active.

The hydrogen system has an integrated nitrogen purge, which is automatically initiated whenever hydrogen flow is commanded off. During a nitrogen purge, both the fail-safe actuator valve and the diverter valve close. The flow control valve opens 25%. A solenoid valves introduces 30 psig nitrogen gas into the fuel line between the flow control valve and the elastomer delivery hose. With the diverter valve closed, the flow path is rerouted from the methane line to the exhaust stack. This action allows the nitrogen charge to push the hydrogen from the hose into the exhaust stack rather than

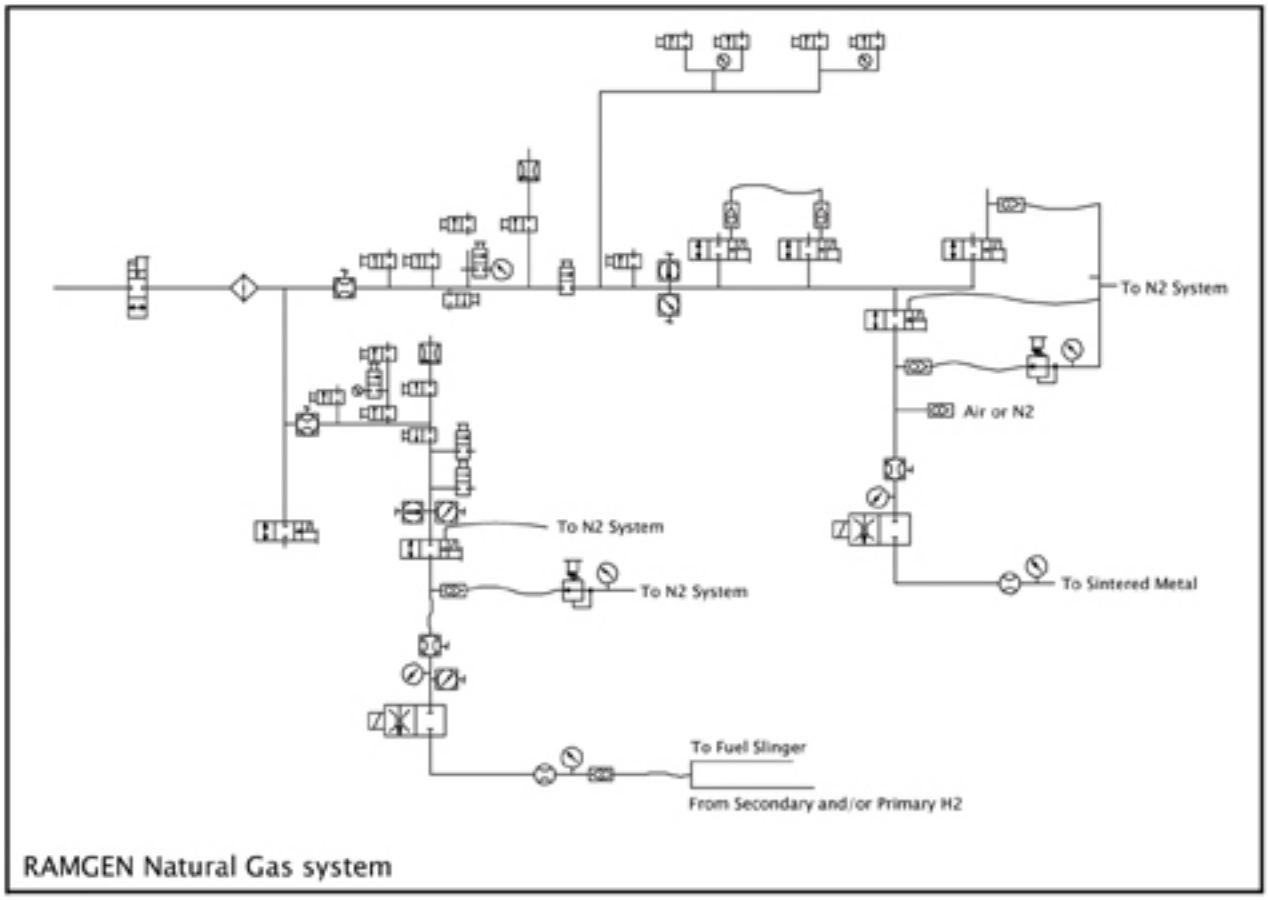

Natural Gas System
Figure 3.33

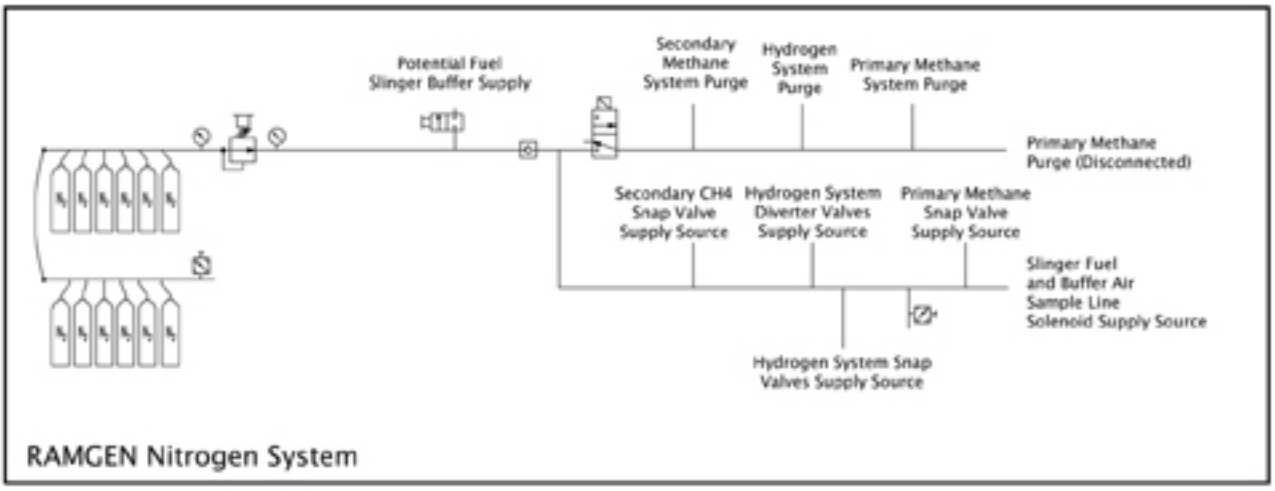

Nitrogen System
Figure 3.34

through the engine. A third solenoid valve opens a bottle fed, 30 psig, nitrogen line between the actuator valve and the control valve. The nitrogen pushes the hydrogen through the partially open flow control valve and into the exhaust stack. The pilot and sintered metal hydrogen lines have identical purge systems.

Additional handling precautions are taken to protect the hardware and personnel. A combustible gas detector and thermocouple are mounted inside the control panel hood to detect a hydrogen leak or a potential hydrogen fire. An automated gas-off and purge sequence is initiated for gas concentrations or temperatures out of acceptable limits.

After full-stop, the hydrogen system is manually vented to the atmosphere outside of the facility. Lines inside the building are vented by manually operating four pressure relief valves. During operation these 350 psig relief valves protect the plumbing between the regulator and the control valve from over pressurization. The vent lines attached to these feed lines are fed a continuous low pressure nitrogen purge.

3.2.12 Engine Inlet

The engine inlet has the dual function of directing intake air flow and providing a mixing volume for fuel and air at design speed operation. Interior components provide routing structure for fuel, seal, and purge gas plumbing.

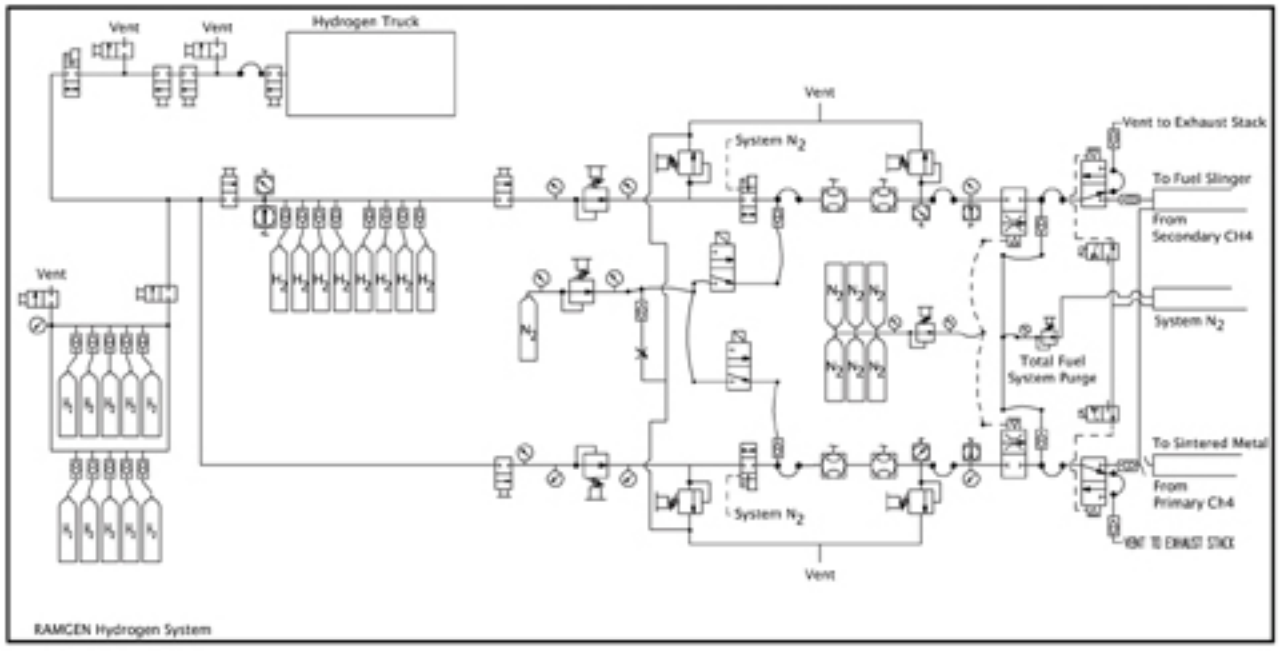

Hydrogen System
Figure 3.35

The inlet flow path is defined by the six -foot diameter inlet housing and by the elliptical fan nose, a straight section of 4 ft. diameter ducting, and the contoured centerbody element. At the rotor face, the annular constriction matches the flowpath height (2.5”). A 20 HP fan mounted between the elliptical nose and the 4 ft. diameter ducting controls low rotor speed air in-flow rates.

Fuel, air, and oil lines are routed through the centerbody via hollow support struts.

Inlet conditions are monitored by a pitot tube and temperature sensor at the constant cross section area feeding the rotor, ten inches upstream of the combustor inlet.

3.2.13 Exhaust Duct and Exhaust Gas Sampling

Exhaust gases, expelled by the helical strake rotation, are directed to the stainless steel exhaust collector, as shown in figure 3.36. From the collector, combustion products are vented to the roof through a 4 ft. diameter exhaust stack.

A stainless steel liner (0.062" thick) was added to the center of the exhaust collector in order to protect hydraulic lines from radiative and convective heating, as shown in figure 3.36. This liner is suspended 3" from the interior of the collector, and insulated with 1.5" Inswool–HP ceramic fiber blanket.

Combustion products are sampled from the center of the transition element connecting the exhaust collector and the exhaust stack, as shown in figure 3.37. Sampling and analysis are performed with an ECOM AC portable gas analyzer. This is a continuous sample unit, with an integral pump and water catch. Installed gas analysis sensors and ranges are listed in Table 3.1. The seven sampled parameters are recorded at 2 second intervals during engine testing.

Measured Parameter	Sensor Type	Range	Accuracy	Resolution
Oxygen, O_2	Electrochemical	0-21%	2% of reading	0.1%
Carbon Monoxide, CO	Electrochemical	0-4000 ppm	2% of reading	1 ppm
Nitric Oxide, NO	Electrochemical	0-4000 ppm	2% of reading	1 ppm
Nitrogen Dioxide, NO_2	Electrochemical	0-500 ppm	2% of reading	1 ppm
Combustibles, C_xH_y	Pellister	0-6%	2% of reading	0.01%
Ambient Temperature	IC Sensor	0-250°F	3 Degrees	1°F
Stack Temperature	Type K Thermocouple	0-1600°F	3 Degrees	1°F

Gas Composition Monitoring
Table 3.1

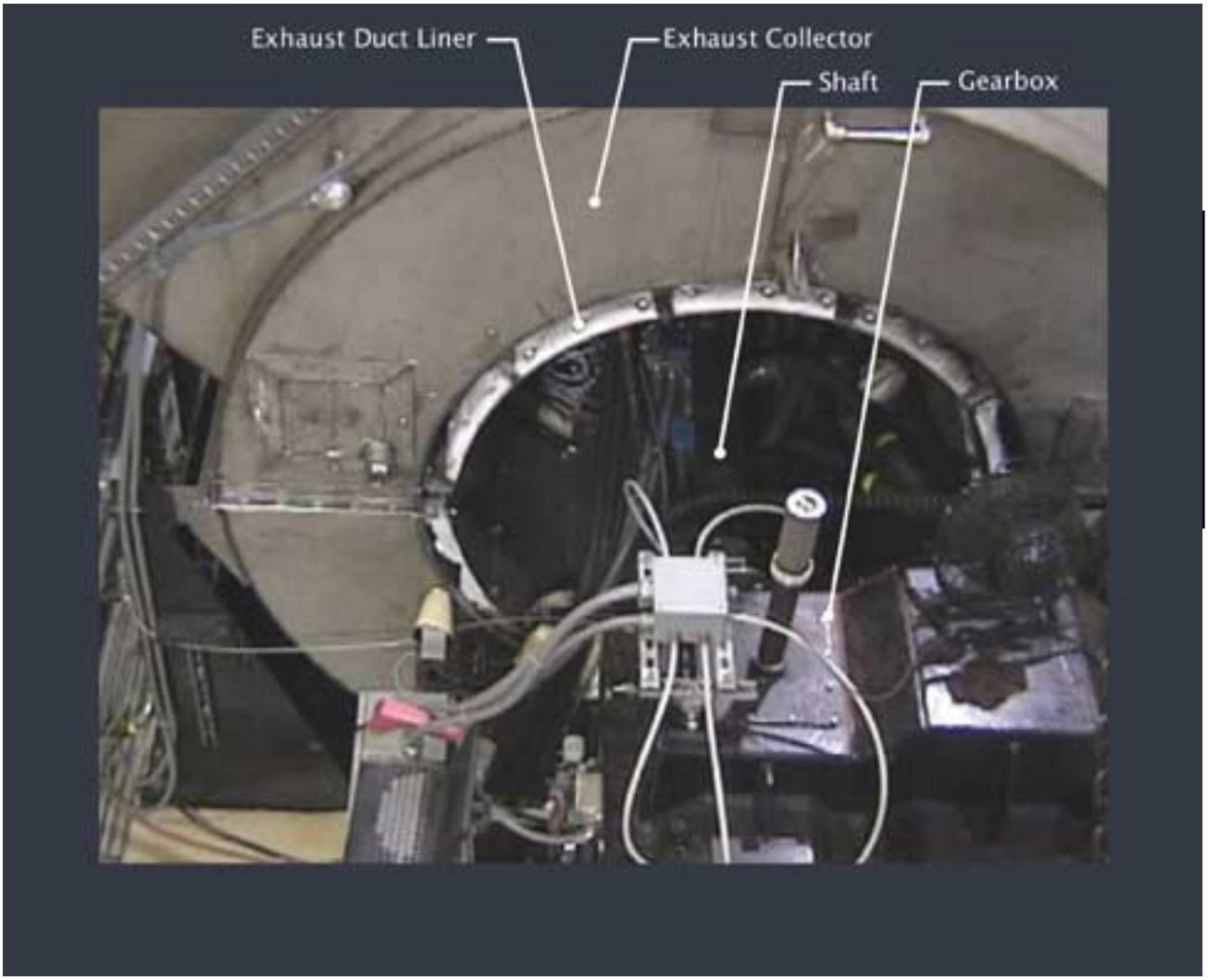

View of Exhaust Collector From Above
Figure 3.36

Exhaust Duct and Engine Case
Figure 3.37

3.3 Control and Diagnostic Equipment

Tests conditions are controlled remotely with the Supervisory Control and Data Acquisition (SCADA) system. A schematic of the integrated engine and control system is shown in figure 3.40. The SCADA system interfaces with a standard programmable logic controller (PLC), with one remote I/O rack in the Motor Control Center and with another in the switchboard in the POC engine control room. The main PLC rack also monitors the vibration and shaft position sensing equipment. The entire control system is powered by an uninterruptible DC power system and can therefore operate without utility power.

Instrumentation monitored by the SCADA system includes a full Bentley-Nevada vibration and shaft position monitoring system, Land infrared temperature monitoring equipment, gas composition analyzers, pressure, temperature and flow measurement equipment. The SCADA system is used to continuously record these engine data for control room display and to archive the data for post-test review at a sampling frequency of 1 Hz. The control room is also equipped with a high speed data acquisition system capable of 1 MHz capture. This system is used to monitor combustor temperature, combustor pressure, inlet strake temperature, exhaust strake temperature, and fuel pressure oscillations.

3.3.1 SCADA Interface Screens

Primary engine control and monitoring is performed through the SCADA system using a custom operator interface. The operator can interact with the engine through any of a dozen control screens:

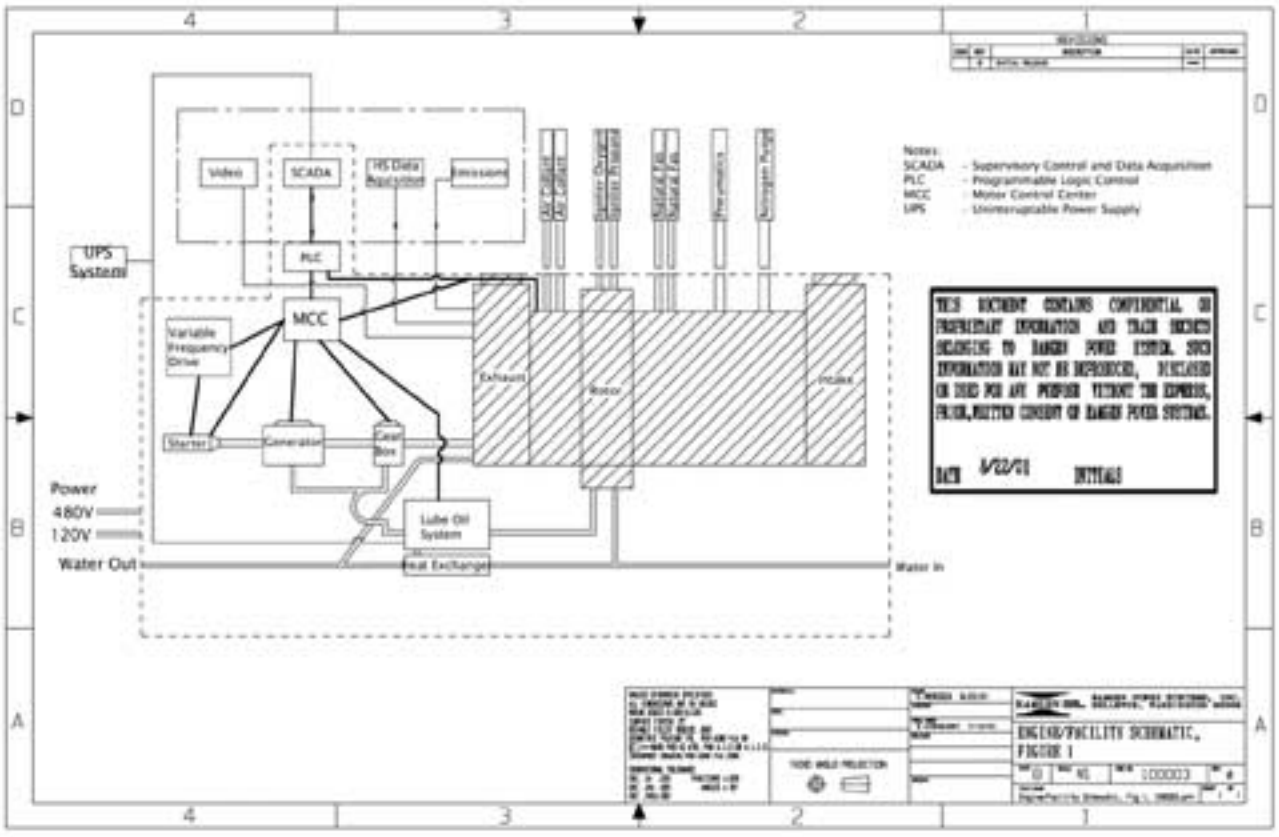

Engine Controls Schematic
Figure 3.40

Alarm Screen

The alarm screen reports violations and related control actions resulting from operation outside of pre-defined limits. An expected operating range is established for each sensor upon its installation. Control system actions for operation outside of this range are also assigned. Typical actions are operator warning display and engine gas-off.

Bearing Screen:

The bearing screen (figure 3.41) is predominantly a report screen. Vibration, lubricant flow rate and lubricant temperature can be monitored for the generator, gearbox and engine bearings. In-flow and return lubricant temperatures in the reservoir, lubricant system in-flow pressure, engine speed, rotor proximity sensor output and lubricant pump operation are also indicated on this display. The sole interactive feature is a control button which allows direct operation of the DC lubricant pump for testing purposes.

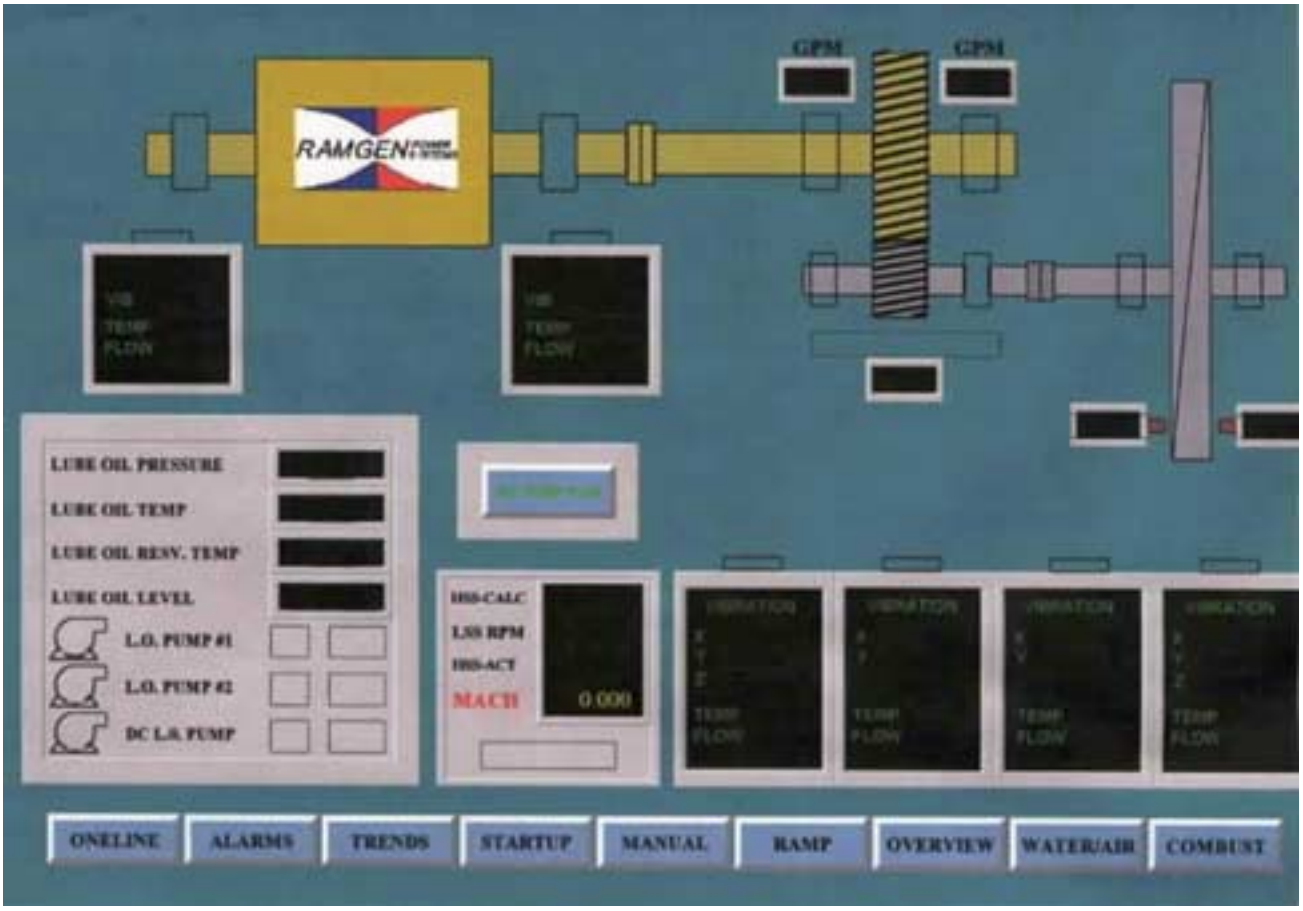

Bearing Screen
Figure 3.41

Test Director Screen:

The test director (figure 3.42) screen is an operation overview report screen. Engine speed, variable frequency drive power, exhaust gas concentration, rotor temperatures, fuel flow conditions and air flow conditions are displayed directly. Additionally, values for fuel flow rates (SCFM), gas concentrations by volume and mass, and BTU value of the combustion gas are calculated and displayed.

Test Director Screen
Figure 3.42

Combustion Screen:

The combustion screen (figure 3.43) is the primary operator/engine interface during non-ramping operation (see the Ramp screen for more information). Through this screen primary and secondary natural gas and hydrogen systems can be activated, and fixed or loop valve control can be selected for the hydrogen system. Based on these selections, the appropriate input boxes for premix and pilot natural gas and hydrogen flow rates will be activated in addition to air film cooling regulator pressure and flow rate controls. The set point input boxes are displayed directly below the actual flow report boxes. Report boxes for combustor floor and strake IR temperatures, exhaust duct temperatures, exhaust duct differential pressure, fuel source pressures, fuel valve positions, rotor proximity sensor output, rotor speed, variable frequency drive power, and exhaust gas composition assist the operator in assessing the combustion process. A trend graph displays information regarding the exhaust duct temperature, the combustor floor IR temperatures, the fuel flow rates and the fuel differential pressure. Current date, current time and run duration are displayed.

Combustor Screen
Figure 3.43

Manual Screen:

The manual screen (figure 3.44) allows the operator to alter some common engine operating parameters without changing the PLC ladder logic. This group is composed predominantly of ignition parameters, gas purge parameters, and commonly altered warning and gas-off conditions. Buttons toggle the ignition system power, ignition system gas supply, ignition system timing light power, ignition blast and ignition blast suppression. Ignition system pre-ignition time, igniter fill time, and fire delay time, fire duration, and igniter pre-purge time can be altered from this screen. Manual operation of the ignition and the hydrogen systems are found on this screen. The delay and duration for this hydrogen purge and for the pilot and premix natural gas line purges can be altered. Flexibility in the delay duration is necessary to account for valve closure response time. Duration changes ensure a thorough purge. Settings can be entered for gas-off wheel space concentration, bearing purge, air film cooling labyrinth seal pressure, air film cooling labyrinth seal temperature, exhaust duct temperature, exhaust gas concentration, 90 degree combustor temperature, 45 degree combustor temperature, air film cooling air temperature, and fuel differential pressure values. Warning values for wheel space gas concentrations can be changed on this screen. A counter, indicating the number of times the engine bearing, oil assist pumps are activated, is displayed (pump action is initiated by a float switch in the oil reservoir). Set points for initiation of the differential fuel pressure boost are on this page.

A manual data trigger button is also found on this screen. Normal data post processing extracts operational data for hot run engine conditions, based on the 90 degree IR combustor temperature. This override button applies the appropriate bit toggle to facilitate cold data capture.

The final block on the manual screen controls the position of two solenoid valves. The valves are used to open gas sample lines to two Drager portable gas analyzers. The analyzers remotely sample wheelspace, oil vent, pilot fuel, and buffer air gases.

Manual Screen
Figure 3.44

Oneline Screen:

The oneline screen (figure 3.45) reports power generation parameters. Protective relay status, generator winding temperatures, engine speed, Volts (kV), Amps (A), power (MW), apparent power (MVAR), and power factor are displayed.

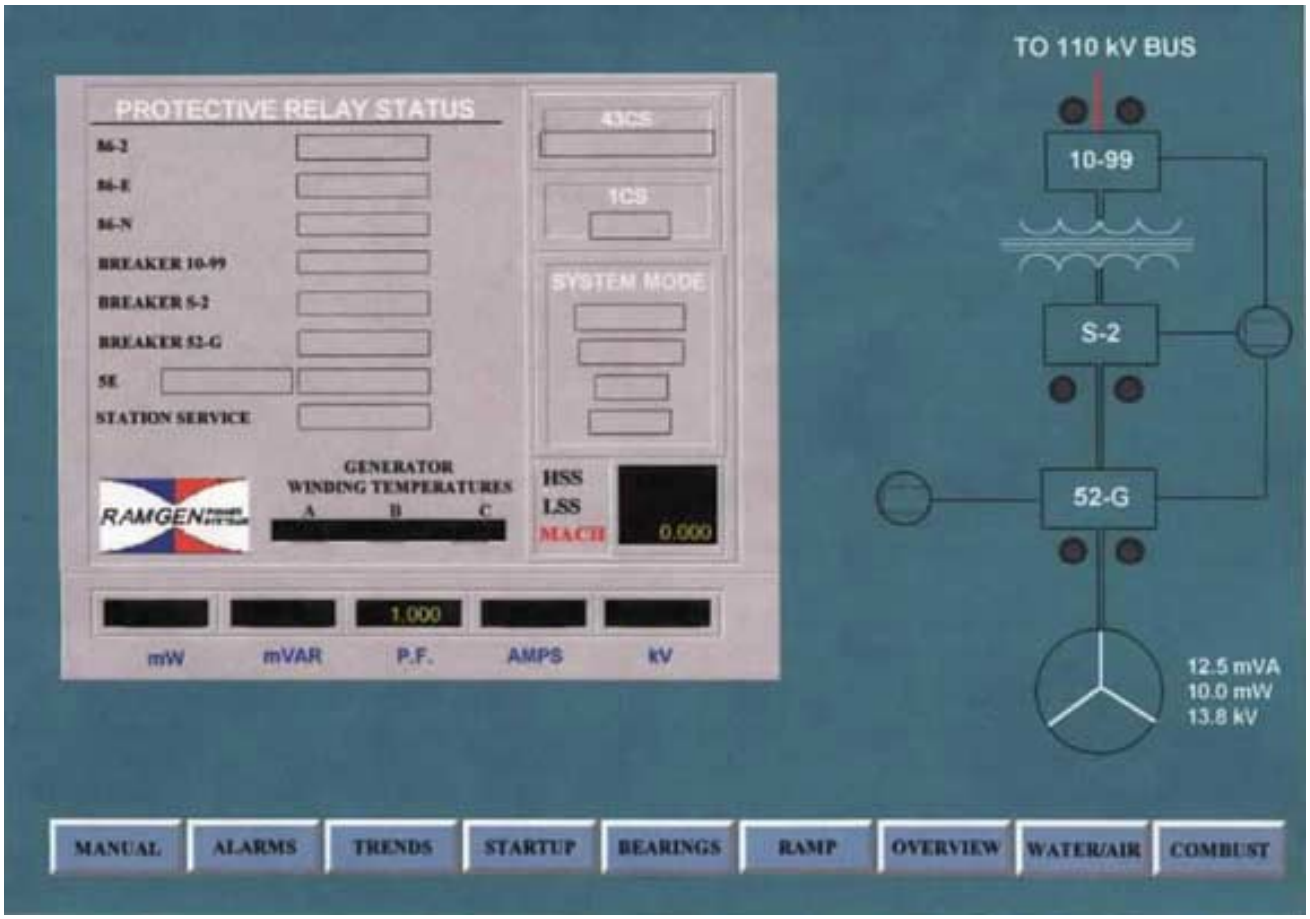

Oneline Screen
Figure 3.45

Overview Screen:

The overview screen (figure 3.46) is a general engine report screen. Values are displayed for Mode, Operation, Engine, Speed, Electrical, and Intake Air parameters in addition to temperature values presented on the schematic of the engine.

The Operation section indicates whether the engine is in start, online, stopping or stopped mode.

The Engine section contains containment temperature, intake differential pressure, intake total pressure, air accumulator pressure, bearing purge pressure, containment methane concentration, center body methane concentration, exhaust duct methane concentration, intake wheel space methane concentration, exhaust wheel space methane concentration, intake labyrinth seal temperature, exhaust labyrinth seal concentration, intake wheel space pressure, intake wheel space temperature, exhaust wheel space pressure, exhaust wheel space temperature, air film cooling slinger temperature, air film cooling labyrinth seal temperature.

The Speed section displays the low speed rpm, as taken from a tooth counter on the low speed side of the gearbox; the high speed rpm, calculated from the low speed rpm and the gear ratio; the high speed rpm, as determined by a proximity sensor counting bolt head passes on the high speed side of the gearbox; and Mach number calculated from comparison of the rotor speed to the local speed of sound.

The Electrical section contains Volt (kV), Amp (A), power (MW), apparent power (MVAR), and power factor information for generated power.

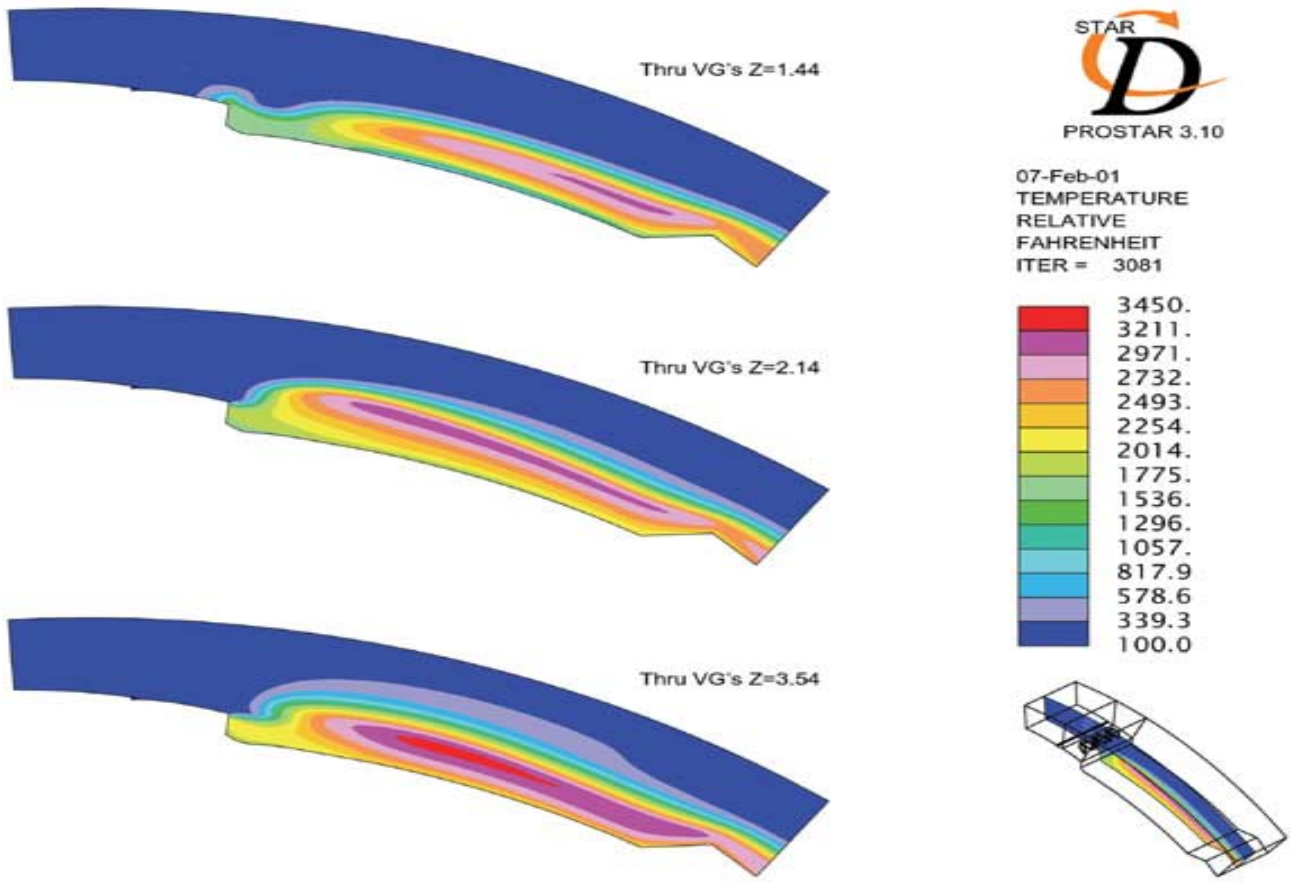

Overview Screen
Figure 3.46

The Intake Air section contains the screen's only control. The desired fan speed can be entered as fan set point. The section also displays the fan status, normal or run; the intake air velocity, calculated from intake total and differential pressures; and the fan rpm. The fuel section indicates the main natural gas line hut-off valve position, premix natural gas flow rate, pilot natural gas flow rate, premix hydrogen flow rate, pilot hydrogen flow rate, and total. All flow rates are in standard cubic feet per minute.

The last element of the overview screen is a diagram of the engine with temperatures. Three temperatures for the starter motor windings, three temperatures for the generator windings, a gearbox bearing temperature, two exhaust duct temperatures, the intake and exhaust labyrinth seal temperatures, the 90 degree combustor IR temperature, the center body temperature, the containment temperature, and the intake duct temperature are overlaid on the diagram. Nitrogen purge pressure, nitrogen tank pressure, run time, intake duct relative humidity and calculated intake air density are also displayed.

Ramp Screen:

The ramp screen (figure 3.47) is used to develop fuel and air ramps suitable for acceleration of the rotor to design speed. While a ramp is active, settings on the combustion screen cannot be changed. On the ramp screen, a fuel control button activates the methane system. A single/multiple ramp toggle selects between one and up to three ramp sections. The number of ramps is set in the number of ramps box. The screen displays the current rotor speed, pilot natural gas flow rate, air film cooling flow rate, air regulator set pressure, and pilot hydrogen flow rate. Below each report box, the operator can

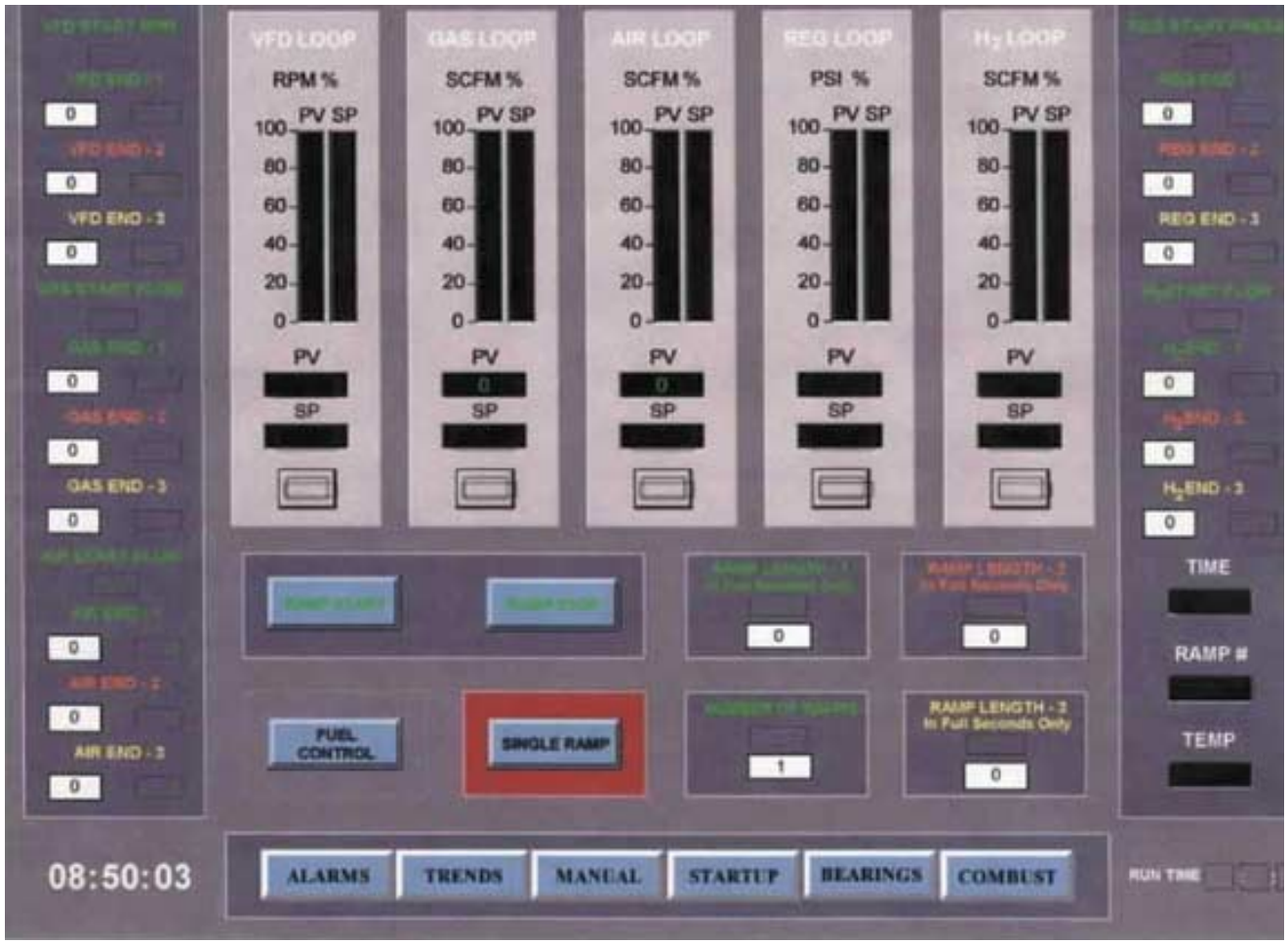

Ramp Screen
Figure 3.47

input ramp end point values for the set number of ramps. An additional box is provided for the duration of each ramp in second. Each ramp is linear from the current engine condition to the set end point. The slope of the ramp is dictates by the ramp duration and end point. When executing the ramps, valves will obey fixed position or loop control based upon the settings on the combustion and the startup screens. The ramping process is initiated by selecting the ramp start button. The ramp stop button suspends the current ramp and holds all controlled parameters in their current state.

For each ramp, a set of five bar graphs display the actual parameter value and the set point valve in percent complete. The rotor speed, pilot natural gas flow rate, air film cooling flow rate, air regulator set pressure, and pilot hydrogen flow rate bar graphs offer a visual indication of the ability of the valve and control to deliver the commanded ramp. A button at the bottom of each graph suspends the current ramp at its current condition. The number of seconds completed in the current ramp, the current ramp number, and the 90 degree combustor IR temperature are also displayed on the ramp screen.

Start Screen:

The start screen (figure 3.48) allows the operator to bring the engine from a complete stop to a running condition. Two knobs control the start process. The unit control knob is first switched to run. This setting initiates a series of software steps which sequentially start the system components. Once the system is powered, the unit control knob is switched to the start position. Next the variable frequency drive knob is switched to the on position. A VFD status box displays VFD status, on/off; VFD faults; power input; power output; Amperage; starter motor temperature; low speed VFD set point,

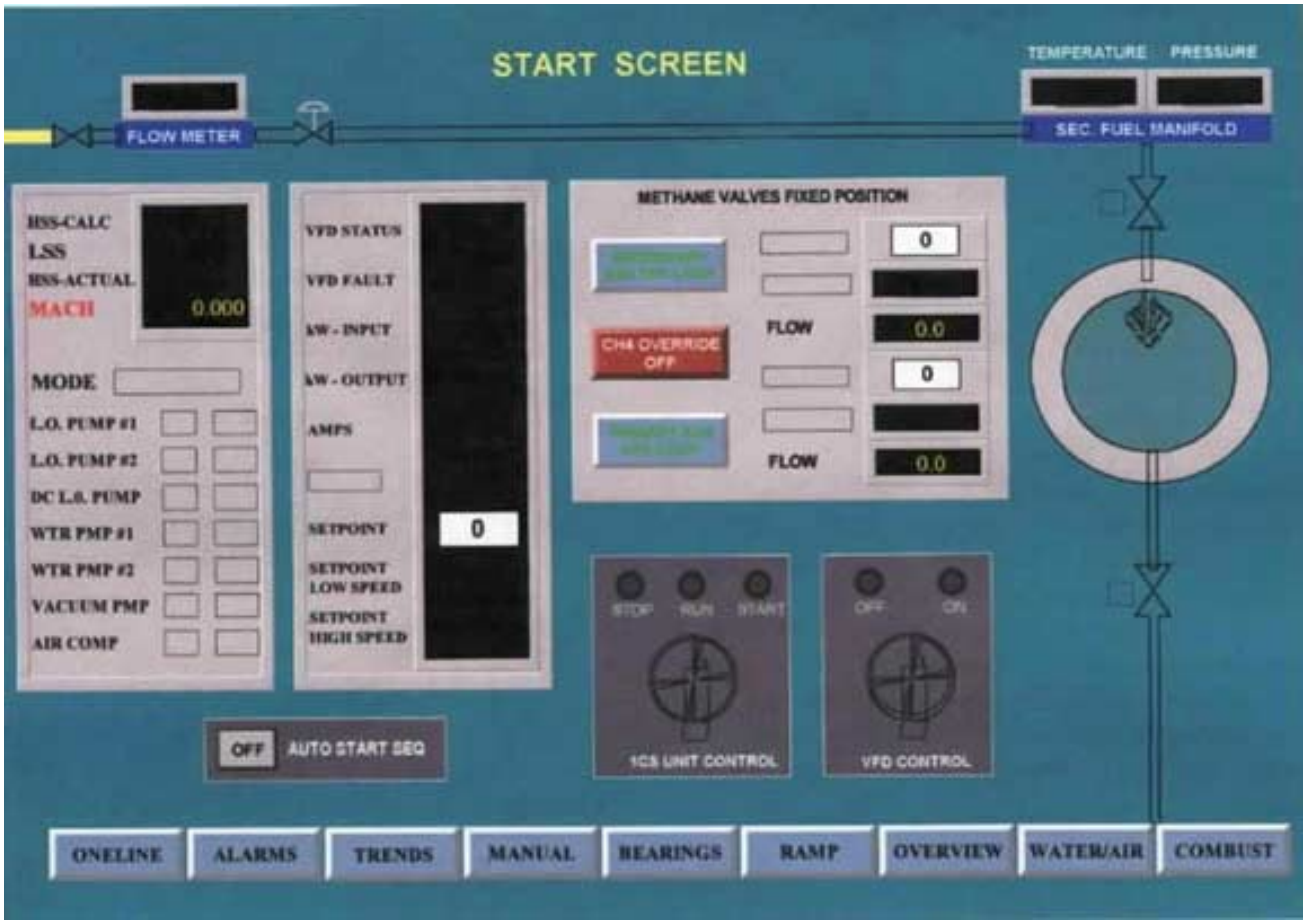

Start Screen
Figure 3.48

from VFD rpm calculation; and high speed VFD set point. Additionally, an input box is provided to set the VFD/starter motor speed. Three buttons control the methane flow. The first button is a natural gas system override. When active, this button allows bypass of the normal operating constraints for component level testing of the natural gas system. The remaining two buttons dictate fixed or loop valve control of the premix and pilot natural gas valves. In the fixed valve control position, flow rate set point boxes are active for natural gas control. Loop controlled flows must be entered from the Combustion screen. Additional boxes in this section report natural gas flow rates, premix turbine meter output, premix line pressure, and premix line temperature. A report section displays engine speeds, operating mode, lube oil pump operating conditions, water pump operating conditions, vacuum pump status, and main air compressor. The final button on this screen activates the auto start sequence. When active the auto start sequel will initiate the ramp defined on the ramp screen immediately after engine light.

Step Screen:

The step screen (figure 3.49) defines operating conditions for single button initiation from the combustion screen. These parameters are necessary for transition from power consumption to power generation. Premix and pilot hydrogen and natural gas and air film cooling flow rates can be preset on this screen.

Step Screen
Figure 3.49

Trends Screen:

This screen shows (figure 3.50) parameter trends. The screen displays real time 90 and 45 degree combustor IR temperatures and exhaust duct temperature. A graph displays exhaust duct temperature, VFD/starter motor power, VFD current, pilot gas flow rates, premix natural gas flow rate, rotor speed, VFD regeneration power, 90 and 45 degree combustor IR temperature, exhaust duct gas composition, and pilot hydrogen flow valve position for the previous 15 minutes.

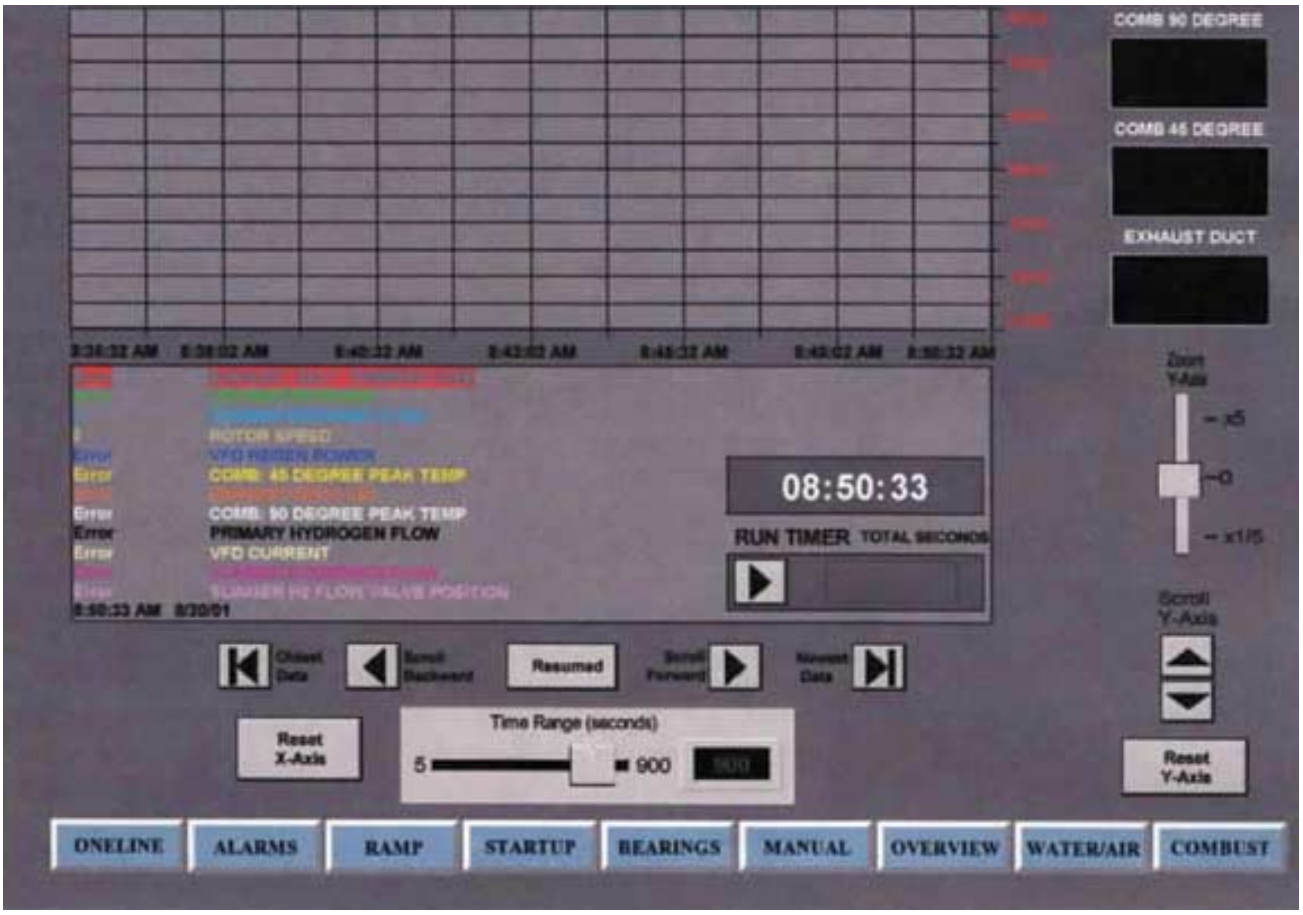

Trends Screen
Figure 3.50

Water/Air Screen:

The water/air screen (figure 3.51) dictates control parameters for the compressed air system, the cooling water system, and the cooling fans. The screen is broken into four sections: air system, water system, fans, and controls. The air system section reports accumulator pressure, air film cooling air manifold temperature, air film cooling air pressure, main air compressor status, air dryer status, auxiliary compressor pressure, auxiliary compressor status, and vacuum pump status. Button controls exist to cycle power to the auxiliary compressor and to bypass the AFC system controls for component testing. The water system section reports the cooling water manifold temperature and pressure, water reservoir temperature and level, engine case, internal and external cooling jacket, water temperatures and flow rates, heat exchanger flow rate and water pump status. The fan section reports the intake fan speed and the water-cooling system, heat exchanger fan speeds. Controls are provided to cycle water system fan power and to adjust the water system fan speeds. The controls section has button s for water pump power cycling, pressurizing the hydrogen system, exercising the flow valves, cycling the intake fan power, and bypassing the hydrogen system for component testing.

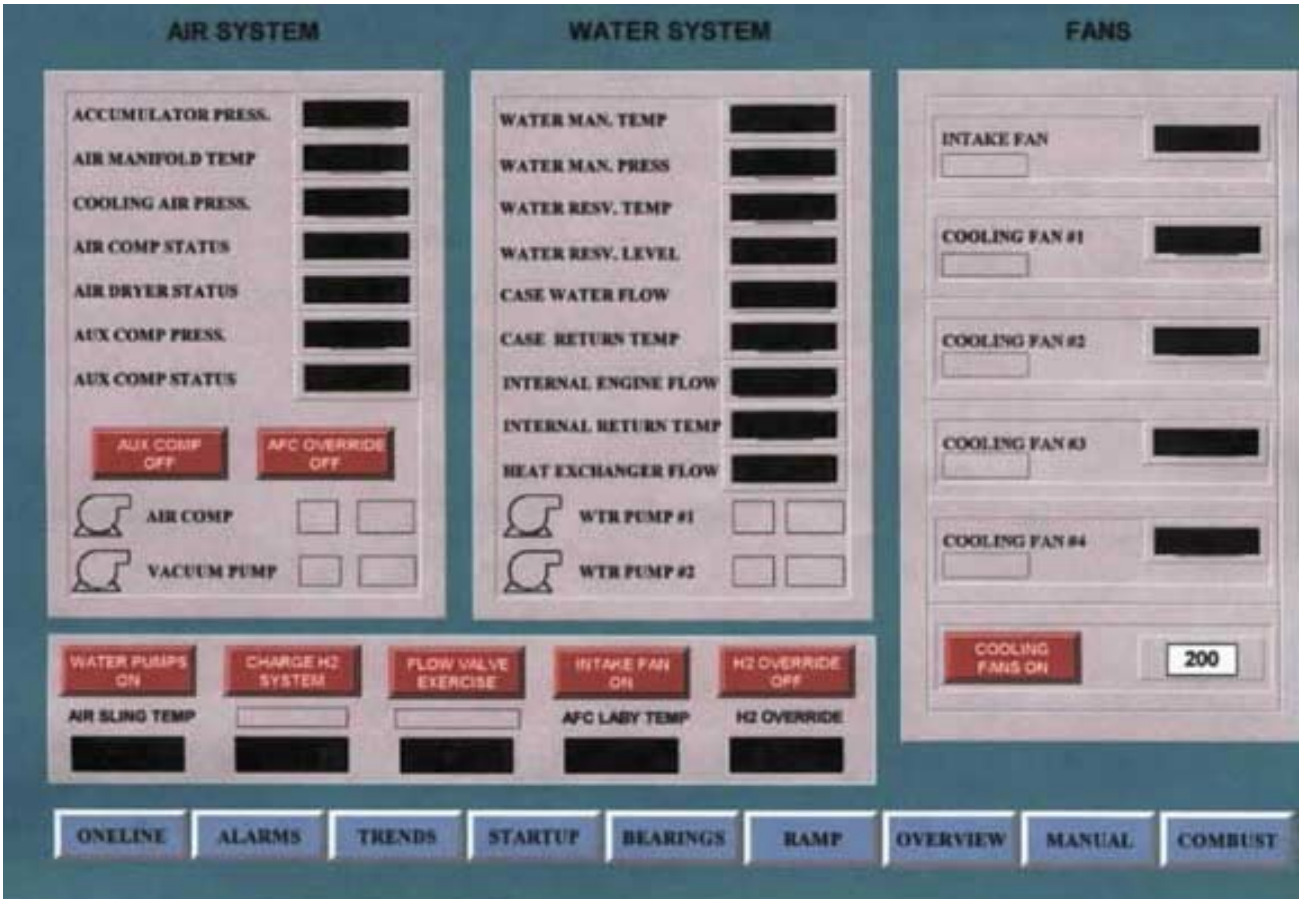

Water/Air Screen
Figure 3.51

3.3.2 High-Speed Data Acquisition System

A high-speed data acquisition system compliments the SCADA system, adding combustor scale monitoring capabilities. With sampling rates to 1 MHz, the system is able to detect temperature and pressure changes within the burner and flow path. The high-speed system is comprised of an eight channel analog-to-digital converter and an array of high speed transducers. The static pressure and rotor temperatures along the ramjet flow path are measured using high speed piezoelectric pressure transducers and IR thermometers mounted in the stationary engine outer casing. Four IR thermometers monitor combustor, nozzle, intake strake and exhaust strake temperatures, and two pressure transducers sample the flow path. Redundant sensors enable full historical coverage of the ramjet's helical flow path. The pressure and temperature traces, as a function of circumferential distance around the rotor, are reconciled in phase with magnetic and optical azimuthal rotor location detectors. The resulting traces provide a valuable diagnostic of the variation of static pressure along the ramjet flowpath. Additional high-speed sensors have been periodically added to monitor fuel system and wheel space pressure oscillations, segment thermal growth, and shaft vibration.

3.3.3 Video Monitors

Four video cameras allow visual monitoring of the engine during operation. Two cameras, one wide and one narrow focus, view the exhaust strakes through lenses in the exhaust duct. A third camera views the engine shaft and the exhaust bearing plate. The fourth camera looks at the intake fan and strakes. The condition of the exhaust plume and the occurrence of seal tip rub can be evaluated with these cameras. The wide and narrow focus exhaust cameras and the high speed data stream are recorded on VHS tape during testing.

3.4 Engine Operation and Personnel Requirements

3.4.1 Typical Test Plan

Although a variety of tests were conducted during the contract period, a standard test procedure was followed.
A test consisted of:

- Assembly of the test equipment
- Activation of electrical and mechanical control systems
- Safety checkout of test equipment and facility
- Activation of one Hz data acquisition system
- Cold spin of the engine at 800 rpm
- Safety and function checks of fuel system, ignition system and instrumentation
- Ignition
- Ramp of rotor speed to operational speed (Mach 1+)
- Testing at operational speed
- Selective recording of 50 to 100 kHz engine data
- Termination of gas flow
- Controlled rotor ramp to full stop
- All test equipment set to a safe mode
- Engine inspections
- Field processing of data

The drafting of a test plan preceded a standard test session. The test plan consisted of:

- Up-to-date hardware configuration list
- Review of previous test series (update daily)
- Statement of test series objectives
- Data log sheet
- Ramp Sheet: A detailed map of ignition, ramp, and steady state valve timing, flow rates, and any special instructions (note: The Ramp Sheet is test specific. Hence, each engine ignition sequence will have an associated Ramp Sheet)

3.4.2 Personnel Requirements

All tests were conducted with the safety of the test personnel of primary importance. The responsibilities of the minimum personnel for safe and efficient testing are described below.

Test Director (TD):

Most engine operations are requested by the TD and implemented by the Engine Controller and test staff. All pertinent pre-test, test, and post-test observations of merit are funneled through the TD.

The TD provides the test plan and sees that it is implemented. Modification of the test plan, real-time, is often initiated by the TD and conveyed to the Engine Controller and test team. The TD typically will monitor the TD data screen, while interacting with the other members of the team as required. Interaction typically involves requesting a specific control setting to be entered by the Engine Controller, requesting the status from the Safety Officer or the Panel Operator, or requesting a data save event from the High Speed Data Operator.

Engine Controller (EC):

The Engine Controller operates the engine control console. This individual enters all engine settings not controlled by manual valves. During engine start-up, spin, run, and shutdown, the engine control console is continually manned by the EC or his/her qualified substitute. The EC typically operates autonomously (i.e. without specific commands from the Test Director) during much of non-hot fire operation, depending on the comfort level of the EC and Test Director. During gas flow operations, ignition, run, and shutdown, the Test Director verbally directs the EC. The EC has authority and ability to abort a test, without specific instructions from the Test Director, if an immediate and significant dangerous condition manifests itself.

The EC is not mandated to monitor any specific parameter, except as instructed by the Test Director. Typically, the experienced Engine Operator / Test Director team will identify specific critical aspects or parameters of the test, and work together to monitor this information real-time by judiciously choosing appropriate data monitoring screens.

High Speed Data Operator (HSDO):

The High Speed Data Operator (HSDO) has the responsibility of continually monitoring the real-time combustor temperatures and pressures from ignition to gas-off.

During ignition, the HSDO will announce if ignition was successful ("both combustors lit") or if one or no combustors have lit ("gas off", followed by an explanation).

During run, the HSDO will operate the sampling system such that the real-time data is appropriately scaled for real-time evaluation. Any new or anomalous temperature or pressure traces are conveyed by the HSDO to the Test Director immediately. Typically, the HSDO and Test Director will discuss this feature real time. It is the responsibility of the HSDO to call for "gas-off" if an immediate and significant dangerous condition manifests itself.

At the request of the Test Director, the HSDO will can save a discreet batch of High Speed Data. (File size makes it impractical to save all high-speed data during a complete test.)

If, during the course of a test, one or both of the combustors is extinguished, the HSDO will call an immediate "gas-off".

Panel Operator (PO):

The Panel Operator controls the hand-operated switches for the starter motor, gas system, and ignition system. Initiation of engine spin-up, gas flow, and ignition require the participation of the PO. Typically, the Test Director will request these events. The Engine Controller will make the appropriate keystrokes to prepare for the event, and then the Engine Controller will request the appropriate manual switch to be thrown by the PO.

During engine operation, the primary responsibility of the PO is to shut off the engine gas flow immediately following the "gas-off" command. If any test personnel request "gas-off" during the course of a test, the PO will immediately turn off the gas. The Test Director typically gives the "gas-off" command at the conclusion of a successful test.

The PO has the added responsibility to monitor the combustor temperature (one second data) continually during hot fire. Typically, the Test Director will request audible temperature feedback from the PO. If the PO observes a temperature above a pre-determined limit, the PO has the responsibility of going to "gas-off" autonomously.

Safety Officer (SO):

The Safety Officer monitors the intake and exhaust cameras for anomalous conditions. Broadly, a condition in which sustained sparking is visible at the rotor or engine case constitutes an anomalous condition. An atypical plume also is an anomalous condition. It is prudent for a new SO to be directly trained by a previous SO.

The SO conveys any non-typical engine behavior, evident on the intake and exhaust cameras, to the Test Director. The SO can command "gas-off" prior to notifying the Test Director if an unsafe condition occurs. The Panel Operator will immediately turn off the engine gas flow.

Additional test personnel may be involved in implementation of a specific test plan or specialty test. Standard safety practices are followed by all additional personnel, and enforced by the Safety Officer.

3.5 Inspections and Life Cycle Assessments

The purpose of this section is to outline the means, techniques and tools required for the post run inspection of the combustors in the prototype engine. Access is through a six-inch diameter port that has been milled into the engine case (figure 3.52) and through stainless steel tubes that lead into the wheel spaces (figure 3.53).

Boroscope Access Port
Figure 3.52

Combustor Access Port
Figure 3.53

The inspection process comprises five distinct procedures: 1) Temperature history of the hot-gas flow path, as indicated by color change in thermographic paint, 2) Measurement of any radial strake growth towards the engine case, 3) Measurement of radial growth in the segment floor (i.e. web creep), and 4) Measurement of any surface irregularities in the combustor floor. These four inspections are performed through the large case access port. The fifth post-test inspection involves using a boroscope to check the condition of the rim clips. This inspection utilizes the stainless steel wheel space access tubes (figure 3.52).

3.5.1 Thermographic paint inspection

The temperature history of the combustor is determined by the use of thermographic paint, which has the The

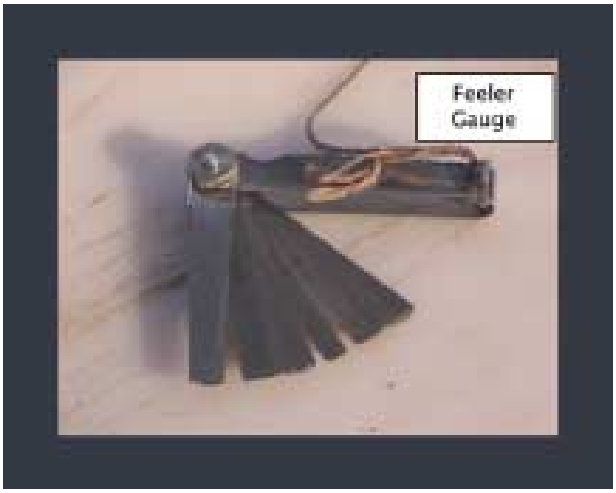

Feeler Gauge
Figure 3.56

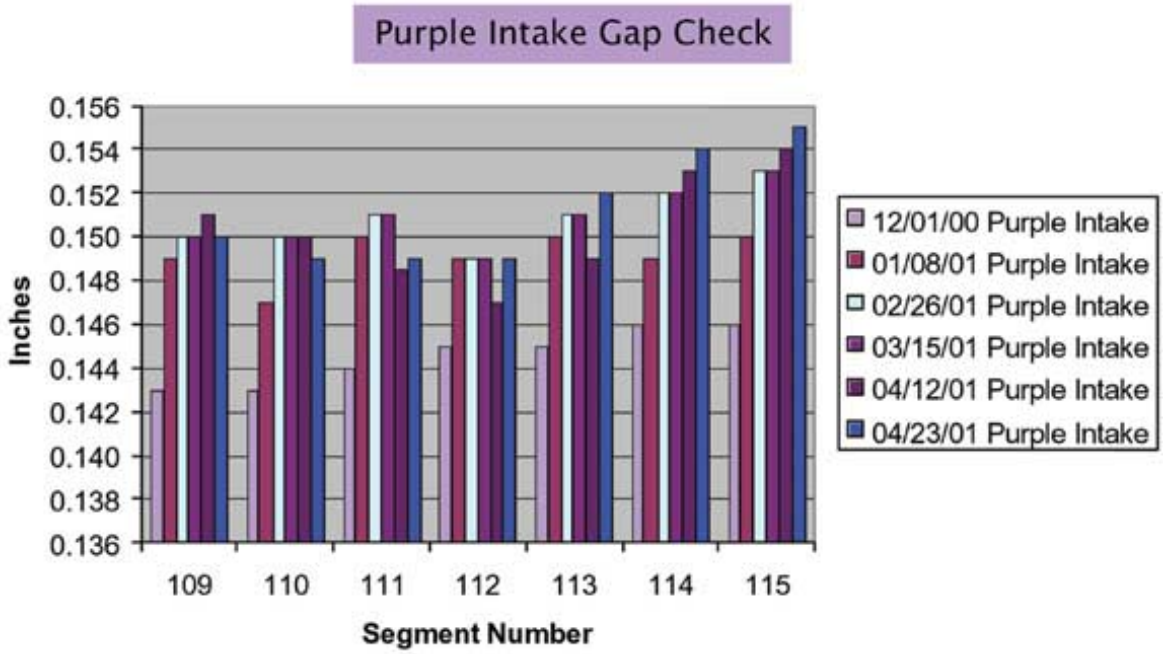

Strake Growth Inspector Results
Figure 3.58

procedure for the temperature inspection requires locking out the starter motor and installing the manual rotor turning gear. The access plug is then removed to permit viewing of the combustors. While using a high intensity light source, the rotor is slowly turned such that each combustor can be inspected (figure 3.54), and photographe for later analysis.

3.5.2 Radial strake growth

This inspection detects radial strake growth (creep) due to centrifugal loading and combustor heating. The results of this effort help to determine the useful duty cycle of the component parts and therefore help to determine the duty cycle of the combustor itself.

Using the same safety procedures as above, the rotor is rotated until the center of the segment in question is aligned with a scribe mark that is on the top face of the inspection port, as shown in figure 3.55. A tapered feeler gauge (figure 3.56) is then employed to measure the distance from the strake to the engine case, as shown in figure 3.57. The results of a series of inspections are shown in figure 3.58.

quality of a color change when exposed to a changing temperature environment. The paints used most often are *Thermax* SC610 and SC560 and MC277-7 yellow. The SC610 is a single change paint that changes from red to white when exposed to a temperature of 1165 F for ten minutes. The SC 650 is also a single change paint that changes from orange to white when subjected to a temperature of 1036 F for ten minutes. The MC 277-7 yellow is a multi change paint that will change different colors for varying temperatures and exposure times.

3.5.3 Radial segment growth

This is a check for segment creep at the floor of the combustor (segment web creep). A change in combustor floor height at this location would indicate inadequate combustor cooling.

This inspection is accomplished with the use of a depth micrometer and a precision 1.436-inch thick block. The rotor is

rotated such that the scribe mark is aligned with the center of the segment in question. The micrometer with a 12-inch rod installed is placed within the guide marks on the access port rim and a measurement is taken to the face of the precision block that has been placed on the center line of the segment.

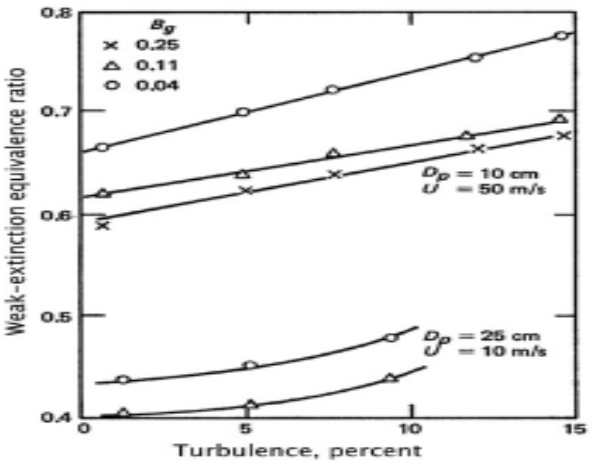

Modified Depth Gauge
Figure 3.63

Combustor floor irregularities:

The purpose of this inspection is to discover and measure any combustor floor irregularities such as raised bubbles from excessive loading or general damage. This is accomplished using a small depth micrometer with .142-inch spacers installed at the base of the tool. The spacers raise the tool above the level of the floor in order to obtain accurate measurements, as shown in figure 3.63. The tool is placed such that it spans the centerlines of two segments with the measurement rod directly above the feature to be measured. The measurement is taken, and subtracted from the spacer height to arrive at the height of the feature.

Internal rim clip inspection:

This inspection checks the condition of the rim clips and rim clip screws. The clips help align and retain the rim segments, and are an integral part of the air and fuel delivery systems.

The inspection is performed using the *Olympus* boroscope and a digital camera, shown in figure 3.65. The boroscope lead is threaded into half-inch stainless steel tubes that lead into the engine wheel spaces. Once inside, the articulated lens body can be adjusted to obtain the clearest image. The rotor is then turned slowly as the rim clips are photographed and checked for misalignment or looseness. Figure 3.66 shows a view of a rim clip during inspection.

Boroscope
Figure 3.65

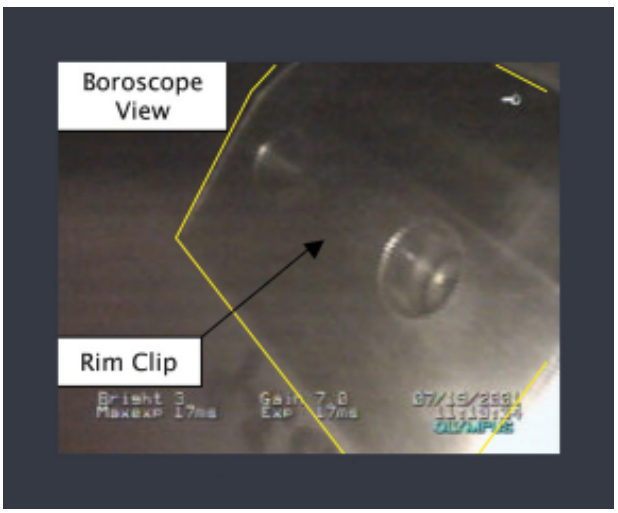

Rim Clip Inspection
Figure 3.66

4.0 Results and Discussion

Task 1.0 focused on the testing and evaluation of the Ramgen engine, particularly the operation of the thrust module. The ideal operation of the thrust module is illustrated in figure 4.1. The figure shows a section cut through the circumferential centerline of the ramjet flowpath shown in figure 4.2. The various gasdynamic processes in the inlet, combustor, and nozzle are schematically represented in figure 4.1, for a coordinate reference frame fixed to the moving rotor wall.

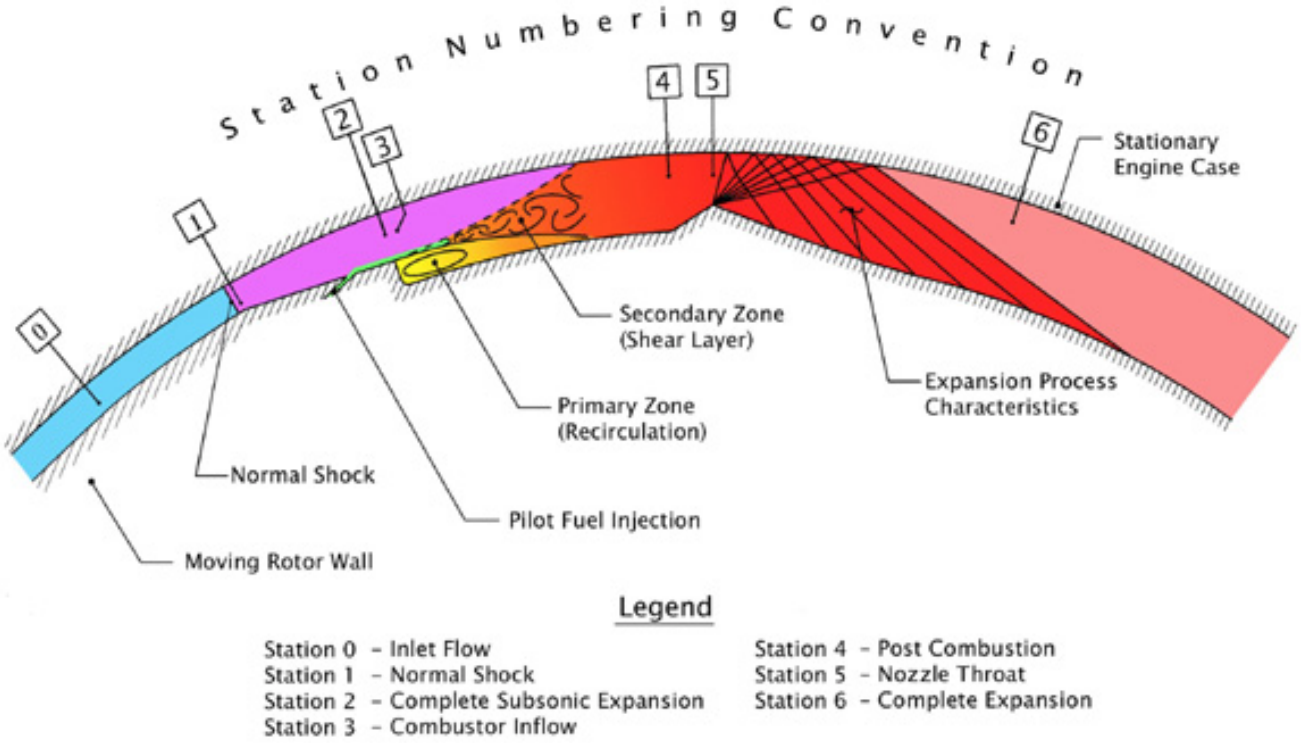

Ramjet Flowpath Station Definitions
Figure 4.1

As indicated in figure 4.1, the flow enters the ramjet inlet at Station 0 with a centerline velocity equivalent to the tangential speed of the inlet centerline. The inflow velocity is determined by the radius of the ramjet flowpath centerline and the rotation rate of the rotor. The Mach number at Station 0 is simply the local tangential velocity divided by the local speed of sound.

The flow then encounters a normal shock between Stations 0 and 1. This normal shock inlet is simple in design, aerodynamically robust, and, for inflow Mach numbers below 1.5, capable of achieving high total pressure recovery (above 93%). This type of inlet does suffer from excessive losses for inflow Mach numbers above 1.5.

The supersonic constant area diffuser, between Stations 1 and 2, accepts the outflow from the normal shock inlet at a local Mach number of approximately 0.8. The subsonic diffuser decelerates the flow in a nearly loss-free process. The flow is slowed to a speed of approximately M ~ 0.3 at which point it enters the combustor.

Figure 4.1 shows a dump combustor, between Station 2 and Station 4. Figure 4.1 includes a schematic representation of the recirculation flow-field which is formed immediately downstream of the dump or rear facing step, Station 3. The recirculation zone behind the rear-facing step serves as the flame-holding zone for the combustor. In addition to the recirculation zone, the flow downstream of the rear-facing step includes a shear layer that is also a combustion zone. Issues regarding fuel-air mixing within the recirculation zone and shear layer are addressed in Section 4.2.2. An analysis of the residence time and flame-holding requirements for the Ramgen engine combustor are discussed in Sections 4.1.2 and 4.2.3 respectively.

Fuel is supplied to the combustion process in the Ramgen combustor in two different ways. The first source of fuel, or primary fuel, is homogeneously mixed with the air that flows into the ramjet inlet through the subsonic diffuser, and then into the combustor, as depicted in figures 4.2 and 4.3. The fuel injection and mixing process occurs upstream from the ramjet rotor at a station where the engine air stream is at atmospheric pressure. When premix is supplied to the ramjets in this way, highly efficient combustion and low pollutant formation levels can be achieved. The methods of introducing primary fuel were discussed in Sections 3.2 and 3.2.6.

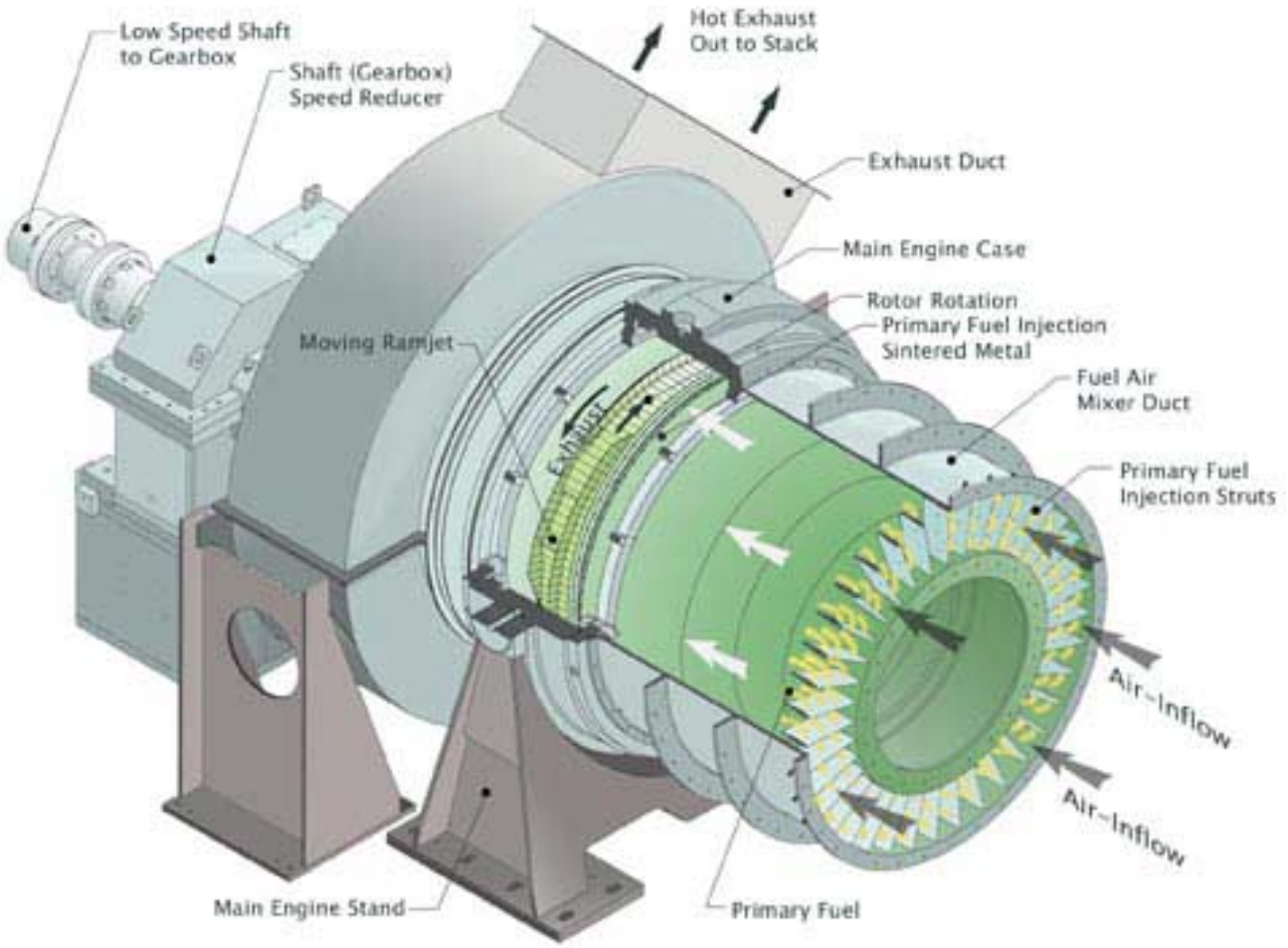

Ramgen Engine Assembly
Figure 4.2

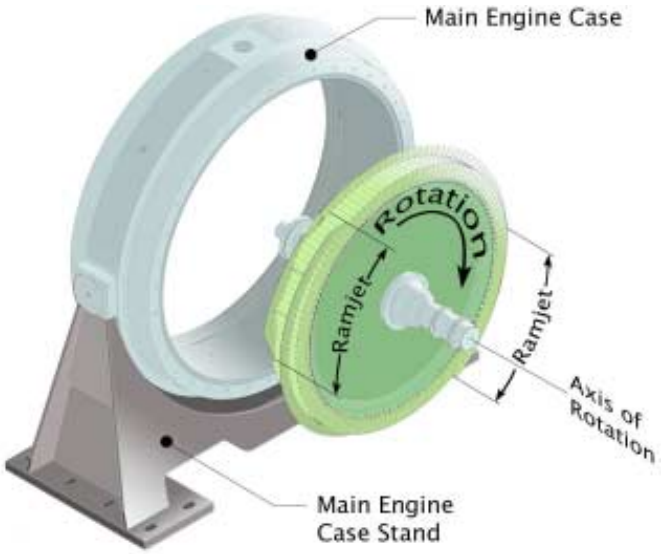

Ramjet Rotor with Stationary Engine Case
Figure 4.3

The second fuel source, or pilot fuel, is used to stabilize the combustion process during the acceleration of the engine from ignition to operating speed. The pilot fuel is injected immediately upstream of the burner. Figure 4.1 shows the location of the injection of pilot fuel through a thin-wall slot just upstream of the rear-facing step. The wall slot forms a thin layer of pure fuel directly adjacent to the wall at the station of the rear-facing step. The pilot fuel is then entrained directly into the recirculation zone. This stabilizes a hot combustion process at all rotor speeds, including situations when premixed fuel concentrations fall below the lean-extinction limit. The method for introducing pilot fuel was described in Sections 3.2.3 and 3.2.5.

Because of the high combustion temperatures sustained by the combustor, it was necessary to cool the walls using air film cooling and protecting the combustor surfaces with thermal barrier coating. The effectiveness of these cooling techniques are discussed in Section 4.2.4.

The end of the combustor is defined by the nozzle throat at Station 4 and Station 5. This geometric contraction works together with the heating of the flow in the combustor to accelerate the flow until it reaches M = 1 or chokes at the nozzle throat. See Section 4.1.1 for a more complete discussion of nozzle throat choking.

When the flow reaches M = 1 at the nozzle throat, the subsequent area increase in the nozzle between Station 5 and Station 6 causes the flow to accelerate to supersonic velocities. When the flow eventually leaves the ramjet at Station 6, it does so at a much higher velocity than when it entered at Station 0.

It is important to note that the processes presented and discussed above are for the engine operating at a given speed. As the speed of the engine changes, the thermodynamic and fluid mechanic states at each of these stations are also varying. There are situations where these variations of station properties can cause an instability or extinction of the combustion process. Section 4.2.1 includes a discussion of operating the engine under these variable-speed conditions.

4.1 Performance Summary

The sections that follow summarize the performance of the Ramgen Engine, as well as some of the key issues which affect this performance, including: nozzle choking, combustor residence time, combustor heat loading, seal tip leakages and emissions. Also included are studies related to the DOE contract subtasks. These studies include ignition/ramping/ steady-state operation, flame-holding, fuel mixing, air film cooling/thermal barrier coating, rotor drag tests and noise monitoring and mitigation.

Before exploring such details, it is worth reviewing some of the major hardware iterations or combustion configurations undertaken throughout the course of the contract. Table 4.1 below summarizes the operational days, total number of rotor spins tests and duration, test quantity (non combusting and combusting) as well as number of runs to Mach one and higher. The last row provides the totals for each column.

Experimental Test Duration Summary

Start Date	End Date	Operation Days	Engine Spin (hrs)	Number of Tests	Hot Fire Total (hrs)	Hot Fire Mach 1+ (hrs)
9/29/00	11/29/01	10	6	73	4.5	0
11/29/00	1/29/01	22	100	200	12	4
1/29/01	3/29/01	22	65	180	15.6	1.3
3/29/01	5/29/01	20	43	80	10.4	1
5/29/01	7/29/01	3	2	6	0	0
	Totals	**77**	**216**	**539**	**42.5**	**6.3**

Table 4.1

As can been seen from the table, the rotor speed was increased from Mach one near the beginning of CY 2001 to enhance inlet performance by augmenting inlet shock strength. In the nine months of testing, the Ramgen Engine accrued over 200 hours of testing, with slightly under 20% (42.5 hours) devoted to hot, combustion tests. The balance was on cold flow spin tests to diagnose/trouble shoot experimental issues and ensure mechanical integrity of each hardware configuration.

Throughout the testing phase, a variety of hardware configurations were investigated with several goals in mind. Much of the efforts centered on enhancing fuel-air mixing between the high velocity core flow through insertion of Vortex Generators (VGs) upstream of the pilot fuel slot. By creating streamwise vorticity (turbulence), the VGs enhanced the diffusion of the thin fuel layer into the core airstream. Other configurations were aimed at improving the flame stabilization of the baseline (rearward facing step) flame-holder by increasing flame surface area. Still other concepts examined various pilot fueling strategies. Table 4.2 below summaries the major configurations tested, including the fuel type (methane and/or hydrogen), features added, and maximum rotor speed attained.

Summary of Experimental Test Configurations

Name	Sub Name	Fueling			Fuel		MAX RPM	Addition. Features	Notes
		Sint.	Prim.	Slinger	NG	H2			
STEP	Baseline*	Y	Y	Y	Y	Y	4000	none	Rich Burn
PYLON	5-Hole	N	Y	Y	Y	Y	4300	3/8" VGs	flamehold
	1/8" Hole	N	X	Y	Y	Y	4300	none	High P4
	½" Hole	N	X	Y	Y	Y	4300	none	High P4
	16-Hole	N	X	Y	Y	Y	4300	none	High P4
VGs	¼" Tall*	X	X	Y	Y	Y	4000	none	No effect
	3/8" Tall	X	X	Y	Y	Y	4200	none	Better
	1.5" Tall	X	X	Y	Y	Y	4300	none	Too Mix
	¾" Tall	X	X	Y	Y	Y	4300	none	Average

* Tested prior to contract initiation

Table 4.2

The Vortex Generators yielded the highest thrust of all the hardware configurations, but as will be explained later, they produced the most unstable combustion dynamics. This was often mitigated through use of increasing levels of hydrogen during the ramping period.

In the sections which follow, each of the above configurations will be examined in more detail, paying close attention to overall combustor performance, mixing enhancements, residence times, and flame-holding capabilities. This section will also address combustor liner cooling and rotor drag testing, finally ending with a treatise of engine noise assessment and mitigation schemes.

4.2 Studies

Detailed studies are presented in sections 4.2.1. through 4.2.6.

4.2.1 Study: Ignition, Ramping, and Steady State Operation

4.2.1.1 Introduction

The unique operating principle of the Ramgen engine requires an ignition system, flame holder, and rotor ramping procedure different from a typical land-base gas turbine engine. Unlike a gas turbine engine, the combustor rotates with the shaft. Centripetal acceleration at the combustor during full speed operation is 566,000 ft/sec^2, or 17,600 equivalent g's. A conventional ignition system that travels with the combustor is impractical in this environment. Likewise, the flame holder and pilot fuel delivery system must be designed not only for high temperature and vibration, but also to withstand the g-load at design speed. This dicates: 1) a stationary ignition system, and 2) pilot flame holding device of low mass and high strength.

The process that is required to define a repeatable and robust ramp relies on both applied theory and empirical methods. The sections that follow discuss ignition, ramping, and steady state operation of the Ramgen engine.

4.2.1.2 Ignition

A timed spark, in a charge of premixed propane and oxygen, results in simultaneous ignition of the combustors. The fuel/ oxidizer mixture, orifice size, and timing have been optimized for an ignition effectiveness of 90 to 95%, depending on the flame-holder configuration. Ignition is initiated at a rotor speed of 800 rpm.

Figure 4.25 shows a typical pre-ignition trace obtained from the high-speed data acquisition system at sampling rate of 10 kHz. Note that the rotor rotational speed is 800 rpm, or 13.333 cycles/second. Hence, the figure shows 2.667 rotations of the rotor. The location of each thrust module is indicated by sets of magnets in the rim clips of key thrust module segments, which are detected by a hall-effect sensor on the stationary engine case. The lower trace shows pressure as measured by a piezoelectric pressure transducer in the stationary case.

Ignition is verified by monitoring the high-speed data system for consistent indications of heat in both combustors. Figure 4.26 shows an example of a successful ignition detected. This particular test was conducted with ¾" vortex generators (VGs) between the fuel slot and the rear-facing step. Both combustors are lit, as can be seen by the repeating temperature trace over 2.667 rotations of the engine. The spectral response of the Land Infrared Thermometer is 0.7 μm to 2.0 μm, a wavelength band appropriate for low interference from products of complete combustion and typically a reasonable

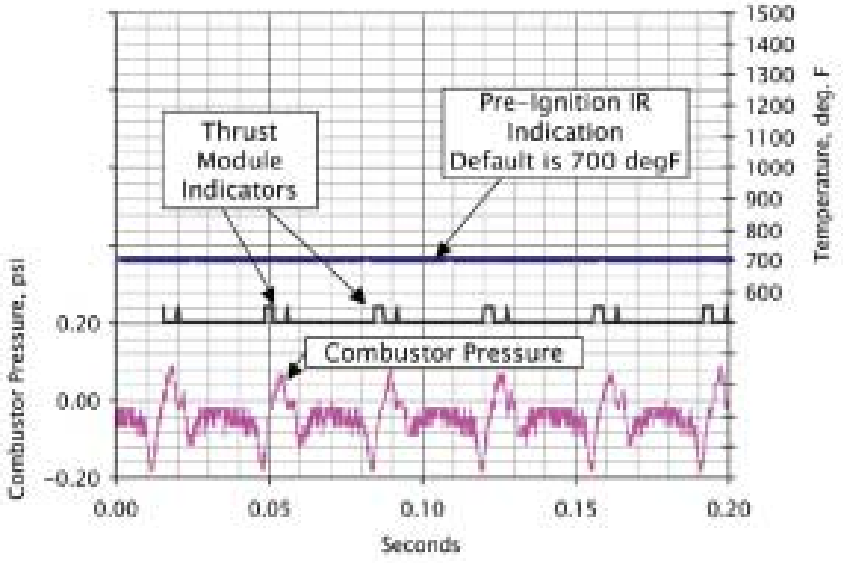

Pre-ignition Combustor Temperature Trace at 10 kHz Sampling Rate and Rotor Speed of 800 rpm
Figure 4.25

measurement of metal temperature (depending on emissivity of the metal surface or thermographic paint). Note in figure 4.26 that the indicated temperature fluctuates more than one would expect for true metal temperature variances. This may be due to interference from byproducts (CO_2 or H_2O) of combustion in the spectral range of the detector.

Figure 4.27 shows a single rotation of the rotor at 800 rpm with both combustors holding flame. The locations of the major features of the thrust module, as detected by a magnetic sensor on the engine housing, are shown schematically for reference. It is immediately clear that flame holding occurs directly behind the rear-facing step, as indicated by the rapid temperature rise.

The forward section of the combustion chamber (approximately 5 to 7 inches along the floor, or approximately 5 step-heights) is the location of the recirculation zone required for flame holding at higher speeds. This is apparent during the two-minute period when the rotor is held at 800 rpm with stable combustion, prior to ramping. A consistent thermal trace develops in the forward half of the combustor, fluctuating by approximately +/-50 F. The rear of the combustor and the nozzle fluctuate by approximately 200 F, indicative of a zone dominated by incomplete combustion, turbulent flame, and unsteady combustion. This is noted as the shear zone on figure 4.27.

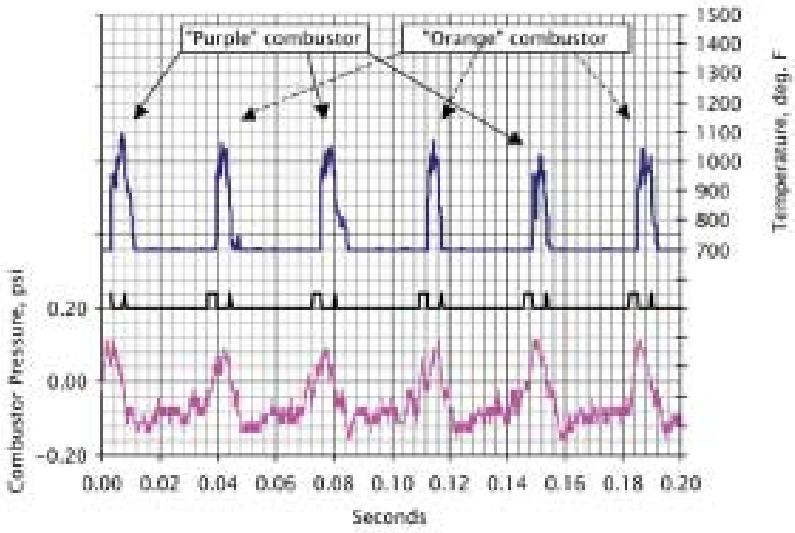

Ignition of Both Combustors Verified by Combustor Temperature Trace at 10 kHz Sampling Rate and Rotor Spped of 800 rpm
Figure 4.26

The test shown in figure 4.28 was conducted with ¾" vortex generators down steam of the fuel slot and up stream of the rear facing step. After ignition, the rotor speed is held constant for two minutes prior to ramping. This allows thermal transients to asymptote toward stable conditions as the air film cooling is increased from 50 scfm to 150 scfm. Throughout the stabilization period, the high-speed (10 kHz) temperature trace indicates flame holding in both the recirculation zone and the shear zone.

In general, a low air film cooling flow rate at ignition prevents quench during the start transient. After ignition, an increase in air film cooling is required. This can be seen in the comparison between figure 4.28, in which the air film coolant increase was simultaneous with ignition, and figure 4.29, in which the air film coolant increase was delayed to 75 seconds after ignition. The temperature rise without additional air film cooling is 100 degF in 75 seconds (and rising), vs approximately 30 degF in 75 seconds (and stable).

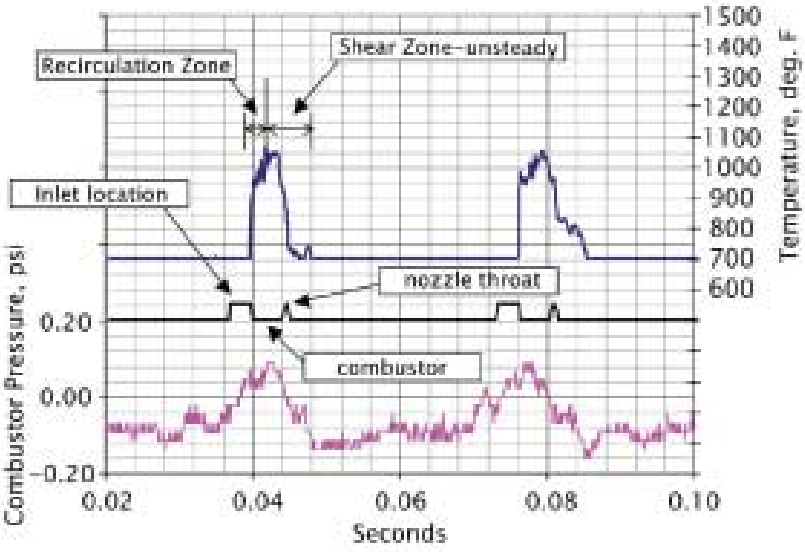

One Rotation of the Rotor with Both Combustors Lit
Figure 4.27

4.2.1.3 Ramp to Operational Speed

A typical ramp-to-speed is shown in figure 4.28. After ignition, the speed is held constant at 800 rpm for two minutes, followed by a continuous and linear increase in rotor speed to 4300 rpm. Control of air film cooling and pilot fuel is typically automated during the ramp. For most configurations, the air film cooling ramp and pilot fuel ramps are broken into three discrete ramps: from 800 rpm to 2000 rpm, 2000 rpm to 3000 rpm, and 3000 rpm to 4300 rpm. A single linear ramp of air film cooling and pilot fuel with rotor speed is not practical, as the fluid-dynamic characteristics of the combustor change as rotor speed increases.

As shown in figure 4.28, air film cooling is increased from 150 scfm to 200 scfm between 800 rpm and 2000 rpm with a ramp acceleration of 400 rpm per minute. A more aggressive air film cooling increase overpowers the recirculation zone

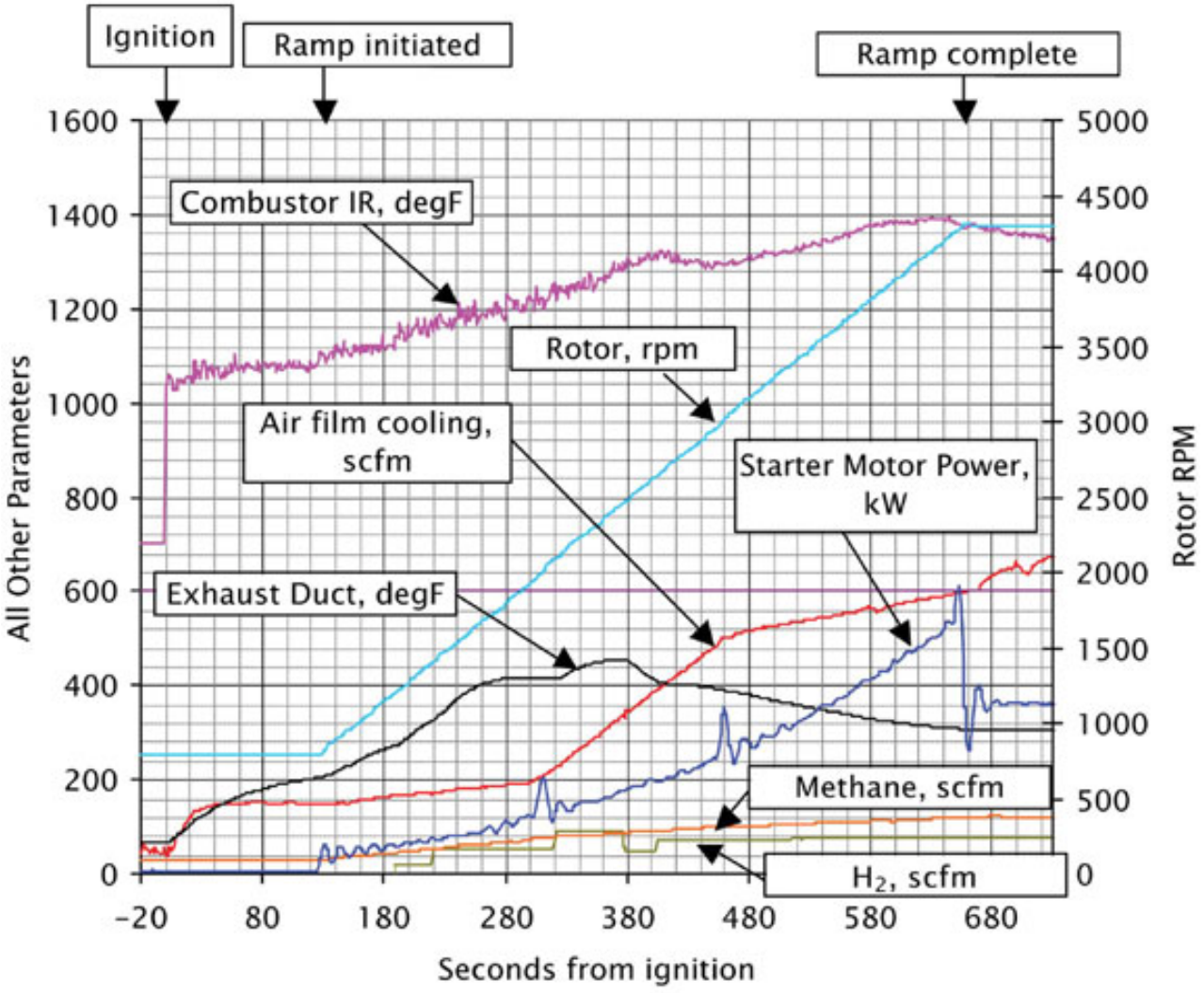

Ignition, Ramp, and Stabilization at Mach 1.1
Figure 4.28

behind the step and extinguishes flame holding. Below 2000 rpm, burning is generally apparent in both the recirculation zone and the shear layer.

For a rotor speed from 2000 rpm to 3000 rpm, the combustor flow field has stabilized sufficiently for increased air film cooling. In the test shown in figure 4.28, the air film cooling is increased from 200 scfm to 500 scfm.

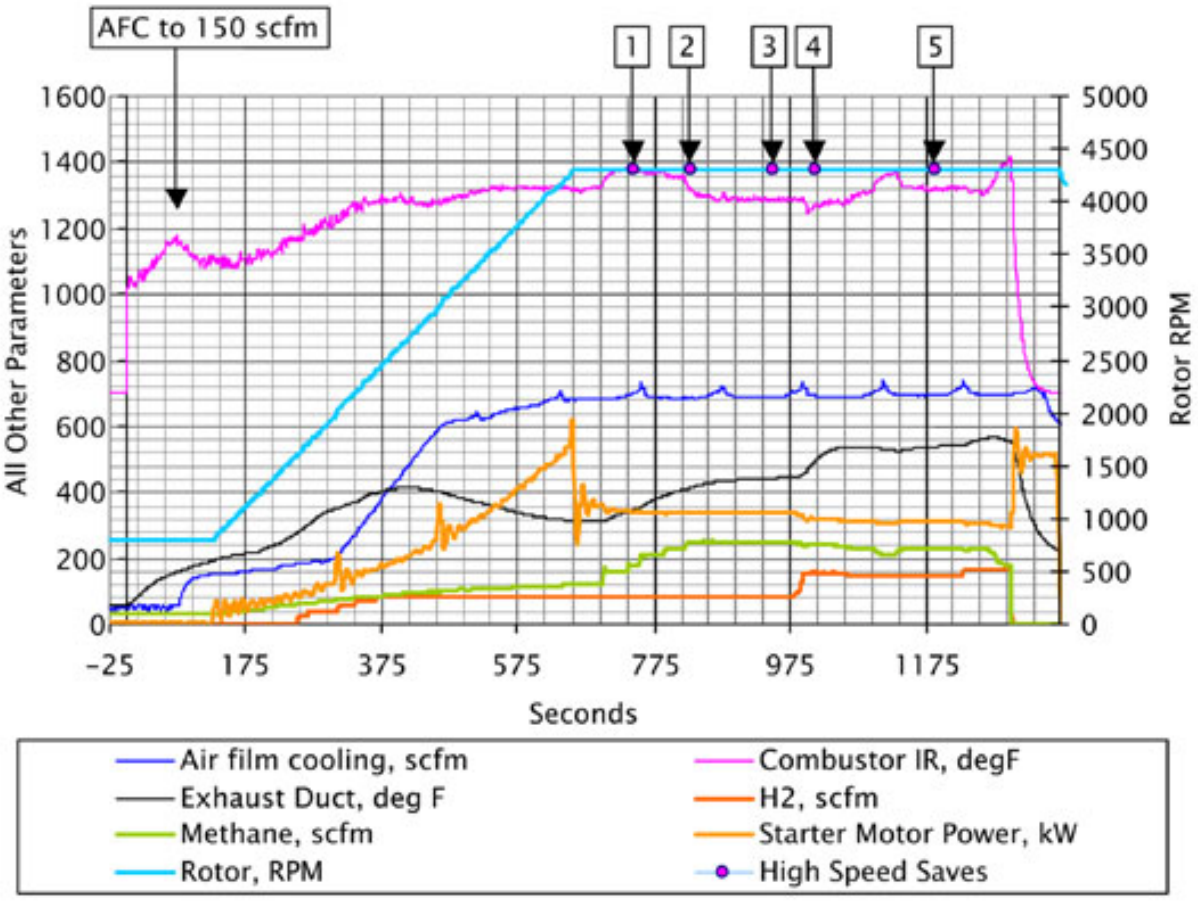

Typical Test (02_22_01 T162327) with 3/4" Vortex Generators Prrior to Rear Facing Step
Figure 4.29

Generally above 2000 rpm, flame holding is limited to the recirculation zone. The burn in the shear layer, as implied by the indicated temperature of the combustor, is reduced as the overall residence time of the combustor drops with increasing speed. Simple modeling of the combustor as a perfectly stirred reactor with an equivalence ratio (CH4 only) of .51, predicts that flame holding above 2000 rpm is not possible without a recirculation zone. Although this model is overly simplistic, it can be surmised that a critical rotor speed will be reached in which the shear zone burn will be unable to hold flame independent of the recirculation zone. Flame-holding stability is discussed in more detail, relative to steady-state engine operation.

Flame holding behind the rear-facing step is well established for a rotor speed between 3000 rpm and 4300 rpm, and air film cooling is effective at controlling combustor heating with a flow rate increase from 500 seconds to 600 seconds.

The variable frequency drive holds the rotor at 4300 rpm at the top of the ramp. Note that there is some drive power oscillation as the rotor speed is stabilized. The power output required to maintain the spinning load is a critical indicator of the overall performance of a thrust module configuration. A typical test matrix begins after the rotor speed and drive power load is stable.

4.2.1.4 Test Matrix

Figure 4.29 shows a test with ¾" vortex generators installed. One uncommon feature of this test is the delay in air film cooling increase from 50 scfm to 150 scfm at 80 seconds, as discussed in section 4.2.1.2. This resulted in a rapid rise in combustor floor temperature, followed by an equally rapid recovery when air film cooling was increased. After stabilizing at 800 rpm, the rotor speed, air film cooling flow, and pilot fuel flow were ramped to design speed. The rotor speed was stabilized by the starter motor at 4300 rpm with pilot fuel flow rate of 81 scfm H2 and 120 scfm of CH4. From ignition at 800 rpm to design speed (4300 rpm) took 11minutes in this test.

Following rotor speed stabilization, the pilot methane fuel was increased incrementally while the hydrogen flow rate was held constant. In this test, a number of methane and hydrogen flow rates were investigated, as shown in
Table 4.4. The points labeled 1 through 5 indicate times where the high-speed data stream was recorded. High-speed data, typically sampled at 100kHz, is not continually recorded because of practical limits on data storage.

Typical test (02_22_01 T162327) with 3/4" vortex generators prior to the rear facing step. at Mach 1.1 inlet conditions (4300 rpm)

Sample point	Pilot Methane Flow Rate, scfm (kg/sec)	Pilot Hydrogen Flow Rate, scfm (kg/sec)	Starter Motor Power, kW	Air Film Cooling Flow Rate, scfm (kg/sec)	Indicated Combustor metal temperature, degree F (K)
	121 (.041)	81 (.0034)	361	680 (.41)	1325 (991)
	160 (.054)	81 (.0034)	345	680	1375 (1020)
1	180 (.061)	81 (.0034)	342	680	1375 (1020)
	210 (.071)	81 (.0034)	335	680	1355 (1014)
	230 (.078)	81 (.0034)	335	680	1350 (1009)
2, 3	250 (.084)	81 (.0034)	335	680	1290 (969)
4	240 (.081)	155 (.0066)	320	680	1275 (964)
	210 (.071)	145 (.0061)	310	680	1361 (1011)
5	230 (.078)	145 (.0061)	310	680	1320 (989)
	180 (.061)	170 (.0072)	296	680	1413 (1041)

Table 4.4

4.2.1.5 Analysis of Thrust Module Performance under Variable Fuel Loadings

In Figure 4.29, the combustor temperature at sampling point 1 is greater than the combustor temperature at the top of the rotor ramp (1377F vs 1325F, respectively). Since methane was increased between these two points, it is reasonable to assume that the temperature increase was driven by an approach toward an equivalence ratio of unity. Continuing on Figure 4.29, from point 1 toward point 3, it is clear that the combustor temperature drops as methane is increased, indicating that between point 1 and point 3 an equivalence ratio greater than one is passed, and an overly rich (ie cooler) burn developed. This observation can be extended to all points at a constant rotor speed of 4300.

Figure 4.30 shows the indicated combustor temperature vs a “local” equivalence ratio, based on an estimated air entrainment flow rate. This local equivalence ratio was calculated by determining the stoichiometric equation for each fuel blend (a known function of hydrogen-to-methane ratio), and estimating the air flow rate to the recirculation zone. The baseline air entrainment flow rate was backed out by assuming that the maximum combustor temperature would be nearly coincident with a unity equivalence ratio. Assuming the air entrainment flow rate is the same for all fuel conditions, figure 4.30 was generated.

Also shown on figure 4.30 are four curves indicating an estimated combustor floor temperature, based on adiabatic flame temperature and estimated heat transfer from the gas via radiation and convection. For simplicity, the model assumed constant convective heat transfer coefficients for the effusion-cooled combustor. Comparing the empirical data to the model in figure 4.30, it is clear that the local equivalence ratio is a significant factor in the combustor temperature. All empirical data for this test was taken with 25%<H2<50% by volume, fuel only.

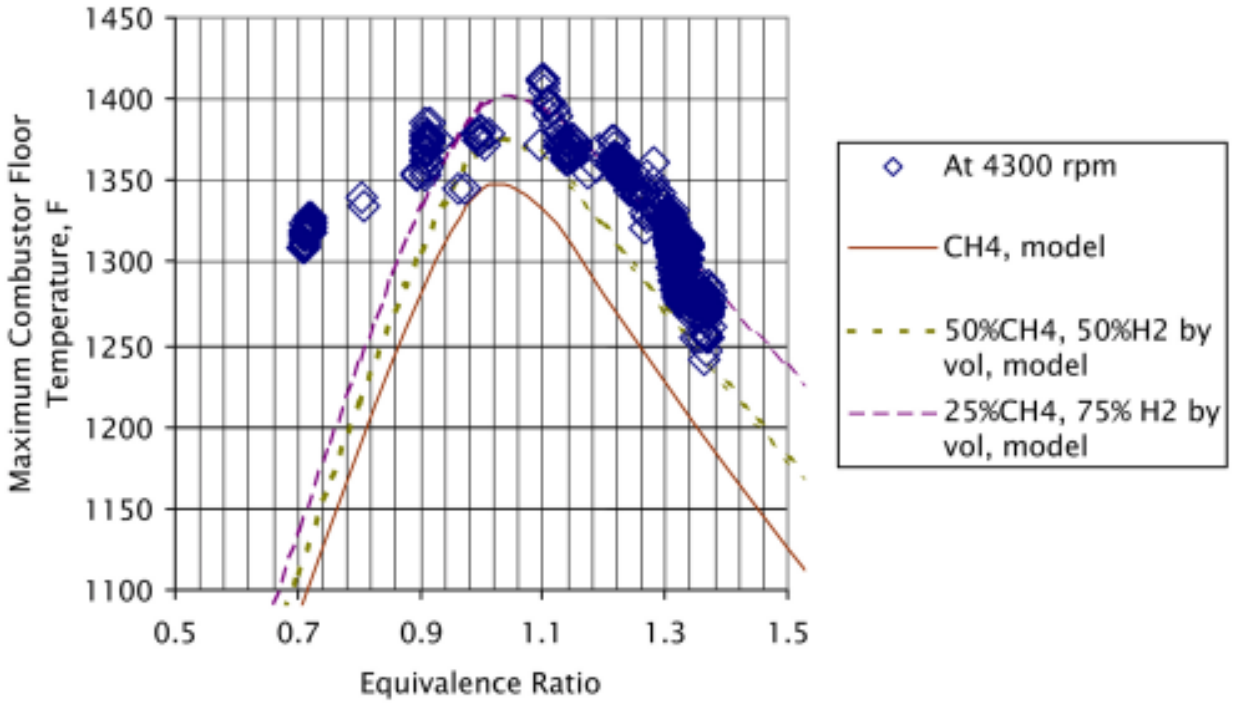

Combustor Floor Temperature, Measured by Infrared Detector, as a Function of Calculated Equivalence Ratio in the Recirculation Zone.
Figure 4.30

4.2.1.6 Chemical Reactor Modeling and High Speed Data at Various Fuel Settings

Details of combustor dynamics are explored by modeling conditions at various fuel set points shown in figure 4.29. Each point indicates where high speed data was recorded for the combustor floor temperature and the combustor pressure, such that modeled data and empirical data can be correlated.

A five element reactor network was used, as shown in Figure 4.33. Two reactor elements were used to model the shear layer that communicates with the recirculation zone. The shear layer half-angle is assumed to be 5 degrees. The recirculation zone length is simulated to be 5 step heights. The entrainment of air from the freestream into the recirculation zone is defined at 3%. All of the fuel is assumed to enter element #1, which is a simulation of the thin layer of fuel, which flows off the step and into the shear layer. The recirculation zone, element #5, receives the fuel by entrainment from element #2. GRI-Mech 2.12 is used as the chemical kinetics mechanism. Quantitatively, the conditions modeled were outside the range of applicability for this mechanism. However, qualitatively, this mechanism is able to predict the correct trends for these conditions. The above conditions and assumptions were fixed for all the high-speed trace points modeled.

4.2.1.6.1 High Speed Data and Chemical Reactor Modeling for Point 1

Figure 4.31 shows a high speed data taker at point 1 (note that point 1 is referenced from figure 4.29). The indicated combustor temperature, as measured by the infrared thermometer is the top curve a representation of the passing combustors is the middle curve, and the combustor pressure (as measured by a dynamic pressure sensor) is the lower curve. A total of 3.5 rotations of the rotor are shown Note that combustor temperatures are relatively consistent from combustor to combustor, and rotation to rotation, but some high speed variation is present. This is due in part to interference of the infrared signal by combustion products and sampling rate aliasing.

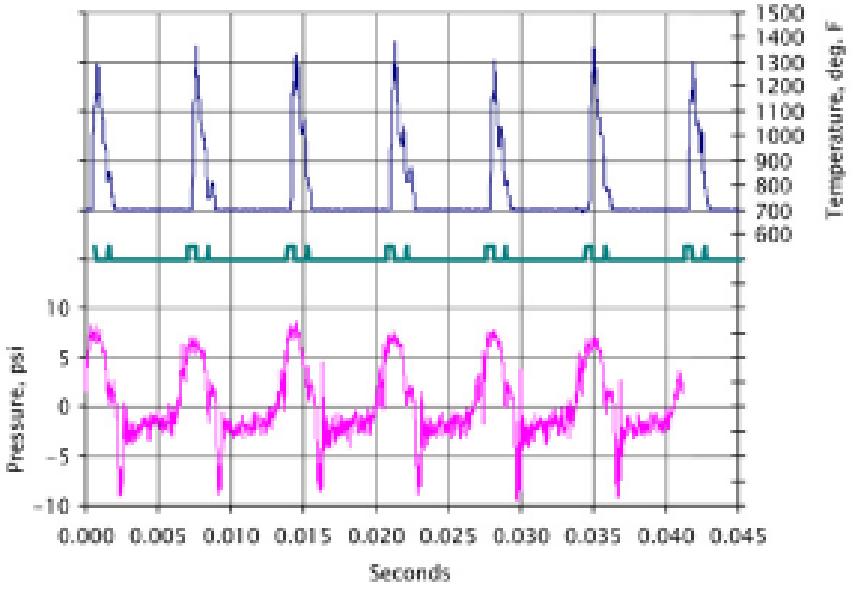

Test at 01_22-01 T163601; High speed (100 Hz) Combustor Temperatre and Pressure at Point 1.
Figure 4.31

Figure 4.32 shows a single rotation of the rotor, at point 1. Note that the combustor temperature indicates the forward half of the combustor (albeit toward the rear of the recirculation zone) is the primary heat release location. The combustor temperature falls off significantly approaching the throat, and more rapidly as the hot gas expands in the nozzle. This temperature fall-off is likely a combination of loss of flameholding ability in the shear zone, some quenching by the freestream air, the track of the infrared thermometer relative to the helix angle of the strake (the infrared thermometer is biased toward the intake side as it passes over the nozzle), and the additive nature of effusion cooling. The pressure profile shows a combustor pressure approximately 7 psi above ambient pressure.

Figure 4.34 shows modeling results corresponding to fuel settings associated with point 1 and figure 4.32. The element with the highest temperature is #2 (2908F), which corresponds to the shear layer near the middle and end of the recirculation zone. The recirculation zone, element #5, is at a lower temperature, 1303F, probably because of the low phi (or low amount of fuel) in that element. The calculated temperatures indicate dependence on phi, except for element #1. Element #1 appears to serve as a mixture element of the bulk flow with the recirculation zone gases because its residence time is lower than the blowout residence time for its phi (1.65). The temperature in the combustor appears to peak in the middle, with a dropoff in temperature toward the end, possibly due to entrainment and mixing of the hot burning gases with the bulk flow air and AFC.

Because chemical reactor modeling assumes extreme states of micromixing for each element (PSR or PFR), the modeling suggests that in order for combustion to be sustained at point 1, there has to be some kind of flameholding outside the recirculation zone or some kind of semi-stable stoichiometric volume in the shear layer.

4.2.1.6.2 High Speed Data and Chemical Reactor Modeling for Point 2

At point 2 (refer to figure 4.29), more CH4 fuel was added. The empirically obtained pressure and temperatures for one rotor cycle are shown in figure 4.35. The corresponding modeling results are shown in figure 4.36. In the model, the effect of fuel addition is that it essentially extinguished combustion in the recirculation zone and the shear layer adjacent to the recirculation zone. Residence times in elements 1, 2 and 5 are below the blowout residence times. The hottest part of the flame is near the middle of the combustor, after the recirculation zone. The qualitative implication from this modeling result is that adding CH4 effectively moved the peak temperature further away from the step, when compared to point 1 (figure 4.34).

Comparing figure 4.35 to figure 4.32, it does appear that the hottest part of the combustor has migrated towards the rear of the combustor, and heat release is present at the throat and in the nozzle (plume). Contrary to the model, the recirculation zone does remain involved in flame holding (compare figure 4.35 and figure 4.36), possibly due to less entrainment of fuel (via element 1) in the experiment compared to the estimate for the model.

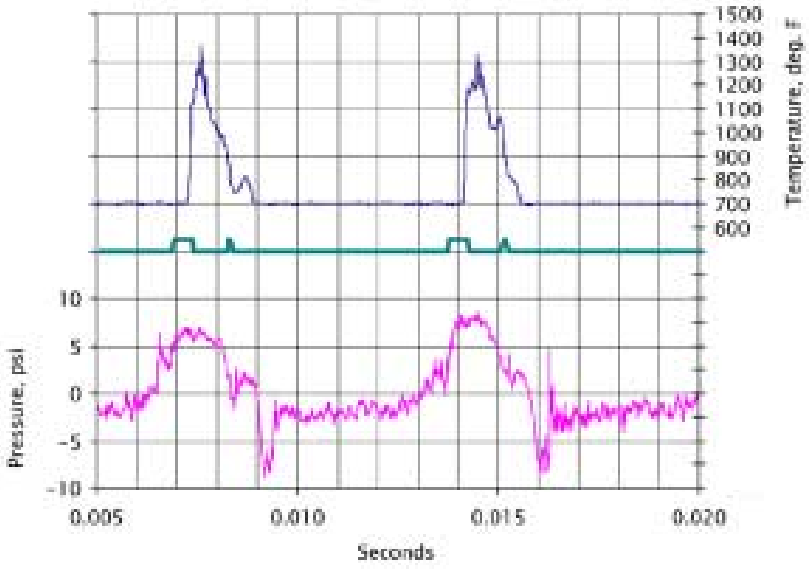

Test 02_22_01 T163601; High Speed (100 Hz) Combustor Temperature and Pressure at Point 1, Single Revolution.
Figure 4.32

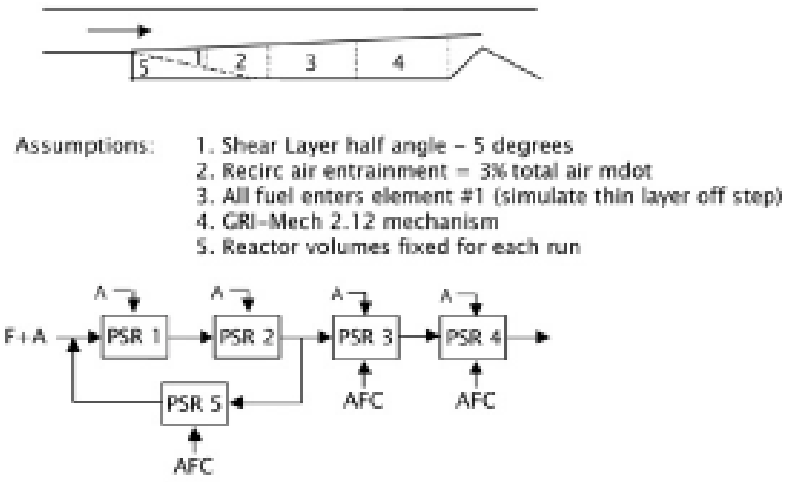

Chemical Reactor Model and Assumptions
Figure 4.33

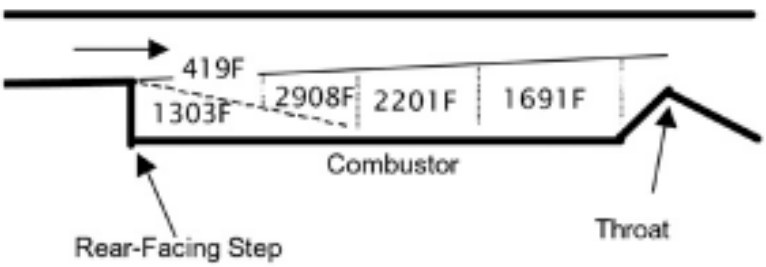

Gas Temperature Modeling Results for Point 1
Figure 4.34

4.2.1.6.3 Chemical Reactor Modeling at Gas-Off

At gas off command (End of Test in figure 4.29), the maximum combustor temperature is 1413F. Combustor modeling results for this condition (48% H2 by volume) are shown in figure 4.37. Note that the recirculation zone residence time is adequate to prevent blowout with additional hydrogen augmentation (compare figure 4.36 and figure 4.37), and consistent with the temperature rise at the end of the test (shown in figure 4.29).

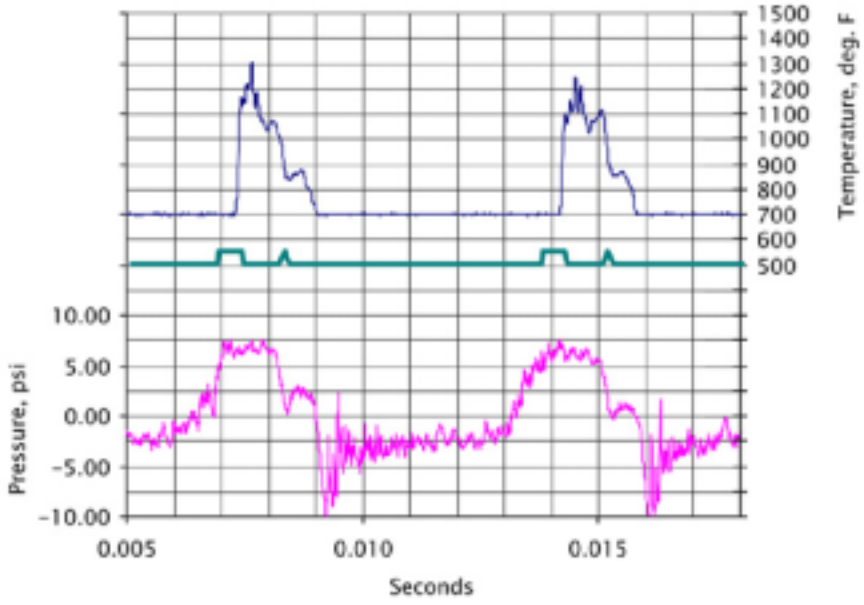

Test 01_22_01 T163727; High Speed (100 kHz) Combustor
Temperature and Pressure at Point 2, Single Revolution
Figure 4.35

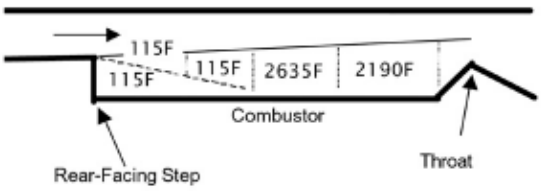

Gas Temperature Modeling Results for Point 2,
refer to Figure 4.32
Figure 4.36

Gas Temperature Modeling Results at Gas-Off,
refer to Figure 4.29
Figure 4.37

4.2.1.7 Blowout Times Versus Equivalence Ratio

Modeling and empirical data discussed above indicate that the performance of the flame holder and combustor is a function of overall stoichiometery, as well as the fuel blend (H2 to CH4 ratio). Chemical reactor modeling was used to calculate the blowout times versus fuel-air equivalence ratio for mixtures of methane/hydrogen fuels, as shown in figure 4.38. The modeling conditions correspond approximately to engine test conditions just above Mach 1 (1.43 atm pressure and 115 deg F combustor inlet temperature).

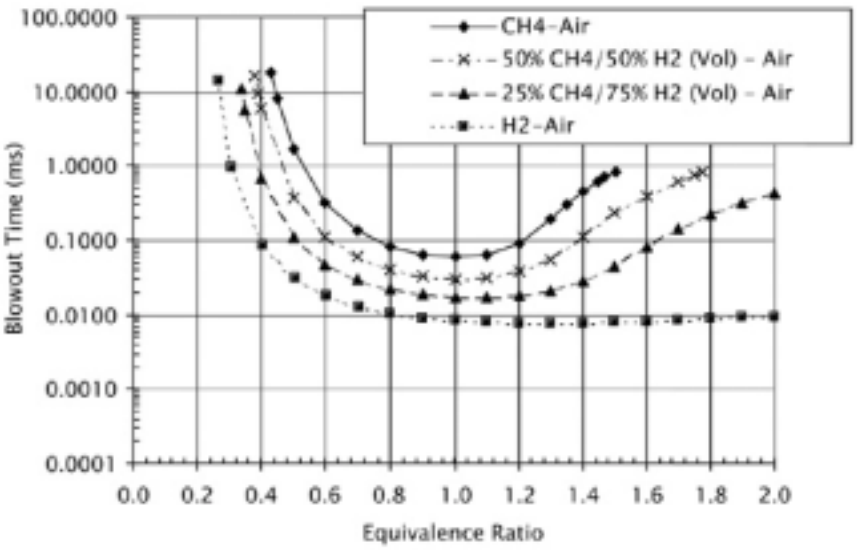

Blowout Times for Various Hydrogen/ Methane Fuel Blends
Figure 4.38

Four curves were generated, corresponding to pure methane, pure hydrogen, 50% methane/ 50% hydrogen mixture (by volume), and 25% methane/75% hydrogen mixture. The curves were calculated for fuel-air equivalence ratios from 0 to 2.0. The minimum equivalence ratio for each of the curves corresponds to the lean extinction limit. For the pure methane and 50-50 CH4/H2 mixture, the rich extinction limits are also shown.

The curves clearly show the benefits of using hydrogen fuel. For pure hydrogen, the blowout times are one to two orders of magnitude below pure methane. For CH4-H2 mixtures, there is a modest to significant decrease in blowout times, as well as a marked increase in flammability limits, compared to pure methane fuel.

4.2.1.8 Conclusions

Both the recirculation zone of the combustor and the shear layer (off the rear-facing step) play roles in ignition, ramping to operational speed, and flame-holding above Mach 1. Sustaining combustion at operational speed requires a balance between fuel and air film cooling, with operational limits defined by the maximum allowable combustor temperature and combustor quench.

The combustor floor temperature trend can be predicted based on the calculated equivalence ratio of the fuel blend, estimated heat transfer coefficients, and the adiabatic flame temperature. Further, a simple PSR network model qualitatively shows the location of maximum heat release in the combustor, although some weakness remains in determining the fuel entrainment split and detailed fluid dynamics.

5.0 Conclusions

5.1 Objectives and Tasks

The current research and development effort has led to significant advancements in adapting ramjet technology to power generation applications. At maturity, the Ramgen engine will compete with, and potentially surpass, traditional gas turbine engines in terms thermal efficiency, emissions, cost, and versatility. Fundamental experiments have illuminated both solutions to technical challenges, and areas worthy of additional research.

The primary objective of this project was to continue the research, design and development effort begun by Ramgen Power Systems on the Ramgen engine. Support of this primary objective was accomplished by exploring specific areas of interest, listed below.

Testing and Evaluation of the Ramgen Engine

The engine was operated with satisfactory combustion and air film cooling performance at supersonic inlet conditions for extended periods. At the completion of the engine test program, over 500 cold flow, ignition, ramp, and high-speed engine tests were performed. This included 216 hours of engine spin tests, 42.5 hours of hot combustor testing, and 6.3 hours above Mach 1.

Auxiliary System Modifications

Significant engine improvements were realized in the contract period, including upgrades to the thrust modules, monitoring and diagnostic equipment, ancillary components (including drive motor control equipment), and stationary engine components. These modifications led to improved thrust module performance, better engine control, increased inspection capability, improved diagnostics, and increased safety.

Measurement of Rotor Drag

Rotor drag tests were performed with thrust module components replaced with bare rim segments. This led to accurate measurement of disk drag, independent of thrust module geometry. This data allowed quantification of module thrust, decoupled from parasitic losses.

Control of Tip Seal Leakage

Tip seal leakage was minimized by the use of replaceable seals. Tip seals were designed such that thermal growth of the combustor segment, combined with centripetal acceleration, caused rubbing of the stainless steel tip seals on the hardened engine case. This resulted in minimal tip seal gap under normal operating conditions. Test results and analysis make it clear that minimizing tip seal gap is an area worthy of further investigation.

Boundary Layer Bleed Evaluation

The prototype Ramgen engine uses a simple boundary layer bleed mechanism consisting of an open passage to the engine exhaust, just upstream of the inlet. The inlet geometry of the prototype engine allowed use of this method, with only slight modification during the contract period.

Combustor Temperature Monitoring

A Land Infrared Radiation Thermometer was adapted to the Ramgen engine to give nearly continuous temperature indications for the combustor wall and floor of the nozzle. This method proved to be a reliable monitor of combustor health, and more robust than discrete temperature measurements that would have been available through a rotor telemetry system.

Evaluation of Fuel Injection/Mixing Methods

Fuel mixing studies investigated performance characteristics of fuel injection through an upstream fuel slot, injection from the stationary engine center body, and injection via a bluff body flame holder. Multiple Vortex Generator (VG) configurations were tested, proving that flame stability could be manipulated with judicious VG sizing. These studies underscored the importance of increasing the shear-layer spreading angle and maximizing the shear area, thereby augmenting flame surface area. Fuel injection configuration via the bluff body flame holder was of secondary importance compared to flame-holder geometry.

Evaluation of Flame Holder Configurations

A bluff body flame holder and multiple Vortex Generator (VG) configurations were evaluated for their ability to enhance flame holding. An optimum VG height for premixing, prior to the rear-facing step, was investigated. The bluff body flame holder increased recirculation zone volume and shear layer surface area. It was found that the heat release zone, and therefore combustion efficiency, could be manipulated by judicious selection of bluff body geometry, and is less influenced by fuel injection distribution.

Combustor Film Cooling Optimization

Air film (effusion) cooling was used to maintain combustor and nozzle surface temperatures below limits dictated by material properties. Air film cooling surface area was increased 50% during the contract period, thermal barrier coating was incorporated, and coolant delivery was optimized. Extensive hot-fire time, under variable heat loading conditions, validated the cooling system.

Noise Monitoring and Mitigation

Noise levels for the prototype engine were measured with an unmuffled intake and exhaust. Thorough analysis of the frequency spectrum made it clear that noise levels can be readily attenuated by a conventional noise enclosure and silencer technology.

Emission Monitoring

The exhaust stack was monitored for NOx, CO, UHC, and CO_2 emissions. Unburned hydrocarbon and CO concentrations were consistent with incomplete combustion, as was expected with the prototype flame holders and combustor configurations. Fuel bypassing the recirculation zone, and insufficient residence time in the shear zone, are clear sources of both CO and unburned hydrocarbons.

5.2 Summary Comments

The improvements, innovations, and tests described in this report resulted in substantial progress toward the primary goal of this continuing research - maturation of the technology of using ramjets for shaft-power production. Extended operation of the thrust modules at Mach 1 with satisfactory combustor performance and air film cooling demonstrated that this technology is viable. Future efforts will work toward optimizing combustor residence time and flame-holding, dealing with unique boundary conditions, minimizing loss mechanisms, and improving combustor cooling. The achievements to date have laid the groundwork for future success.

Appendix 1

The Development of the Ramgen Engine Combustor System

Submitted for Presentation at
ASME Turbo 2002 Conference

Draft
Proceedings of the ASME TURBO EXPO 2002
ASME TURBO EXPO: LAND, SEA & AIR 2002
June 3-6, 2002, AMSTERDAM, THE NETHERLANDS

GT-2002-30084

THE DEVELOPMENT OF THE RAMGEN ENGINE COMBUSTION SYSTEM

Blake C. Chenevert, Donald W. Kendrick*, Ben Trueblood,
Jon Tonouchi, Shawn P. Lawlor and Robert C. Steele
Ramgen Power Systems
Bellevue WA 98005

ABSTRACT

The research and development of a unique combustion engine is presented. The engine converts the thrust from ramjet modules located on the rim of a disk into shaft torque, which in turn can be used for electrical power generation or mechanical drive applications. A test program was undertaken that included evaluation of the pre-prototype engine and incorporation of improvements to the thrust modules and supporting systems. Fuel mixing studies and vortex generators and bluff body flame holders demonstrated the importance of increasing the shear-layer area and spreading angle to augment flame volume. Evaluation of flame-holding configurations (with variable fuel injection methods) concluded that the heat release zone, and therrefore combustion efficiency, could be manipulated by judicious selection of bluff body geometry, and is less influenced by fuel injection distribution. Finally, successful operation of novel fuel and cooling air delivery systems have resolved issues of gas (fuel and air) delivery to the individual rotor segments. The lessons learned from the pre-prototype engine are currrently being applied to the development of a 2.8MW engine. *Keywords:* Gas Turbine, Ramjets, Lean-Premixed, Combustion.

INTRODUCTION

The paper presents the design and development of a fundamentally new kind of power generation device known as the Ramgen engine. These effortshave been aided by the Department of Energy, as part of an initiative to bring viable and innovative energy technologies to market.

The design of the pre-prototype engine represents the application of well-established ramjet principles to power generation. Instead of using a ramjet to provided thrust for a supersonic aircraft or missile, the engine converts the linear thrust from a ramjet into shaft torque, which in turn drives a generator which provides electricity or shaft power for a mechanical drive application. At maturity, the production engine will have a thrermal efficiency rivaling and surpassing conventional gas turbines, with highly competitive CO and NO_x emmisions through its operation in a lean premixed mode. The unique engine design also permits the use of waste fuels, including landfill gas and coal bed methane as well as synthetic (”Syn Gas”) and biomass fuels, for energy production. Such atypical gaseous fuels cannot be currently utilized in conventional gas turbine systems due to the risks of autoignition, flashback, engine wear and inability to ingest atmospheric fuels directly.

The pre-prototype engine was fully assembled in Tacoma, WA in July 1998. Tests occurring in 1999 validated ignition and flame holding at idle rotor speeds, the mechanical integrity of the rotor at supersonic tips speeds, and overall system integrity. Development work conducted between late 1999 to September 2000 focused on improving combustion stability, fuel delivery methods, and air film cooling systems. These efforts resulted in substantial progress toward operation at full rotor speeds (4300 rpm, Mach 1.1 inflow conditions).

---

*Corresponding Author, Technology Leader Aero-Thermal:
dkendrick@ramgen.com

THEORY OF OPERATION: THE RAMGEN ENGINE

Ramjet Technology

The engine is based on ramjet technology which produces propulsive force by increasing the momentum of the working fluid via combustion and expansion through a supersonic nozzle (Heiser and Pratt, 1994). In contrast to other air-breathing engines, the working cycle of the ramjet engine is not accompanied by mechanical compression of the working fluid but rather through a shock system located within the inlet portion of the engine. This makes the ramjet engine the simplest mechanical air-breathing engine to date through its minimal use of moving parts. Figure 1 illustrates the working cycle of the ramjet engine and demonstrates the four fundamental processes: ingestion, compression, heat release, and expansion.

Flame stabilization is typically achieved from a simple flame holder (V-Gutter or equivalent) located at the end of the inlet passage or dump plane and sized for the appropriate flow velocities. The air-fuel mixture entering the combustion chamber is ignited by recirculating hot combustion products comprising the recirculation zone.

The flow within the combustor is subsonic; hence, an initial contraction of the flow area (throat) is necessary to both reduce the internal pressure and accelerate the flow to sonic conditions (Oates, 1997). After attaining sonic velocities, the flow encounters a diverging passage to continue the acceleration process. The addition of the nozzle allows the flow to continue to expand to supersonic exit velocities, until amvient pressure is attained - "ideal expansion".

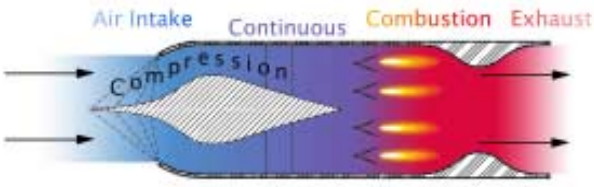

Fig. 1: Ramjet Engine Working Cycle

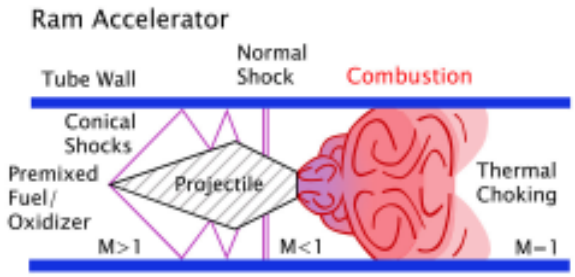

Fig. 2: The Ram Accelerator

A novel variation of the ramjet engine is the ram-accelerator. The ram-accelerator is a unique embodiment of the ramjet process applied to the acceleration of a projectile or payload (Hertzberg et al., 1088, Bogdanoff, 1992). In the ram-accelerator, a tube or barrel is filled with a mixture of fuel and oxidant, commonly referred to as "premix". A projectile is first launched into one end of the barrel with a low supersonic velocity (Mach ~ 1.2). As the projectile travels through the premix, the shaping of the projectile creates a series of oblique, conical shock waves, which coalesce and reflect off the barrel walls as indicated in Fig. 2 (Bogdanoff, 1992, Harsha, 1981).

A normal shock is stabilized in the expanding section of the flowpath formed between the projectile and the barrel wall (see Fig. 2). As the premix passes through the normal shock wave and diffuser, it is compressed and decelerated to subsonic velociies. The combustion process is stabilized behind the trailing edge of the projectile - which acts as a rearward facing step flameholder - whereafter a thermally choking process ensues to maximize exit gas velocity. The duct or flow path formed between the moving projectile and the stationary barrel wall completes the ramjet's flowpath where all the thrust is manifested on the moving projectile. The thrust developed by the ramjet process accelerates the projectile as it moves along the length of the barrel so that it's exit velocity greatly exceeds it's inlet velocity.

The Ramgen Engine

The essential concept of the engine is the incorporation of one or more ramjets onto the rim of a rotor such that the thrust from the ramjets acts tangentially, causing it to rotate at supersonic rim speeds. In this way the thrust from the ramjets is converted into shaft torque.

Figure 3 is an isometric illustration of the high-speed rotor and the stationary main engine case from the pre-prototype engine. The figure illustrates how the two ramjet flow-paths are incorporated into the rim of the high-speed rotor. As shown, the two-dimensional ramjet fowpaths are open on their exterior, or radially outer-most, surface. Closure of the ramjet flowpath is facilitated by the stationary surface of the main engine case. The combination of a ramjet flowpath where one of the ramjet surfaces is moving relative to the other is analogous to the moving projectile and stationary barrel wall of the ram-accelerator. The ramjet flow-paths are mounted on the rim of the rotor as inter-twined helixes at an optimized angle to ensure sufficient inlet length, combustor velocities, residence times and optimized thrust vectors. Combustion products from one ramjet are inhibited from being ingested into its

neighbour by a mechanical searation known as a strake which wraps around the rotor's periphery (Fig. 3). Note that the helix/strake angle dictates the inlet, diffuser, combustor, and nozzle lengths, which in turn dictates the combustor velocity, residence time, and thrust vectors.

The shallow strake angle has a number of implications. Firstly, despite the supersonic rim speeds, the axial velocity of the premix ingested is very low. As a result, the inflow can be delivered to the ramjets with minimal pressure and viscous losses, facilitating a simple atmospheric premixer system. As a consequence, the engine is capable of burning a wide variety of low pressure and sub-quality fuels, including coal-bed methane, low=BTU natural gas (landfill methane), biomass fuels, and hydrogen. Secondly, the "augering" nature of the rotor enables the engine to be self-pumping, drawing in the required flow as determined by the effective flow area of the inlet system.

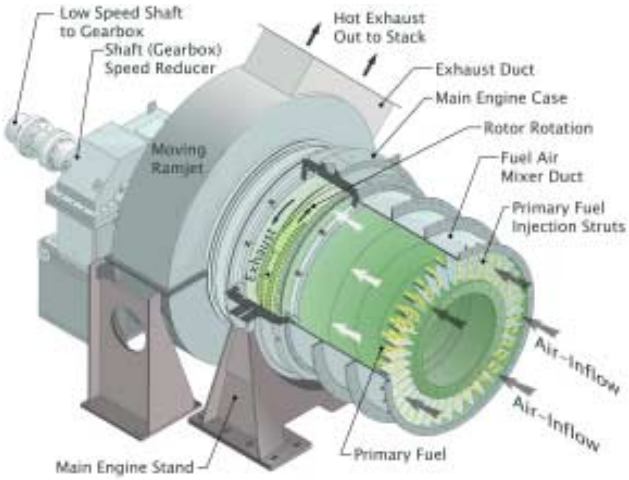

Fig. 3: The Pre-Protype Ramgen Engine.

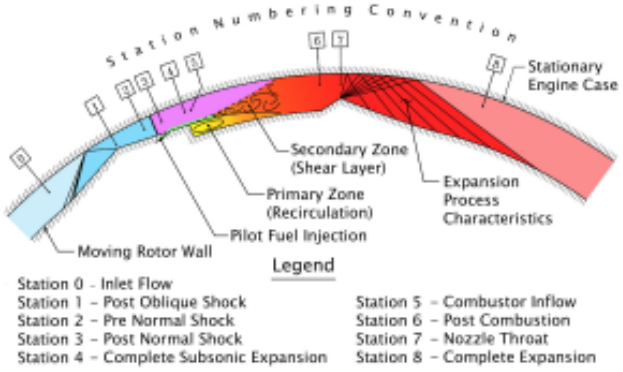

Fig. 4: Ramgen Engine Flow Details.

Figure 4 is a cut-away view depicting the flow path including the supersonic inlet, diffuser, combustor and exit nozzle for the pre-prototype engine. As shown in the figure, supersonic inflow (Station 0) meets the compression surface comprising the inlet. Through a series of Mach waves and strongly reflected shock (emanating from the stationary casing wall), the required inlet compression is achieved. The gas is then diffused through a two dimensional diffuser whereby the static pressure rises to attain required combustor inflow conditions while ensuring no separation along the diffuser's length. A simple rearward facing step flameholder is employed as the baseline flameholder to anchor the combustion activity. Standard diffusion piloting schemes (to be discussed) serve to anchor the flame and ensure acceptable combustion efficiency and acoustic levels. The hot combustion gases are then accelerated to supersonic velocities in the nozzle. The flow continues to expand/accelerate through the diverging portion of the supersonic nozzle until it attains atmospheric conditions - ideal expansion.

Delivery of pilot fuel and cooling air is achieved through incorporation of centrifugal pumps attached to the sides of the engine. Air is delivered to the hot side of the rotor while pilot fuel is delivered to the cold or intake side. Each gas is collected in an annular manifold at the rotor's periphery and then directed to the required segments via internal segment manifolding.

The next sections will describe some of the experimental results of the pre-prototype engine located in Tacoma, WA.

EXPERIMENTAL RESULTS: THE PRE-PROTOTYPE ENGINE

Experimental Set-uup

Engine Layout. Figure 3 illustrates the layout of the pre-prototype engine. The primary fuel employed was industrial grade methane (NG), supplied at a line pressure of 2 atmospheres and ambient temperature. The fuel system was manifolded and accurately measured by Worcester Model 20-755X I/P vales and Sponsler Model SP1-1/2-CB-PH7-8-4-RFX turbine meters. This base fuel was supplemented with pure hydrogen to assess alterations in the ignition delay times and flame speeds on combustor performance. Hydrogen was supplied by a 1200m^3 tube trailer, with an initial supply pressure of 136 atmospheres. Consistent with the methane supply, the hydrogen was regulated and controlled via I/P control valves and turbine meters. Downstream of the metering systems, the hydrogen and methane

lines were joined and routed to the main engine fuel line. To eliminate any hydrogen backflow into the lower pressure methane line, a check valve was installed in the methane line.

Three fuel systems were installed in the engine. The first or primary fuel system was via radial fuel struts located inside the inlet air annulus (see Fig. 3). Due to their upstream location, fuel delivery struts induced a high level of mixedness by the time the mixture reached the rotor. The second or teriary fuel system was via a series of porous metal plates circumferentially arranged around the inlet, downstream of the primary fuel struts. This also achieved a high degree of mixedness due to its upstream location. Both of the fuel systems supply the bulk of the gaseous fuel to the system and required only slightly above atmospheric pressures to operate effectively. The third or pilot fuel system supplied pure fuel to the flame stabilization device (to be discussed) and paralleled similar diffusion piloting schemes (Kendrick et al., 1999, Snyder et al., 1994). Injection of the pilot fuel was either through film-type slots located 1cm upstream of the dump plane (interfacial plane dividing the end of the diffuser with the front of the combustor) and / or through the bluff body flame stabilizer itself. For all of the reported tests, only the diffusion piloting system was employed.

As with typical combustion systems, the engine was outfitted with a variety of instrumentation and diagnostic features to maximize output data from each combustion run. Combustor dynamic pressures and floor temperatures were measured using PCB Model 112A04 piezoelectric pressure transducers and a Land Infrared IR Thermometer Model X0144IRT, respectively. The IR dectector viewed the combustor through a 1cm diameter quartz window and had a spectral range from 700-2000nm to accurately measure the liner floor temperature without significant contamination from such combustion byproducts as CO_2 and H_2O (Eckbreth, 1988). Two additional IR detectors were mounted on the engine inlet and exhaust, and aligned with the axis of engine rotation, to monitor the combustor and nozzle strake wall temperatures. A 3cm diameter quartz port was also added to the exhaust duct in order to view the broadband chemiluminescence via colour video cameras.

The cavities formed between the rotor and the stationary case were purged with air (dried and filtered) to mitigate aerodynamic heating of the wheelspace and prevent accumulation of flammable mixtures. This space was monitored for temperature changes (OMEGA type K thermocouples) and combustibles (Drager Multiwarn II catalytic).

Instrumentation interfaced with the System Control And Data Acquisition System (SCADA), and included emergency shut-off control logic where appropriate. All low speed data (gas flow rates, static pressures and temperatures) were monitored via RSView (Allen-Bradley), while control logic was managed by RSLogics software (Allen-Bradley). All high speed data (dynamic combustor pressures and liner temperatures) were similarly monitored in real time via a PC running a National Instruments WaveView7 system sampling up to 100kHz per channel. Post processing was facilitated via in-house Excel macros and documented in Excel workbooks.

Table 1: Engine Conditions (per ramjet).

Mair (kg/s)	Mfuel (kg/s)	Pilot (%, by - volume)	Fuel -	H2 (%, by volume)	AFC (%, mass total flow)
4	≤ 0.95	0-100%	NG/H2	0-70%	10%

Table 1 details the range of flow conditions for a standard run. The “AFC” depicts the level of air film cooling (liner cooling) required to maintain acceptable combustor floor temperatures and hence mechanical system integrity. Engine starting and ramp up to design point speeds was accomplished with a 447 kW AC starter motor connected to a regenerative variable frequency drive unit (VFD). The VFD also compensates for ramjet thrust generation. The starting motor is required to “start” (Hertzberg et al., 1988) the inlet shock system to initiate positive thrust generation. Combustion was initiated at low rotor speeds via a pulse discharged igniter timed appropriately to the location of the dump plane via magnetic pick-ups.

Flame Stabilizers. Three flame stabilizers were employed in this investigation (Figs. 5 and 6). The first is a 2.5cm high rearward facing step flameholder built into the engine’s floor. The second builds from the first in that it employs vortex generators (“VG’s) 1cm upstream of the step. This configuration was chosen to enhance mixing of the pilot fuel and core airflow and encourage a radial growth in combustion activity. Four sizes were investigated: 1, 1.3, 1.91 and 3.81cm high. The final flame holder concept, “Pylon”, was again an adaptation of the rearward facing step and was chosen to increase flame surface area through creation of multiple shear layers issuing from the dump plane.

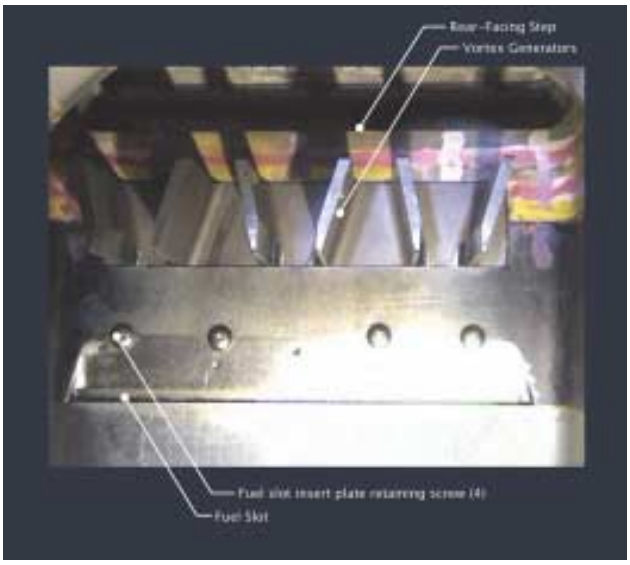

Fig. 5: Vortex Generator Flameholder.

Experimental Results

A timed spark from the Pulsed Discharge Ignitors resulted in the simultaneous igntion and engine speed had been stabilized at 800rpm. The fuel/oxidizer mixture ratio, ignition timing and AFC flow rates were optimized for greater than 95% ignition effectiveness irrespective of the flame stabilizer employed.

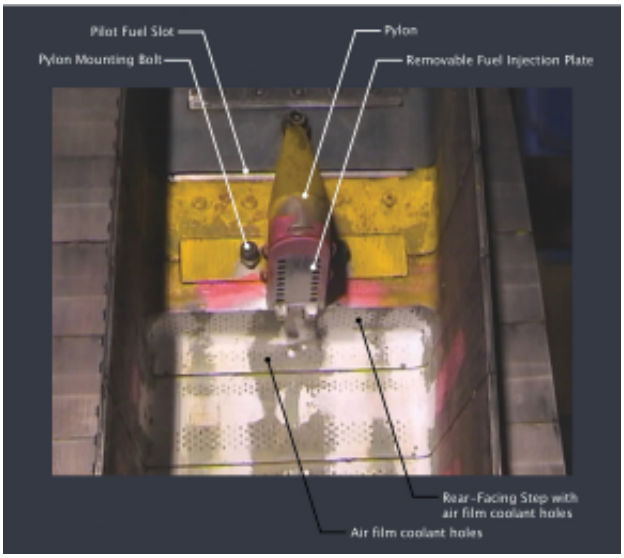

Fig. 6: Pylon and Rearward Facing Step

Igntion was verified by monitoring the high speed data acquisition system and ensuring that both combustors revealed typical floor temperature traces as shown in Fig. 7 below. This particular test was conducted with the 1.9cm tall VGs in place, located between the pilot fuel slot and the dump plane. Both combustors were lit as noted by the successive temperature pulses seen in the plot (top curve). It should be noted that due to the single location of the IR detector at the twelve-o-clock position on the engine cse, adjacent pulses denote opposite combustors. Due to the sampling rate of the detector, the trace gives an accurate measure of the floor temperature as the rotor moves relative to the fixed position of the Land IR. In fact,taking into consideration the rotor's speed and sampling rate, the rotor travels approximately 3mm between successive samples at the design speed (4300rpm). Also noted in the figure is the location of the beginning and end of the 33cm long combustor as determined by magnetic pickups in the stationary engine case - see the square pulse (dump plane and the triangle pulse (throat - middle curve). Also shown is the combustor pressure versus rotor position (bottom curve).

Evident is that the first half of the combustion chamber encompasses the recirculation zone and furthermore, that the location of the shear layer reattachment point is located approximately 20cm downstream of the step (note the location of the maximum floor temperature). A relatively stationary thermal trace develops in the forward half of the combustor, fluctuating within 27K from trace to trace. The latter half of the combustor however, appears dominated by more incomplete combustion zones as evident by substantially greater temperature fluctuations (+/- 120K) between successive cycles.

After stabilization at 800rpm for two minutes, an automated fuel, AFC and rotor ramp schedule was initiated via the Allen Bradley control logic (RSLigics) to attain the desired rim Mach number of approximately 1.1 (4300rpm). This inlet Mach number permits the exit nozzle to choke, and mzximizes available thrust. In practice, the ramp (Fig. 8) is broken down into three separate ramps, which are individually opimized for adequate pilot fuel, AFC and rotor acceleration: 800-2000rpm, 2000-3000rpm and 3000-4300rpm. The main issue of using a single ramp for all the quantities was evident from the video temperature traces during the ramping process. The fluid dynamics and combustion clearly alter as inlet/rotor speeds increase - most likely the combined effects of the non-uniform boundary conditions, increasing flow velocities, centifugal effects and stratification with increasing centrifugal loadings. The AFC flow rates were found to be critical in ensuring a sufficiently robust flame during the ramping process. If not incremented correctly, it would eventually quench the entire combustion process.

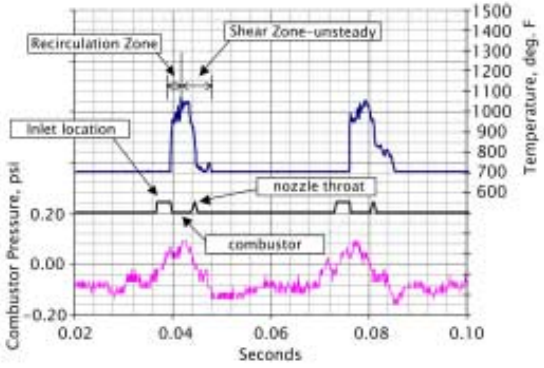

Fig. 7: Single rotor rotation showing combustor floor temperature and pressure traces.

Above 2000rpm, flame stabilization was generally restricted to the recirculation zone. The shear layer combustion, as indicated by the IR traces whose peaks move progressively upstream, was reduced as the overall combustor residence time dropped. Simple reactor modeling of the combustion zone (to be discussed) revealed that above 2000rpm, combustion is only possble in the recirculation zone where local residence times are conducive to methane oxidation. It appears, therefore, that there is a critical rotor speed above which the shear layer combustion is replaced by combustion with the recirculation zone.

The VFD is shown to hold the rotor at 4300rpm after some perturbations at the top of the ramp (Fig. 9). This transient is due to imbalance inrequired motor power transitioning from ramping to steady state operation. The power output required to maintain the engine's speed is a critical factor in the overall performance of the two thrust modules (combustor/nozzle systems). A typical test matrix (varying fuel loading between the three fuel circuits, H_2 addition, etc.) is effectuated after the rotor speed and drive stabilizes.

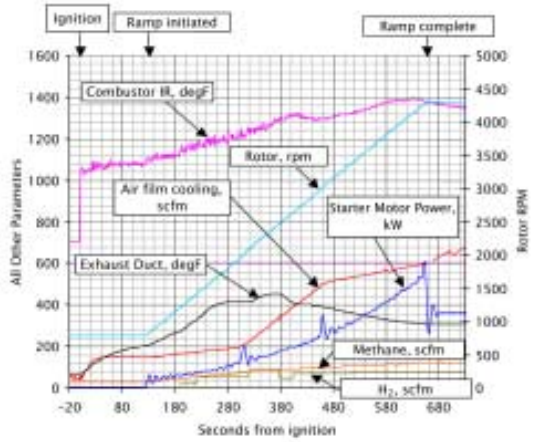

Fig. 8: Ramp Sequence to 4300rpm (Mach 1.1).

Typical Test Sequence. Depicted in Table 2 is a sample test run whereby the methane flow rate was incrementally ramped to a prescribed point, whereafter the hydrogen level was then incremented. Also included on the table is the VFD power required to stabilize the engine rpm at 4300rpm. Decreases in the required VFD is a direct measure of the effectiveness of the thrust modules and hence system efficiency. Points labeled 1 through 5 on the table refer to low speed data points (see Fig. 9) at prescribed operating conditions. Shown in Fig. 9 is a marked drop in the combustor floor temperature between points 1 and 3. If it is assumed that the floor temperature is linked to the bulk average flame temperature, it would seem reasonable that the combustion zone is leaning out with this increase in NG flowrate and hence has passed through the stoichiometric fuel-air ratio. The argument can be extended through all points at a constant rotor speed of 4300rpm. Figure 10 depicts the indicated combustor floor temperature versus local equivalence ratio based on an estimate of the entrained airflow rate into the recirculation zone per the rationale above. The baseline air entrainment rate was determined by assuming that the maximum combustor temperature was coincident with stoichiometric conditions. The figure was then generated assuming the entrainment rate was preserved throughout the exercise.

Pt.	NG (Kg/s)	H2 (Kg/s)	VFD (KW)	AFC (kg/s)	T (K)
	0.041	0.0034	361	0.41	991
	0.054	0.0034	345	0.41	1021
1	0.061	0.0034	342	0.41	1021
	0.071	0.0034	335	0.41	1014
	0.078	0.0034	335	0.41	1009
2,3	0.084	0.0034	335	0.41	969
4	0.081	0.0066	320	0.41	964
	0.071	0.0061	310	0.41	1011
5	0.078	0.0061	310	0.41	989

Table 2: 1.3cm Tall VGs Test Plan

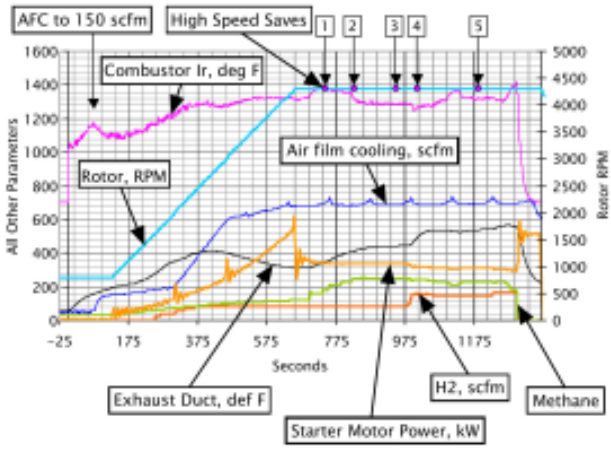

Figure 9: NG and H_2 Addition Test Plan with 1.3cm VGs.

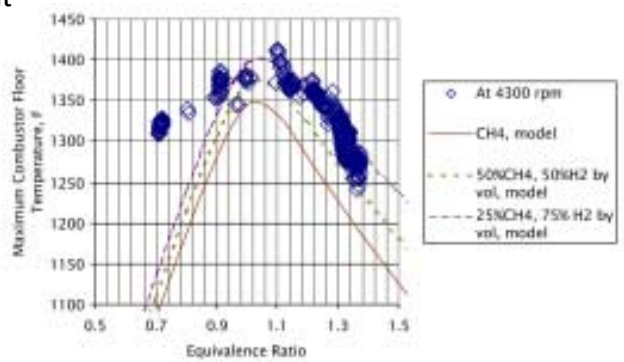

Fig. 10: Combustor Floor Temperatures versus Equivalence Ratio (data and model predictions).

Also shown in the figure are three curves estimating the floor temperature based on a simple, one dimensional model which includes the heat transfer from the gas to the floor (Kreith and Bohn, 1986) and equilibrium calculations (STANJAN) of flame temperatures for each fuel mixture. As demonstrated by the model, it is evident that the local equivalence ratio is a significant factor in determining the gas temperature.

Details of the above combustor are further explored through chemical reactor modeling of the events depicted in Fig. 9. It should be noted that at each of the denoted points, high speed data (IR and combustor pressure traces) were taken. A five element reactor network was used and is shown in Fig. 11. Two reactor blocks (#1 and 2) were employed to model the shear layer which communicated with the recirculation zone (#5). The shear layer half angle was assumed to be 5 degrees (Schlichting, 1979) and extended five duct heights downstream (Ozawa, 1981). The shear layer entrainment rate (as discussed above) was maintained at 3% and all the fuel was assumed to enter element 1 to simulate the thin layer of fuel issuing from the fuel slot. The recirculation zone element received fuel through entrainment from neighbouring elements 1 and 2. The GRI-MECH 2.12 was used to model the chemical kinetics mechanism for NG/H2 oxidation. It will be shown that the model accurately predicted the observed trends of Fig. 9.

Figure 12 shows the high speed data trace at point 1 for one rotation of the rotor. The top curve depicts the temperature while the bottom is the combustor pressure. Apparent is the forward location of the peak heat release within the combustor. A rapid drop ensues in the IR trace as the gas is unable to sustain combustion outside the recirculation zone.

Figure 13 depicts the modeling results corresponding to point 1. It reveals the predicted reactor temperatures based on the assumed flow rates and residence times determined experimentally. The highest temperature is seen to occupy reactor element 2 (2908^{o}F) which corresponds to the shear layer near the middle and end of the recirculation zone, consistent with the high speed trace (Fig. 12). The recirculation zone (element 5) predicts a lower temperature (1303^{o}F), most likely attributed to the reduced fuel-air ratio and increased wall heat transfer at this location. Element 1 appears to be insensitive to local equivalence ratio and behaves more as a mixing element since its residence time is below the required blowoff residence time for its equivalence ratio (Φ = 1.65). The temperature in the combustor is shown to drop off after the centrally located peak, most likely attributed to entrainment of the large, unreacted core flow and AFC flows with the products of combustion.

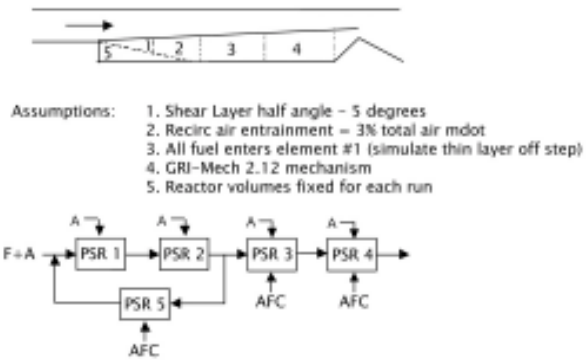

Fig. 11: Chemical Reactor Modeling Network.

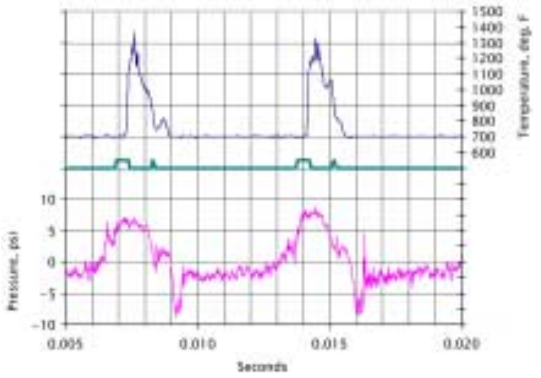

Fig. 12: High Speed Data Trace for Point 1.

A similar analysis is made at point 2. The high speed data trace and reactor network modeling results are shown in Figs. 14 and 15, respectively. As evidenced in both figures, there is a downstream migration in the peak heat release location. The model results show that the fuel addition has quenched most combustion activity in the recirculation zone and shear layer and shifted it downstream. Residence times in the upstream elements (1, 2 and 5) are below the required blowout times required to sustain combustion. The high speed data traces confirm these modeling results as evidenced by the combustion activity near the nozzle. Contrary to the model results is the reduced participation of the recirculation zone in the high speed data. This is most likely due to the model's over-prediction of fuel entering the recirculation zone.

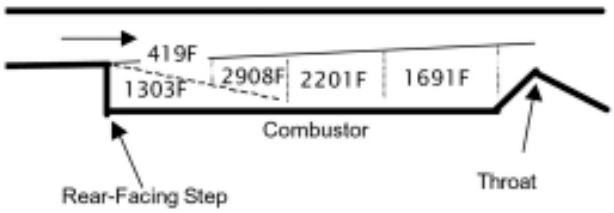

Fig. 13: Gas Temperature Modeling Results for Point 1.

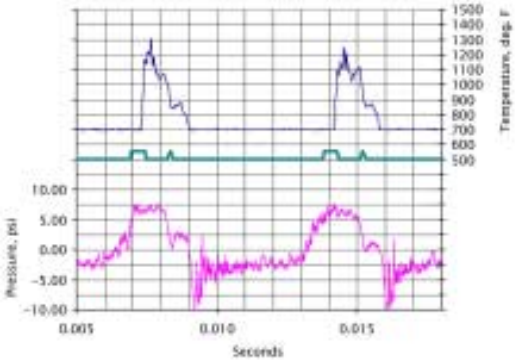

Fig. 14: High Speed Data Trace for Point 2.

At the termination of the experiment, the maximum combustor floor temperature is 1413°F. Combustion modeling results for this condition appear in Fig. 16 below. It appears that the recirculation zone residence times are adequate to sustain combustion with the hydrogen addition (compare Figs. 15 and 16) and such predictions are aligned with the temperature rise at the end of the test (Fig. 9).

Comparisons in Flame Stabilization Configurations. As noted previously, three flame stabilization devices were tested: a baseline, rearward facing step, a rearward facing step and VGs, and a rearward facing step and Pylon. The mechanism for fuel-air mixing and flame stabilization with the baseline rearward facing step flameholder is conventional shear layer mixing and creation of a recirculation zone (Zukoski, 1978). The combustion is sustained by the steady entrainment of the combustion by-products into the shear layer, which ignites the incoming cold charge. The success of this flameholder, therefore, depends on the spreading rate of the shear layer, which must extend to the opposite wall to ensure high combustion efficiency. The inflow shear spreading half angle is approximately 5 degrees (Schlichting, 1979). The angle (ϕ) can be augmented through combustion (Glassman, 1987) by following relation, where S_T is the turbulent flame speed and U is the approach velocity:

$$\phi = \sin^{-1}\left(\frac{S_T}{U}\right) \qquad (1)$$

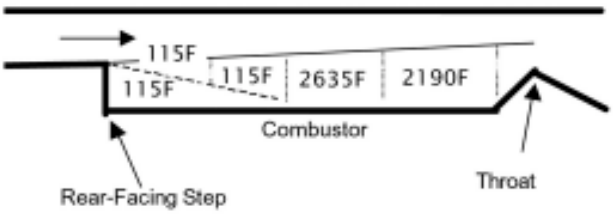

FIg. 15: Gas Temperature Modeling Results for Point 2.

Fig. 16: Gas Temperature Modeling Results for Gas Off.

Recognizing that the spreading angle can be augmented with a fuel with a higher turbulent flame speed, hydrogen was blended with the baseline methane fuel. Note that hydrogen's turbulent flame speed is up to four times methane's flame speed (Glassman, 1987). Test with the baseline rearward facing step revealed poor mixing between the pilot fuel and mainstream airflow. As such, most of the pilot fuel directly entered the recirculation zone, resulting in over-rich conditions. These disadvantageous situations resulted in significant quenching of the combustion directly behind the step, and often shifted the combustion zone toward the centre of the combustion chamber where leaner conditions prevailed. Efforts were focused on enhancing the mixing of the pilot fuel stream with the main core flow with the implementation of the VGs.

Vortex Generators of various heights were examined with the intention of creating sufficient streamwise vorticity to enhance mixing of the pilot and core air flows to radially extend the combustion zone. Throughout the series of tests, it was found that there was a delicate balance between increased mixing (taller VGs) and reduced combustion stabiity. The larger the VGs, the less stable the combustion zone, most likely due to the increased turbulence and quenching activity promoted by the larger struts (Lefebre, 1983). A sample high speed trace is shown in Fig. 17 for the optimal VG configuration (1cm long).

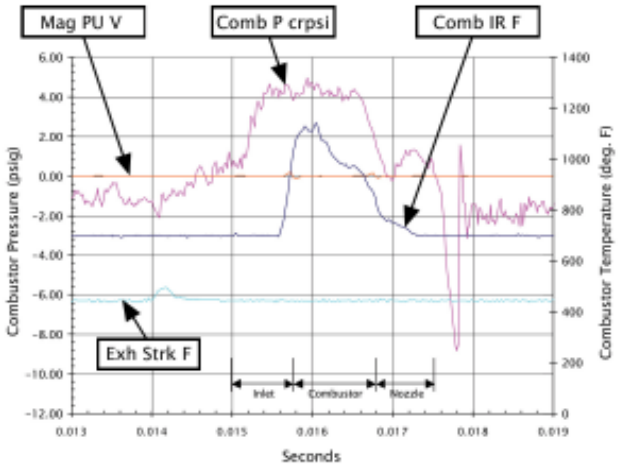

Fig. 17: High Speed Trace for the 1cm Tall VGs.

Fig. 17 shows that there is a greater streamwise distribution in temperature relative to the baseline step and secondly, the combustor pressure is more uniform. This is important since it is this pressure which forces the exhaust nozzle to choke, maximizing system performance.

The VGs provided some improvement with regard to heat release distribution and fuel-air mixing but failed to demonstrate a dramatic decrease in VFD power over the baseline configuration with fuel loading variations. The next series of tests investigated the Pylon design with various configurations in fuel injection (Fig. 6). This concept provides the greatest flexibiity in fuel placement, affords the combustor with the largest possible combustion volume to maximize heat release and provides the largest flame surface area. Such attributes favour an increase in overall combustion efficiency.

Preliminary CFD simulations using Star-CD showed encouraging results (Fig. 18). The pressure based solver was employed using the standard k-ε turbulence model and included the effects of rotation. THe figure depicts total temperature contours through various axial slices of the combustor. Apparent is the radial growth in combustion activity near the centre-line due to the presence of the Pylon. Unfortunately, due to the insufficient blockage afforded by the Pylon and the high momentum of the approach flow, it was ineffective in extending combustion in the axial direction. The design did, however, provide a more homogenous temperature distribution relative to the proceeding designs, irrespective of the fuel injection configurqtion (Fig. 19). This test was conducted with pilot fuel issuing from a single, 32 mm diameter hole from the pylon's faceplate and from the fuel slot along the floor. Due to this more uniform and elevated temperature distribution, combustion intensity and pressures were increased.

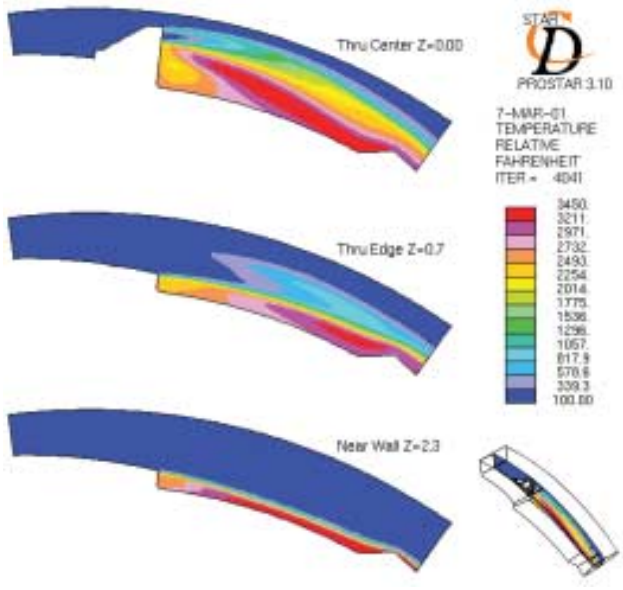

Fig. 18: Temperature Contours from a CFD Simulation of the Pylon Flame Stabilizer.

An overall comparison between VG and Pylon test data is made by comparing corresponding fuel loadings (BTUs of fuel) to VFD power for a rotor speed of 4300rpm. Lower VFD levels for the same fuel (BTU) loading would therefore signify higher system effectiveness. A summary plot appears in Fig. 20. All VG tests are denoted by square symbols while their Pylon counterparts are denoted by diamonds. Apparent is the more compact grouping of the Pylon data. The dotted box, which captures all such runs, further illustrates the fact that increasing fuel loading (expressed in BTU/s) lowers required VFD power. The greater slope and compactness of the Pylon providing increased flame surface area and hence higher burner pressures through increased combustion activity. The net effect is higher ramjet thrust and overall cycle efficiency.

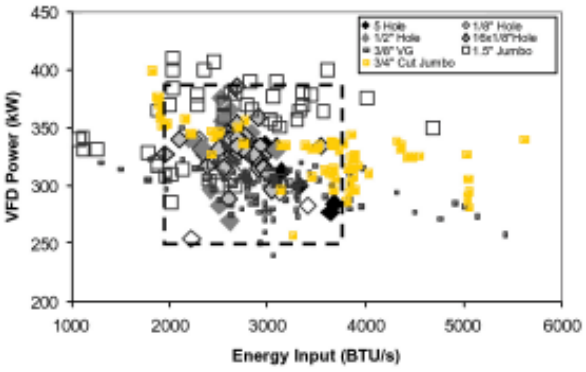

FIg. 20: VFD Comparisons between all VG and Pylon Runs.

CONCLUSIONS

The preliminary results from a pre-prototype engine are presented. The engine is designed to convert the thrust from ramjet modules located on the rim of a disk into shaft torque, which in turn can be used for electrical power generation or mechanical drive applications. Initial combustion tests reveal the importance of flame volume and surface area for increased combustion efficiency, irrespective of fuel injection schemes. Chemical kinetic modeling was shown to accurately depict the essential flow features of a sample test matrix whereby stepwise increases in NG and hydrogen flowrates were separately investigates. The results confirm the visual ovservations that dramatic flowfield variations occur both during ramp up and pilot fuel excursions due to the nature of te engine.

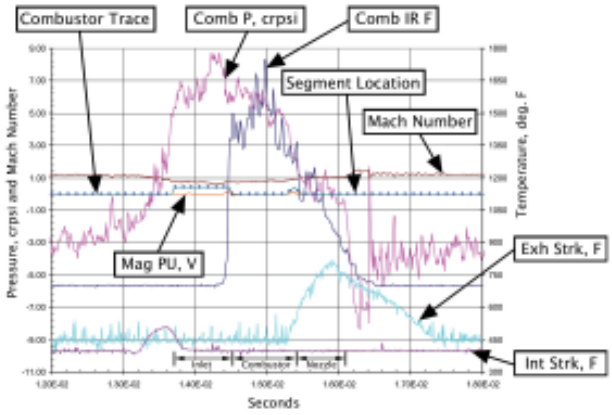

FIg. 19. High Speed for the Pylon Flame Stabilizer with 32mm fuel hole.

REFERENCES:

Bogdanoff, D. W., "Ram Accelerator DIrect Space Launch System: New Concepts," J. Prop. Pwr., Vol. 8, No. 2, pp. 481-490.

Eckbreth, A. C., 1988, Laser Diagnostics for Combustion Temperature and Species, Turnbridge Wells, Kent

Glassmanm I., 1987, Combustion, Academic Press, Orlando.

Harsha P. T. and Edelman, R. B., 1981, "Assessment of a Modular Ramjet Combustion Model," J. Spacecraft, Vol. **19**, No., 3, pp. 430-436.

Heiser, W. H. and Pratt, D. T., 1994, Hypersonic Airbreathing Propulsion, AIAA Ed. Series, Washington

Hertzberg, A., Bruckner, A. P. and Bogdanoff, D. W., 1988, "Ram Accelerator: A New Chemical Method for Accelerating Projectiles to Ultrahigh Velocities," *AIAA Journal*, Vol. 26, No. 2, pp. 195-203.

Kendrick, D. W. , Andserson T. J., Sowa, W. A. , and Snyder, T. S., 1999, "Acoustic Sensitivities of Lean-Premixed Fuel Injectors in a Single Nozzle Rig," *J. of Eng. For Gas Turb. and Pwr.*, Vol. **121**, pp. 429-436.

Kreith, F. and BVohn, M. S., 1986, The Principals of Heat Transfer, Harper and Row, Cambridge.

Lefebre, A. H., 1983, "Gas Turbine Combustion", Hemisphere Publishing.

Oates, G. C., 1997, Aerothermodynamics of Gas Turbine and Rocket Propulsion, AIAA Ed. Series, Washington.

Ozawa, R. I., 1981, "Survey of Basic Data on Flame Stabilization and Propagation for High Speed Combustion Systems", AFAPL-TR-70-81.

Schlichting, H., 1979, Boundary-Layer Theory, McGraw-Hill, New York.

Snyder, T. S., Rosfjord, T. J., McVey, J., Hu, A., and Schlein, B., 1994, "Emissions and Performance of a Lean-Premixed Gas Fuel Injection System for Aeroderivative Gas Turbine Engines," ASME Paper 94-GT-234.

Yungster, S., Eberhardt, S. and Bruckner, A. P., 1991, "Numerical Simulation of Hypervelocity Projectiles in Detonable Gases," *AIAA Journal*, Vol. 29, pp. 187-193.

Zukoski, E. E., 1978, "Afterburners," *The Aerothermodynamics of Aircraft Gas Turbine Engines*, AFAPL-TR-78-52, Ch. 21.

ACKNOWLEDGEMENTS

This effort was funded in part by the Department of Energy under the cooperative agreement #DE-FC26-00NT40, awarded between the period of September 29th, 2000 and August 31st, 2001. The computational support (Star CD) was provided by Combustion Science and Engineering (Columbia, MD).